

**Aviation-Climate Change Research Initiative  
(ACCRI)**

**Subject specific white paper (SSWP) on  
Contrail/Cirrus Optics and Radiation**

**SSWP # V**

**Steve S. C. Ou, PI, Senior Research Scientist**

**K. N. Liou, Co-PI, Distinguished Professor of Atmospheric Sciences**

**Joint Institute for Regional Earth System Science and Engineering  
and Department of Atmospheric and Oceanic Sciences  
University of California, Los Angeles**

**January 25, 2008**

## Table of Content

<b>Executive Summary</b> .....	4
<b>1. Introduction/Background</b> .....	8
<b>2. A Review of Climatic Impacts of Contrail and Contrail-Cirrus</b> .....	10
<b>a. Current state of the scientific research</b> .....	10
• <i>Long-term trends in the coverage and frequency of contrail-cirrus and cirrus occurrence</i> .....	10
• <i>Aerosol-cirrus and contrail-cirrus indirect effects</i> .....	11
• <i>Microphysical and radiative properties on contrails and contrail-cirrus</i> .....	13
• <i>Radiative forcing for persistent contrails and contrail-cirrus</i> .....	14
• <i>Climatic impacts of contrails and contrail-cirrus</i> .....	15
<b>b. Critical role of contrail and cirrus clouds in the climate process</b> .....	16
<b>c. Progress since the IPCC 1999 report</b> .....	16
• <i>Long-term trends in the coverage and frequency of contrail-cirrus and cirrus occurrence</i> .....	16
• <i>Radiative forcing of contrails and contrail -cirrus</i> .....	18
<b>d. Present state of measurements and data analysis</b> .....	18
• <i>Contrail and cirrus climatology based on analyses of surface and satellite observations</i> .....	18
• <i>Satellite remote sensing of contrails and cirrus clouds</i> .....	19
• <i>Satellite remote sensing techniques applicable to contrails and cirrus clouds</i> .....	22
• <i>Ground-based remote sensing of contrails and cirrus</i> .....	25
<b>e. Present state of modeling capability</b> .....	26
• <i>Parameterization of ice crystal microphysics properties in GCMs</i> .....	26
• <i>Modeling optical properties of contrails for input into radiative transfer models</i> .....	27
• <i>Radiative transfer model for application to satellite remote sensing – LBLE model</i> .....	28
• <i>Radiative transfer model for radiative forcing calculation – Fu-Liou model</i> .....	29
• <i>Global climate model – UCLA AGCM</i> .....	30
• <i>Global Contrail-Climate Model - ECHAM4 GCM</i> .....	30
• <i>Regional climate model – WRF model</i> .....	31
<b>f. Current estimates of climate impacts and uncertainties</b> .....	32
<b>g. Interconnectivity with other SSWP theme areas</b> .....	34
• <i>Formation, evolution, and persistence for contrails and contrail-cirrus</i> .....	34
• <i>Contrails and contrail cirrus specific microphysics</i> .....	34
<b>3. Outstanding limitations, gaps and issues that need improvement</b> .....	35
<b>a. Science</b> .....	35
• <i>Long-term trends in contrail-cirrus and cirrus</i> .....	36
• <i>Aerosol-cirrus and contrail-cirrus indirect effects</i> .....	36

•	<i>Microphysical and radiative properties on contrails and cirrus</i> .....	36
•	<i>Radiative forcing of contrails</i> .....	36
•	<i>Climatic impacts of contrails and contrail-cirrus</i> .....	36
<b>b.</b>	<b>Measurements and analysis</b> .....	36
•	<i>Satellite remote sensing</i> .....	37
•	<i>Ground-based remote sensing</i> .....	37
<b>c.</b>	<b>Modeling capability</b> .....	37
•	<i>Modeling optical properties for contrails and cirrus for radiative transfer calculations</i> .....	37
•	<i>Radiative transfer models</i> .....	37
•	<i>Global and regional climate modeling</i> .....	38
•	<i>Global distribution and properties of super-saturation, aerosol, and thin cirrus</i> .....	38
<b>d.</b>	<b>Interconnectivity with other SSWP theme areas</b> .....	39
•	<i>Detection and prediction of ice supersaturation</i> .....	39
•	<i>Chemistry within emission plumes</i> .....	39
•	<i>Contrail cirrus development</i> .....	40
•	<i>In situ measurements of aerosol composition and small ice crystals</i> .....	41
•	<i>Properties of heterogeneous ice nuclei from natural and anthropogenic sources</i> .....	41
<b>4.</b>	<b>Prioritization of research needs for tackling outstanding issues</b> .....	42
<b>5.</b>	<b>Recommendations for best use of current tools for modeling and data analysis</b> .....	45
	<b>References</b> .....	47
	<b>Figures</b> .....	60

## Executive Summary

In this subject-specific white paper, we present a literature survey of past and current developments regarding the impact of contrails and contrail cirrus on the radiation field of the Earth's atmosphere and climate. A number of recommendations for future long-term and short-term actions that are required to comprehend and quantify this important subject are subsequently outlined.

We first present a survey on the background of the basic problem of aviation's impacts on climate and climate change, followed by a discussion of perspectives based on conclusions of the 1999 Intergovernmental Panel on Climate Change (IPCC) Special Report, and the doubling and tripling growths of aviation industry in the next 20 to 40 years as projected by the Next Generation Air Transportation System, United Nation International Civil Aviation Organization, European Union Nations, and the United Kingdom. In response to the pressing need for further study of the potential impact of aircraft emission on climate and environment, a "Workshop on the Impacts of Aviation on Climate Change" was organized and held in Boston, MA on June 7-9, 2006, and a report on the findings during this workshop was later published.

We then review the definition of contrail and the classification of short-lived and persistent contrails and contrail-induced cirrus clouds. The coverage of contrails and contrail-cirrus clouds (~0.1%) has been found to be much smaller compared to that of naturally formed cirrus clouds (>20%). However, their radiative effects are not negligible and, because of indirect effect and feedback, their potential climatic impact could be substantial, particularly in the vicinity of flight corridors where contrail and contrail-induced cirrus formations are frequent. We point out that the radiative forcing of aviation produced contrails in the past is at least twice as large as the contribution of aircraft CO<sub>2</sub> emissions alone. Finally, estimates of the annual growth rate of cirrus clouds (~0.1%/yr) and the global contrail radiative forcing are presented.

### State of Science

Persistent contrails and contrail-cirrus that are formed in the upper troposphere and lower stratosphere may play an important role in regulating the radiation balance in the Earth-atmosphere system through the competition between the solar-albedo and greenhouse effects that are determined by the ice crystal microphysical and radiative properties within these clouds. The major issue is whether increasing jet air traffic will enhance the generation of additional cirrus clouds, which can lead to an amplification of global warming caused by the build-up of carbon dioxide and other trace gases in the atmosphere.

We have presented past and current progress in estimating long-term trends of the coverage and frequency of occurrence of contrail and contrail-cirrus clouds. Most works after the publication of the 1999 IPCC report focused on the estimate of long-term frequency trend using meteorological data, satellite observations, and numerical weather model products on global and regional scales, as well as the study of radiative forcings of contrails and contrail cirrus by means of satellite data and radiative transfer calculations. Surface observations and satellite data all show that the trend of cirrus cloud cover increased in the past 50 years and that the formation of cirrus clouds has been more frequent in winter and spring near flight corridors. It is anticipated that this increasing trend will continue as a result of increased aviation-induced contrail cirrus formations that tap hitherto cloud-free supersaturated air.

The 1999 IPCC report estimated that the direct radiative forcings of persistent contrails and contrail-induced cirrus are about  $0.02 \text{ W m}^{-2}$  (with a range of uncertainty from  $0.005\text{-}0.06 \text{ W m}^{-2}$ ) and anywhere

between 0 and  $0.04 \text{ W m}^{-2}$ , respectively. Estimates of contrail radiative forcings vary from near zero to  $0.03 \text{ W m}^{-2}$ . A number of GCM results show that surface warming produced by contrails is between  $0.2$  and  $0.3^\circ\text{C/decade}$ . These values must be updated and further assessed in light of new observations and an improved physical understanding of the microphysical and optical properties of contrails and contrail-cirrus.

Lastly, we discuss the issue of aerosol indirect effects on the microphysical and radiative properties of ice clouds, essential to the study of the climatic impact of contrails and contrail-cirrus. The indirect effects are complex and their quantifications require a concerted effort involving laboratory and theoretical research, modeling approach, and *in situ* observations in the atmosphere.

### **Present state of measurements, data analyses, and modeling capability**

The long-term contrail and cirrus trends have been compiled using satellite and manual surface observations and ground-based instrument measurements. We report a comprehensive data archive of contrail observations from the surface, compiled by the Global Learning and Observations to Benefit the Environment program. We have also provided a list of satellite remote sensing instruments and retrieval techniques that are applicable to contrails and contrail-cirrus studies, including a discussion of the current capability of ground-based remote sensing instruments.

A number of models for contrail research have been developed, and we identify seven state-of-the-art parameterization programs and models, including parameterization of ice crystal microphysics properties in GCMs, the unified theory of light scattering by ice crystals developed by Liou, Takano and Yang, the LBLE radiative transfer model for satellite remote sensing developed by Takano and Liou, the delta 2/4-stream radiative transfer model for radiative forcing calculations developed by Fu and Liou, the UCLA GCM, the European ECHAM4 global contrail-climate model, and the WRF model for regional study.

### **Current estimate of the uncertainties on the climatic impact of contrails and contrail-cirrus**

The major debate has focused on the magnitude of radiative forcing and surface warming generated by contrails. Large uncertainties exist in global and regional radiative forcing and surface warming, as determined by observations and modeling studies. This suggests that past and current studies of contrail climate impact are inconclusive and not definitive. However, it is pointed out that the radiative and climatic effects, though small globally, could be substantial on a regional scale, as illustrated by a number of regional modeling studies, a subject requiring further exploration and investigation.

### **Outstanding scientific limitations**

Primary sources of data that can be used to estimate the long-term trends in contrail-cirrus and cirrus clouds suffer from uncertainties due to manual operation and high-altitude measurements, limitations in geographical coverage, and low temporal and spatial resolutions. The aerosol indirect effects on the microphysical and radiative properties of cirrus clouds are critical in the discussion of climate and climate change involving contrails and cirrus clouds, but these effects are complex and difficult to quantify by mean of *in situ* observations and/or modeling approaches. Comprehensive and systematic *in situ* measurements of contrail and contrail-cirrus have been extremely limited because of the requirement of high flying aircraft and the development of accurate and durable sampling instruments. Modeling approaches, on the other hand, are limited by insufficient understanding of the physical and chemical processes that control ice formation in the presence of aerosols. It would seem that it is

important to reduce these uncertainties before resolving the contemporary issues of the magnitudes of radiative forcing and surface warming.

Due to their narrow geometrical shapes, detection of the freshly formed and young contrails by space-borne sensors and ground-based lidar and radar has been a difficult task. Moreover, satellite contrail detection algorithms using split-window bands suffer from a drawback: cirrus clouds with similar linear shapes can be misidentified as contrails. Further development of the satellite and ground-based remote sensing techniques to infer the microphysical and optical properties of contrails is needed, along with *in situ* observations for validation of ice microphysics and the single-scattering properties.

It appears that current GCMs have had difficulty in predicting supersaturation in the upper troposphere and the lower stratosphere region. Many cloud schemes in GCMs compute cloud fraction based on an empirical function of the grid-mean relative humidity that may not be applicable to stratiform cirrus clouds, which are known to be long-lived and can be transported over many grid boxes of a large-scale model during their lifetime.

In addition to the above uncertainties and limitations, there are other issues related to the study of climatic impact of contrails, including uncertainties in the global distribution of water vapor, aerosols, and thin cirrus; detection and prediction of ice supersaturation; chemistry within emission plumes, contrail-cirrus development; the concentration of small ice crystals; and the physical and chemical properties of heterogeneous ice nuclei from natural and anthropogenic sources.

### **Prioritization of research needs**

*In situ* observations and ground-based remote sensing of contrail cirrus and aircraft emission plumes using high-flying aircraft and accurate and durable sampling instruments are needed for the study of the aerosol and contrail indirect effects on the microphysics and radiative properties, modeling of the microphysical and radiative properties for contrails, and the development of ice crystal single-scattering parameterization. These research activities can be costly, and their planning and preparation can be time-consuming. Laboratory measurements of the optical properties for ice crystal clouds can mitigate the uncertainty in current models and parameterizations. In addition, the airborne and remote broadband and narrow-band radiometric measurements, combined with collocated and coincident ice crystal *in situ* observations can be used to validate atmospheric and surface contrail radiative forcings computed by radiative transfer models. However, we rank the priority for this research category as “low” in regard to cost and time.

For global and regional model studies that address direct and indirect effects involving contrails, understanding of the basic mechanism for ice crystal formation is required to improve parameterization of heterogeneous ice nucleation rates. Data collected from coordinated atmospheric *in situ* measurements of the ice crystal and aerosol properties would assist in the development of physical parameterizations so that the contrail direct and indirect effects could be physically simulated in global models. The estimated cost for modeling efforts would be much smaller than *in situ* measurements, and the required time would also be shorter, perhaps on the order of one to two years. We rank this research category as “medium priority”.

An integrated use of satellite observations will improve the dependability of estimating the long-term trends of contrails and contrail-cirrus and complement the study of aerosol indirect effect. Research-grade broadband radiometric observations from satellites can be used directly for the investigation of radiative forcing produced by contrails and contrail-cirrus. Radiative transfer

calculations can also utilize satellite-retrieved ice crystal microphysical and optical properties as input. Furthermore, integrated satellite observations can be combined with collocated surface observations, meteorological soundings and ground-based remote sensing measurements to further improve accuracy of the detection of contrails and contrail-cirrus. Therefore, satellite observations would be very useful in advancing our understanding in the climatic effect of contrails. The cost for conducting this line of research would be relatively inexpensive, if a suitable number of focused validation experiments using existing facilities could be configured. We rank this research category as “high priority”.

### **Recommendations for best use of current tools**

We would suggest two current tools for contrails-climate research and development. First, MODIS cloud mask and products, with their superior spatial and spectral resolution, can be used to study long-term trends in the coverage and frequency of contrail-cirrus and cirrus occurrence in conjunction with AVHRR and GOES imager data. Another complementary dataset for estimating contrail long-term trends would be the CALIPSO/CALIOP cloud mask products, which have recently become available. MODIS cloud mask and products can also be analyzed to study aerosol-cirrus and contrail-cirrus indirect effects.

With reference to the modeling aspect, it appears that the best regional model that has been developed so far is the WRF model. We suggest that this model coupled with a spectral radiative transfer and ice microphysics parameterizations be used to simulate the formation, evolution, and dissipation of contrails and contrail cirrus using input from flight track and jet fuel consumption information, and that the simulation results be compared with the independent remote sensing results determined from MODIS and related cloud products.

## 1. Introduction/Background

Aviation appears to be one of the world's fastest growing sources of greenhouse gases, such as carbon dioxide, water vapor, and nitrogen oxide. The increase in the global surface temperature produced by greenhouse warming has been linked to the occurrence of more frequent extreme weather events such as floods, droughts, hurricanes, and blizzards, leading to catastrophic damages of property and loss of lives (US Environmental Protection Agency 2007). The 1999 Intergovernmental Panel on Climate Change (IPCC) Special Report contains a detailed study of the impact of aviation on the global atmosphere. Major findings from this report include: (1) Aviation produces around  $6 \times 10^8$  tons of carbon dioxide annually and globally; (2) it accounts for 3.5% of global warming from all human activities in 1990; and (3) aircraft emitted greenhouse gases will continue to rise and could contribute to about 15% of global warming from all human activities by 2050. Since the publication of the IPCC 1999 report, air traffic has been continually growing, particularly in the United States, Europe, and eastern Asia. In fact, the Integrated Plan for the Next Generation Air Transportation System (NGATS) proposed by the Joint Planning and Development Office (JPDO) created by the U. S. Congress demands that air transportation services grow from 2004 to 2025 by three fold (NGATS 2004). A similar projection of the aviation growth has been suggested by the United Nation International Civil Aviation Organization, the European Union, and the United Kingdom (Bows et al. 2005).

In view of the aviation activities projected over the next few decades, it is vitally important that immediate and effective actions be taken to understand the nature of the problem and to assist policy makers in making informed decision to protect the environment from potential threat by the inadvertent modifications of climate. Thus, the potential impact of aircraft emissions on current and future climate of the Earth-atmosphere system has become a serious environmental issue that challenges the aviation industry (e.g., Waitz et al. 2004). In response to this challenge, the NGATS/JPDO and the Partnership for Air Transportation Noise and Emissions Reduction (PARTNER) convened a panel of scientists to participate in a "Workshop on the Impacts of Aviation on Climate Change" in Boston, MA, June 7-9, 2006. The major goal of this workshop was to assess and document the present state of knowledge of the climatic impacts of aviation. A report of findings and recommendations from this workshop was later published (JPDO and PARTNER 2006).

Among the aircraft-emitted greenhouse gases, water vapor contributes to the formation of contrails and cirrus clouds, which effectively transmit solar radiation, but block terrestrial infrared radiation that could produce warming of the Earth-atmosphere system. A contrail or condensation trail is defined by Appleman (1953) as the upper-level ice crystal cloud generated by jet aircraft flying in the upper troposphere and lower stratosphere (UT/LS). Contrails were first observed behind low-flying propeller-driven aircraft in 1915, but have now become a common sight in the skies over the United States and Europe, particularly near airports. They are visible line clouds produced by water vapor emitted from aircraft flying in sufficiently cold air. Emerging from the exhaust of jet engines, water vapor is drastically cooled in the extremely cold environment so that saturation with respect to liquid water can be quickly reached (Schumann 1996). Following the thermodynamic principle as described in Appleman (1953), small water droplets can be formed through heterogeneous nucleation on the emitted soot and sulfuric acid aerosols, which serve as cloud condensation nuclei (CCN). Measurements have shown that saturation with respect to liquid water are usually reached in the fresh plume (age < 0.5 sec) closely behind the aircraft and that contrails would not form if the environment is only ice-saturated (Jensen et al. 1998a; Kärcher et al. 1998; Schumann et al. 2000). Because the environment temperature in UT/LS is generally below  $-40^{\circ}$  C, freshly formed water droplets would then instantly freeze to become contrail ice crystals (Schumann 2002).

In an extremely dry atmosphere, such as the typical condition of UT/LS, contrail ice crystals may not grow to sufficiently large sizes before they undergo complete sublimation. In this case, there would be no visible contrail line behind the aircraft. However, in an adequately moist atmosphere, these ice crystals can continue to grow to a much larger size through water vapor deposition and coalescence processes and become visible at 10-30 m behind the aircraft. In a sub-saturated (with respect to ice) atmosphere, contrail lines only last for a short time period on the order of minutes and these are classified as “short-lived contrails” (Minnis 2002). Two examples of these contrails are shown in **Fig 1 (a)** where a pair of trails forming behind the aircraft gradually dissipated. Some contrails can persist for a much longer time period in an ice-saturated or ice-supersaturated atmosphere and are grouped as “persistent contrails”. In an ice-supersaturated atmosphere, emitted soot particles may serve as ice nuclei (IN) upon which natural ice crystals are formed by means of contact or immersion nucleation (Jensen et al. 1998b). The resulting mixture of contrail and natural ice crystals is classified as “contrail-induced cirrus” (hereafter referred to as “contrail cirrus”). **Figure 1(b)** shows examples of persistent contrail and contrail cirrus. This picture was taken by L. Nguyen, NASA LaRC on January 26, 2001 at eastern Virginia. Distinct crisscrossing persistent contrails are shown along with contrail cirrus at high altitudes and spread to a much wider extent than the younger contrails formed below. No clear-cut age threshold can be detected between short-lived and persistent contrails. Bakan et al. (1994) observed that a group of persistent contrails in the region of flight corridors of heavy air traffic over Europe can merge together and grow into cirrus cloud forms, producing similar radiative characteristics (blocking sunlight) as natural cirrus.

Contrails and contrail cirrus transmit, reflect and absorb the incoming solar radiation and, at the same time, transmit and absorb/emit thermal infrared radiation (Liou 1986). It has been noted that they can directly affect climate through these radiative processes (Murcray 1970; Kuhn 1970; Changnon 1981). The net radiative effects of contrails containing nonspherical ice crystals have not been comprehensively quantified, because their composition and structure are poorly understood (Sassen 1997). Although the coverage of contrails and contrail cirrus ( $\sim 0.1\%$ ) is much smaller compared to the coverage of naturally formed cirrus clouds ( $>20\%$ ), their potential climatic impact nevertheless cannot be ignored, particularly near flight corridors where air traffic is heavy and contrail formations are frequent. **Figure 2(a)** displays an estimated linear contrail coverage over a  $2.8^\circ$  grid resolution based on a parameterization of contrail formation adjusted to match the linear contrails observed from satellites, using air traffic data from 1992 and 10-year global analyses of relative humidity and temperature at selected pressure levels (Sausen et al. 1998; Minnis et al. 2004). Black and white boxes represent the boundaries for the land and ocean air traffic regions, respectively. **Figure 2(b)** shows the geographical distribution of average total contrail cover computed by Gulberg (2003) using the IFSHAM model. The global mean contrail cover determined from this work is  $0.06\%$ , which is somewhat less than the IPCC (1999) estimate of  $0.1\%$ . The geographical distributions of contrail coverage from different numerical models shown in Figs. 2(a) and 2(b) are qualitatively similar and reveal that contrail coverage is largely confined to main flight route and flight frequency. High contrail covers up to  $5\%$  are shown to center around the northern United States and western European metropolitan areas.

Due to numerous factors, including the lack of *in situ* observations and detailed modeling studies, the climatic impact of contrails has not been well understood. In the 1999 IPCC assessment report (IPCC 1999), contrails and their effects have been recognized as one of the largest outstanding uncertainties in the study of air traffic impact on the atmosphere. Moreover, Sausen and Schumann (2007) indicated that even though current civil aviation is only responsible for just  $2\%$  of total anthropogenic  $\text{CO}_2$  emissions, its impact on environment and climate will be a matter of special concern in the context of anthropogenic global warming since aviation is among the fastest growing economic

sectors. It has been stated in a number of assessments (e.g., Shine et al. 1990; Brasseur et al. 1998; Schumann et al. 2001; Ramaswamy et al. 2001; Sausen et al. 2005) that the radiative forcing of current aviation is at least twice as large as the contribution from aircraft CO<sub>2</sub> emissions alone, caused by persistent contrails and contrail cirrus and by the aircraft emitted NO<sub>x</sub>, H<sub>2</sub>O, and particles.

A significant increase in aviation traffic in recent years has resulted in a noticeable increase in the frequency of occurrence of contrails and contrail cirrus. For example, Minnis et al. (2004) showed a trend in cirrus increase by about 0.1%/yr over the continental USA between 1971 and 1995, and attributed it exclusively to the aviation traffic increase during this period. The radiative and climatic effects of contrails and contrail cirrus appear to have become an important subject for scientific research and in public policy domain. Despite a large degree of uncertainty regarding contrail cover and its ice crystal size and shape, the globally and annually averaged radiative forcings have been estimated. For subsonic aircraft emissions, an estimated positive radiative forcing of 0.02 W m<sup>-2</sup> with an uncertainty of more than a factor of two was reported for the year 1992 (IPCC 1999). However, for the year 2000, this number was increased to 0.03 W m<sup>-2</sup> (IPCC 4<sup>th</sup> Assessment Report, Forster et al. 2007). The mean radiative forcing due to contrails is smaller than that produced by tropospheric aerosols. However, the projected increase in future air traffic could cause the direct climatic effects of contrails comparable to those generated by certain types of tropospheric aerosols.

Under the support of the current FAA program, we have undertaken a survey of available literature and relevant information sources via network websites and put together a focused and in-depth overview of the present knowledge and understanding of scientific principles, uncertainties, and requirements in conjunction with the climatic impacts of contrails and contrail cirrus. In this subject-specific white paper (SSWP), we present the results of our literature survey and provide a number of recommendations for future actions that are required to comprehend and determine the climatic impacts of contrail and contrail cirrus. Section 2 contains a review of the current status of the subject, progress that was made since the IPCC 1999 report, the present state of satellite and ground-based remote sensing as well as modeling capabilities, current estimate of the climatic impact of contrails, and interconnectivity with other SSWP areas. Section 3 lists outstanding limitations, gaps and issues that need improvement. Section 4 prioritizes research needs, followed by recommendations for short-term research in Section 5.

## **2. A Review of the Climatic Impacts of Contrail and Contrail Cirrus**

### **a. Current state of the scientific research**

- *Long-term trends in the coverage and frequency of contrail-cirrus and cirrus occurrence.*

The primary concern in studying the climatic effects of contrails has been the record of the long-term trend of contrails and contrail cirrus. There are four primary data sources that can be used to address this question: manual surface observations of cloud cover, meteorological soundings of temperature and humidity profiles, ground-based measurements by active remote sensors, and satellite data. Each source has its limits. Surface manual observations suffer from insufficient geographical coverage and inaccuracy due to subjective judgment. Humidity soundings display a large degree of uncertainty at high-altitude. Ground-based remote sensing is restricted in geographical coverage. Polar-orbiting and geostationary satellite remote sensing instruments are limited by their temporal and spatial resolution and coverage. We note that surface observations have been continuously used for the compilation of contrail statistics. Machta and Carpenter (1971) first reported secular increases in the amount of high cloud cover in the absence of low or middle clouds at a number of midlatitude stations in the United States between 1948 and 1970. Changnon (1981) analyzed records of monthly sky cover, sunshine and

temperature in Midwestern United States (10-state) areas for the period 1901-1977 to discern long-term trends. The sky cover data shows a long-term increase in cloudy days and decrease in clear days since 1901. **Figure 3** displays that for a 10-year increment period, the average cloudy days for the south-central area increase from 112 days during the 1901-1910 period to 172 days for during 1968-1977 period. In a separate report to the National Science Foundation, Changnon et al. (1980) further illustrated that high-cloud cover increased from 1951 to 1976 over many Midwestern cities and theorized that such an increase in high clouds could be due to the increase in commercial air traffic. Seaver and Lee (1987) also found more cloud cover, less sunshine and a decrease in the number of clear days over large regions of the United States since 1936.

Liou et al. (1990) analyzed cirrus-cloud cover over Salt Lake City based on surface observations between 1949 and 1994. In this study, the three-hourly weather observations reported by the National Weather Service at Salt Lake City International Airport were used to determine the sky cover information. For each observation, the cloud amount, which is quantified in tenths of the sky coverage, cloud type and visibility were recorded. **Figure 4** shows the time series of the mean annual high cloud cover and domestic jet fuel consumption. Based on a student-*t* test, the time series of high cloud coverage can be separated into two periods: 1949-1964 (period 1) and 1965-1982 (period 2). The high-cloud covers for periods 1 and 2 are 11.8% and 19.6%, respectively. The average high-cloud cover for period 2 matches the one for 1965-1969 compiled by Machta and Carpenter (1971). In the time series of domestic jet fuel consumption a sharp increase in the mid-60's occurred corresponding to a substantial increase in high-cloud cover. As shown in Fig. 4, increased cirrus cloudiness has also been detected in climate data from other stations in the mid-western and northwestern United States that are located in major upper-tropospheric flight corridors (Frankel et al. 1997). Based on correlation between the trends of cirrus cloudiness and jet fuel consumption, increase in cirrus clouds over the last 50 years could be partially attributed to an increase in air traffic (Study of Man's Impacts on Climate 1971).

Observations in Germany indicated that the frequency of high clouds during sunny hours increased from 45% in 1954 to 70% in 1995. Over the same period, global radiation during sunshine hours decreased by about 10% (Rebetez and Beniston 1998). A similar increase in high-cloud frequency has also been observed for cloudy conditions (Liepert et al. 1994, Liepert 1997). Boucher (1999) analyzed the surface manual observation reports over North America for the period 1982–1991 and found a decadal increase of 5.6% for the entire region and 13.3% over heavy air traffic areas. The author also reported a global trend of 1.7% per decade over land and 6.2% per decade over the oceans.

A comprehensive analysis of jet aircraft contrails over the United States and Europe using satellite infrared imagery was reported in IPCC (1999). In 1992, aircraft line-shaped contrails were estimated to cover about 0.1% of the Earth's surface on the annually averaged basis but with larger regional values (e.g., 0.5% over central Europe between 1996 and 1997). It is anticipated that global contrail coverage will increase by about 0.5% by 2050 (IPCC 1999).

- *Aerosol indirect effects*

Due to the global increase in air traffic, aircraft-emitted water vapor and soot particles mostly composed of black carbon (BC) are continuously infiltrated into the UT/LS, which could cause accelerated increase in contrails and cirrus cloud occurrence. Aerosols affect the atmospheric radiative transfer through their direct interaction with solar radiation (referred to as direct radiative effect) and through their interaction with clouds (referred to as indirect effect). Compared to cloud radiative effect, the aircraft-emitted aerosol direct radiative effect is quite small because of small aerosol optical depth. However, the formation of contrails through heterogeneous ice nucleation processes that involve

aerosols could change the vertical and horizontal distributions of clouds and water vapor amount. Based on satellite remote sensing studies, Seinfeld (1998) theorized that some cirrus clouds in fact evolve from contrails. The increase in cloudiness associated with additional IN and water vapor can lead to a substantial enhancement of cloud radiative effects.

Ice crystals in high clouds can be formed by the homogeneous freezing of solution droplets at temperatures below  $-37^{\circ}\text{C}$ , and by the heterogeneous freezing of insoluble or partially insoluble particles. BC is one of the major IN candidates (Cantrell and Heymsfield 2005). Aircraft-injected BC particles may serve as IN via deposition nucleation. Laboratory studies have shown that the surrogates for IN in the atmosphere are significant contributors to atmospheric heterogeneous IN populations, and that heterogeneous freezing rates increase with particle size under the same thermodynamic conditions (e.g., Archuleta et al. 2005). BC is generally quite hydrophobic, but could become hydrophilic after exposure to sulfuric acid, and therefore can act as immersion IN. DeMott (1990; 1999) showed in the laboratory that soot particles can act as heterogeneous IN at temperatures between  $-25^{\circ}\text{C}$  and  $-40^{\circ}\text{C}$  and below  $-53^{\circ}\text{C}$ . More laboratory data are now becoming available for characterizing ice nucleation on aerosols.

Aerosol indirect effects on the microphysical and radiative properties of cirrus clouds are important for the study of climatic impact of contrails and contrail cirrus, but these effects are complex and difficult to quantify based on a modeling approach (Seinfeld, 1998). Attempts to mechanistically relate aerosols number density to cloud formation in general circulation models have focused on the initiation of warm/liquid clouds. Much less attention has been given to the study of the potential impacts of aerosols on high-altitude ice clouds for the reasons stated above. Parameterizations for homogeneous and heterogeneous ice nucleation have been developed by various researchers (e.g., Kärcher and Lohmann 2002; DeMott et al. 1997; Gorbunov et al. 2000, Kärcher and Lohmann 2003; Liu and Penner 2005; Kärcher et al. 2006). Some significant steps in quantifying the indirect effect from anthropogenic aerosols have been made by using GCMs. For example, Jones et al. (1994) estimated aerosol indirect effect by performing a series of simulations for the annual mean distribution of low-level cloud droplet effective radius at cloud top using the Hadley Center GCM. **Figure 5(a)** shows the global distribution of cloud top effective radius, while **Fig. 5(b)** displays its instantaneous change due to changes from natural-only aerosols to total aerosol concentration. There is a general decrease in effective radius throughout most of the Northern Hemisphere and over most of the land areas, particularly around major industrial regions.

Measurements of BC at the level where ice clouds form have been extremely limited due to the requirement of high flying aircraft and limitation of our understanding of the physical and chemical processes controlling ice formation in the presence of aerosols, particularly heterogeneous ice nucleation (Cantrell and Heymsfield, 2005). An adequate understanding of aerosol-cirrus cloud interaction must be derived from *in situ* microphysical measurements. However, it is difficult to isolate and quantify aerosol indirect effects based solely on *in situ* observations, because of measurement uncertainties and sampling considerations, as well as a separation of these effects from the natural variability of meteorological conditions.

In view of various problems encountered in the quantification of aerosol indirect effects based on direct *in situ* observations, an alternative approach to study the aerosol-cirrus and contrail-cirrus indirect effects is through satellite observations of ice clouds and aerosols, making use of an extensive suite of space-based instruments that are currently available along with collocated and coincident *in situ* aerosol measurements. These observations contain rich and valuable information that can be used to investigate the relationship between aerosols and ice cloud formation. Along this line, correlation of the MODIS

observed ice crystal effective radius and the level of aerosol loading during the Indian Ocean Experiment (INDOEX) revealed a significant aerosol impact on ice cloud particle size (Chýlek et al. 2006).

- *Microphysical and radiative properties of contrails and contrail cirrus*

The radiative forcings of contrails and contrail cirrus depend on their optical properties, which are in turn a function of the ice crystal size and shape distributions. Because *in situ* observations on contrails have been limited, their microphysical properties are largely unknown. Following is a summary of findings based on available *in situ* microphysical measurements. Knollenberg (1972) first used an optical-array spectrometer on board NCAR Sabreliner aircraft and made *in situ* microphysical measurements of ice crystal size distribution, *IWC*, and total ice water budget within its own contrails and the resulting cirrus uncinus clouds. He found that, like cirrus clouds, the *IWC* of contrails depends on temperature, humidity, vertical velocity of air, fall out of ice crystals, and possibly radiative cooling. Konrad and Howard (1974) provided an insightful morphology of contrail cirrus and fallstreaks as viewed by ultra-sensitive radars. From the late 70's to the early 90's, high-altitude *in situ* observations mostly focused on natural cirrus clouds.

In 1996, the Subsonic Aircraft Contrail and Cloud Effects Special Study (SUCCESS) field campaign carried out over Kansas during a 5-week period (April 8-May 10, 1996) provided unique microphysical measurements of the size and shape characteristics of ice crystals that were not previously available. SUCCESS used scientifically-instrumented aircraft and ground-based measurements to investigate the effects of subsonic aircraft on contrails, cirrus clouds and atmospheric chemistry (Toon and Miake-Lye 1998). Airborne platforms used during SUCCESS include a medium-altitude DC-8 and a high-altitude ER-2, both of which were based at the NASA Ames Research Center, Moffett Field, California and a T-39 aircraft based at the NASA Wallops Flight Facility, Wallops Island, Virginia. During the SUCCESS observation period, all three NASA aircraft were deployed at the Salina campus of Kansas State University. A series of flights, averaging one every other day during this period, were made near the ARM-SGP site. Flights were also made over the Gulf of Mexico to utilize an oceanic background for remote sensing measurements. In order to achieve experimental objectives, the DC-8 aircraft was used as an *in situ* sampling platform, carrying a wide variety of instruments for sampling gases and particulate matters, and radiometric measurements. Major cloud microphysics measurement instruments included a multi-angle aerosol spectrometer probe (MASP, Baumgardner et al. 1995), a video ice particle sampler (VIPS, Heymsfield and McFarquhar 1996), a cloudscope (Arnott et al. 1995), a Pi-Nephelometer (Lawson et al. 1998), and a FSSP. The T-39 aircraft was used primarily to sample the exhaust from other aircraft. It also carried a suite of instruments to measure particles and gases. The ER-2 aircraft carried the MODIS Airborne Simulator, which was used as a surrogate for MODIS, so that remote sensing observations could be related to the *in situ* parameters measured by the DC-8 and the T-39.

Based on analysis of the data gathered during SUCCESS, Heymsfield et al. (1998) examined the evolution of contrails to precipitation trails using the data collected from various instruments, including PI, VIPS, and a PMS 2D-C imaging probe with a lower detection limit between 50 and 100  $\mu\text{m}$ . Goodman et al. (1998) used an impaction technique to sample ice crystals in the exhaust trail of a Boeing 757, and found that ice crystals in the contrail of about 1 minute old had a unimodal size distribution, with an equivalent volume radius of less than 10  $\mu\text{m}$  and an effective radius of about 2  $\mu\text{m}$ . The crystal habits at the observed temperature of  $-61^{\circ}\text{C}$  were predominantly hexagonal plates (75%), columns (20%) and few triangular plates (<5%). Lawson et al. (1998) sampled a persistent contrail generated by the DC-8 during SUCCESS and found that, after 40 minutes, the core of the contrail

consisted of mostly small particles ( $L = 1 - 20 \mu\text{m}$ ) with a concentration larger than  $1000 \text{ l}^{-1}$ , but the concentration of large particles ( $L > 300 \mu\text{m}$ ) was less than  $10^{-6} \text{ l}^{-1}$ . In contrast to the core, the contrail boundary consisted of one order-of-magnitude less small particles, but three order-of-magnitudes more large particles with the shape of columns and bullet rosettes that are typically found in natural cirrus.

In the area of lidar observations of contrail microphysics, Freudenthaler et al. (1996a) found that strong depolarization produced by contrails containing growing particles a few minutes old revealed nonspherical shaped particles. Sassen and Hsueh (1998) analyzed the data from a ground-based polarization lidar during SUCCESS to study contrails and cirrus clouds evolved from contrails. They found that contrail-cirrus is distinctively different from natural cirrus clouds. Contrail-cirrus tends to be thin ( $\sim 50 - 500 \text{ m}$ ) and can generate coronas indicative of long-lasting small ( $20 - 30 \mu\text{m}$ ) particles. Jensen et al. (1998c) conducted a case study of the persistent contrail evolution in a sheared environment by simulating contrail evolution using a large-eddy simulation model with detailed ice microphysics. Simulation results were compared to satellite and *in situ* measurements of the persistent contrails inferred from the SUCCESS experiment. Using large ambient super-saturations and moderate wind shear in simulation, ice crystals with maximum dimensions greater than  $200 \mu\text{m}$  were generated within 45 minutes after emission by depositional growth.

- *Radiative forcing for persistent contrails and contrail cirrus*

Aircraft emission of water vapor and particles, as well as the creation of contrails, could lead to a change in global cloudiness. A number of atmospheric GCM studies that investigated the impacts of injecting water vapor on creating contrails (e.g., Ponater et al. 1996; Rind et al. 1996) also illustrated the potential importance of these impacts on climate. Persistent contrails are detectable both by surface observation and satellite remote sensing, and their impact on radiative forcing can be evaluated. Fahey et al. (1999) presented the 1992 IPCC estimate of direct radiative forcing from persistent contrails of about  $+0.02 \text{ W m}^{-2}$  with a range of uncertainty from  $+0.005$  to  $+0.06 \text{ W m}^{-2}$ . This estimate is limited to immediately visible, quasi-linear persistent contrails. The radiative forcing associated with contrail formation is a consequence of aircraft activity, and its impact on climate can be directly estimated by various measurement techniques and modeling approaches. Cirrus clouds generally exert a net positive radiative forcing as a result of the domination of longwave greenhouse effect relative to solar albedo effect. Fahey et al. (1999) reported that the 1992 IPCC estimate of the radiative forcing from aircraft-induced cirrus clouds is positive and may be comparable to contrail radiative forcing. The magnitude of this radiative forcing remains very uncertain. A range for the best estimate of the globally averaged radiative forcing due to contrails could fall between 0 and  $0.04 \text{ W m}^{-2}$ .

The importance of contrails in changing regional and global radiation budgets has been assessed in several modeling studies. Using a one-dimensional radiative transfer model along with specified contrail microphysical properties and atmospheric conditions, Fortuin et al. (1995) estimated that, with 0.5% cloudiness, contrails may produce a radiative forcing at the top of atmosphere (TOA) of  $-0.15$  to  $0.3 \text{ W m}^{-2}$  for the Atlantic flight corridor. Minnis et al. (1999) calculated the TOA radiative forcing for the year 1992 with a similar approach and found a net global radiative forcing of  $0.01 \text{ W m}^{-2}$ . The radiative forcing for heavy air traffic regions is much higher with maximum values reaching  $0.71 \text{ W m}^{-2}$  over northern France and  $0.58 \text{ W m}^{-2}$  near New York City. Contrails have important effects on regional climate and for the time period when the upper atmosphere is saturated or supersaturated with respect to ice. Moreover, Fortuin et al. (1995) and Strauss et al. (1997) suggested that the maximum instantaneous radiative forcing directly under a contrail, assuming 100% contrail cover, could have values from  $-30 \text{ W m}^{-2}$  to  $60 \text{ W m}^{-2}$ . Such a large radiative forcing could lead to a change in the surface temperature by a few degrees K. Strauss et al (1997) also found that an additional 0.5% contrail cover could cause a

warming of 0.05K. Thus, although the global mean magnitude of radiative forcing produced from contrails is relatively small, as compared to the estimated anthropogenic greenhouse effect, contrails could have a significant impact on regional climate.

- *Climatic impacts of contrails and contrail cirrus*

Non-black, semi-transparent high cirrus clouds are known to produce surface warming, and warming in the lower troposphere caused by the thermal IR fluxes emitted from the cloud. The degree and extent of warming are controlled by the cloud's radiative property and its physical position in the atmosphere as well as feedbacks associated with thermodynamic processes involving cloud formation. Earlier model simulation results show that high clouds above about 8 km produce a warming effect at the surface: the degree of this warming is a function of cirrus cloud optical depth (or emissivity) (Freeman and Liou 1979; Liou and Gebhart 1982). Research efforts pertaining to cirrus clouds and climate have been comprehensively reviewed by Liou (1986) and Liou (2005), both of which also pointed out the importance of cirrus formation from contrails.

Grassl (1990) presented the importance of contrails in the upper troposphere and additional water vapor in the lower stratosphere in conjunction with the radiation budget of the Earth-atmosphere system. Liou et al. (1990) specifically studied the climatic effects of contrail-cirrus by using a two-dimensional cloud-climate model, in view of the fact that the increase in contrail-cirrus has been primarily confined to midlatitudes. This model was a combination of a two-dimensional energy balance climate model (Liou and Ou 1981, 1983, Ou and Liou 1984) and an interactive cloud formation model (Liou et al. 1985) that generates cloud cover and liquid water content based on thermodynamic principles. The effects of contrail cirrus cover on cloud formation and temperature field were investigated by increasing the cloud cover between 20 and 70°N, roughly corresponding to the location of most jet aircraft traffic. A 5% increase in high-cloud cover leads to a substantial amplification in high-cloud cover increase (15%) at 20- 40°N, caused by an increase in specific humidity. Low and middle clouds also increase slightly because of the additional moisture supply. Overall, enhanced downward thermal IR emission from additional high clouds causes a temperature increase in the troposphere of the lower latitudes. **Figure 6** shows zonally mean changes in atmospheric and surface temperatures due to increases in high cloud cover of (a) 5%, and (b) 10%. For both experiments, there is a maximum temperature increase in the lower troposphere of the tropics due to a significant increase of humidity in that region. This is in contrast to the results simulated from fixed relative humidity and non-interactive cloud cover, in which the maximum temperature increase occurs in the polar region. Hansen et al. (2005) also produced the maximum temperature increase in the lower troposphere of the tropics for a 4xCO<sub>2</sub> experiment using the GISS GCM. Temperature increases above 5 km are generally reduced with increasing height. The surface albedo feedback effects are also substantially reduced. The temperature increase due to a 5% increase of cloud cover under the condition of interactive cloud cover is less than that of fixed cloud cover, because of the increase in low and middle cloud covers in the former experiment. A 10% increase in high-cloud cover in the perturbation experiment shows a temperature increase of more than a factor of two (relative to a 5% increase in cloud cover) in the troposphere, because additional high clouds are formed due to the humidity feedback effect. In the case of a 5% increase in high-cloud cover, surface temperature increases by about 1 K, but varies with latitude. When the increase in high clouds was doubled, a surface temperature increase of about 2.5 K was obtained in the experiment. In summary, all perturbation experiments involving high-cloud cover increase indicate increases in atmospheric and surface temperature caused by a positive greenhouse feedback from cloud cover and specific humidity.

## **b. Critical roles of contrail and cirrus clouds in climate processes**

Persistent contrails, contrail cirrus, and natural cirrus clouds formed in UT/LS play a significant role in regulating the radiation balance of the Earth-atmosphere system, and so their presence must be recognized as a crucial component in understanding the inadvertent human-induced climate change problem (Liou 1986). Short-lived contrails are not expected to have significant impacts on climate change due to their extremely small coverage and relatively short durations of existence. Persistent contrail and cirrus cloud temperatures are low ( $< -20^{\circ}\text{C}$ ), and many of them are composed of irregularly shaped ice crystals. Because of their high altitude and cold temperature, they can act as a thermal blanket by absorbing (and therefore trapping) the upward thermal infrared radiation emitted and transmitted from below the cloud, the same as the “greenhouse effect”, which warms the Earth-atmosphere system. At the same time, these clouds can also reflect the incoming solar radiation referred to as the “solar albedo effect”, which serves to cool down the Earth-atmosphere system. Balance between these competing radiative effects determines the net impact of high clouds on our climate system. The relative importance of the greenhouse vs. albedo effect is dependent on the cloud microphysical and optical properties of clouds (Ackerman et al. 1988; Stephens et al. 1990; Fu and Liou 1993; Ou and Liou 1995), which in turn are governed by atmospheric circulation and water vapor distribution.

In summary, the major issue is whether increase in cirrus clouds related to increasing jet air traffic would enhance or suppress the global warming produced by the build-up of carbon dioxide and other greenhouse gases. Another important issue is whether there are other unknown mechanisms that might have contributed to a global increase in cirrus clouds in recent years. Resolving these issues is vitally important to planning future air traffic operation.

## **c. Progress since the IPCC 1999 report**

- *Long-term trends in the coverage and frequency of contrail-cirrus and cirrus occurrence.*

Chen et al. (2001) estimated contrail occurrence frequency over the Taiwan area based on flight frequency and meteorological data, and found that contrails form more frequently in winter and spring than in summer. Zerefos et al. (2003) examined changes in cirrus-cloud cover in association with aviation activities at busy air traffic corridors based on the ISCCP data set covering the period 1984 – 1998. The results show increasing trends in cirrus-cloud cover between this period over the air traffic corridors of North America, North Atlantic Ocean, and Europe. Minnis et al. (2003) used two years of data from surface observers at 22 military installations scattered over the continental United States to estimate mean hourly, monthly, and annual frequencies of daytime contrail occurrence. During both years, persistent contrails were most prevalent in winter and early spring, but less frequent during summer and occurred simultaneously with cirrus clouds 85% of the time. Although highly correlated with the air traffic fuel consumption, contrail occurrence is also governed by meteorological conditions. Minnis et al. (2004) further collected and analyzed surface observations from 1971 to 1995 and showed that cirrus clouds increased significantly over the northern hemisphere oceans and the United States, while decreasing over other land areas except over Western Europe, where cirrus coverage was relatively constant. It was pointed out that surface observations are consistent with satellite-derived trends over most areas and that it is most likely that the cirrus trends in the U. S. are correlated with air traffic. The cirrus increase is a factor of 1.8 greater than that expected from the current estimate of linear-contrail coverage, suggesting that a spreading factor of the same magnitude could be used to estimate the maximum contrail effect.

Wylie et al. (1994, 1999, 2005) used NOAA High Resolution Infrared Radiometer Sounder (HIRS) polar-orbiting satellite data from 1979 to 2001, a 22-year record, to determine the frequency of detected high cloud in the upper troposphere (**Fig. 7**). The CO<sub>2</sub> slicing method was used to infer cloud amount and height. They estimated that thin cirrus ( $\tau < 0.7$ ) covers about 20% in the mid-latitude region and over 50% in the tropics. High clouds show a small but statistically significant increase in the Tropics and the Northern Hemisphere. The HIRS analysis differed from the International Satellite Cloud Climatology Project (ISCCP, Rossow and Schiffer), which shows a decrease in both total cloud cover and high clouds during most of the 22-year period.

Schumann (2005) presented the formation, occurrence, properties, and climatic effects of contrails. The global cover by lined-shaped contrails and their radiative impact is smaller than that assessed in an international assessment in 1999. To help alleviate uncertainty in the air traffic contribution to cirrus increase, Minnis et al. (2005) analyzed linear contrail coverage over the North Pacific Ocean using the NOAA-16/AVHRR data during a 4-month period in 2002 and 2003. Manual evaluation of the automated contrail detection method revealed that it misclassified, on average, 32 % of the pixels as contrails and missed 15 % of contrail pixels. After a correction for detection errors, the contrail coverage over the domain between 25° and 55°N and between 120° and 150°W varied from a minimum of 0.37 % in February to a maximum of 0.56 % in May. The annual mean coverage, after correcting for the diurnal cycle of air traffic, is 0.31 %, a value very close to earlier theoretical estimates for the region. The average contrail optical depth is 0.24, corresponding to a mean longwave radiative forcing of 14.2 W m<sup>-2</sup>.

Duda et al. (2003, 2005) estimated contrail frequency and coverage over the contiguous United States (CONUS), using hourly meteorological analyses from the Rapid Update Cycle (RUC) numerical weather prediction model and commercial air traffic data for a 2-month period during 2001. The contrail frequency over the CONUS was computed directly from RUC analyses using several modified forms of the classical Appleman criteria for persistent contrail formation. Various schemes for diagnosing contrails from the RUC analyses were tested. Palikonda et al. (2005) derived linear contrail coverage, optical depth, and longwave radiative forcing from NOAA-15 and NOAA-16 daytime AVHRR data over CONUS, southern Canada, northern Mexico, and the surrounding oceans. Contrail coverage averaged 1.17% and 0.65% based on the early-morning NOAA-15 and mid-afternoon NOAA-16 observations, respectively, for the areas and times common to both satellites. The estimated combined maximum coverage for the entire domain was ~1.05% during February, while a minimum of 0.57% occurred during August. The annual mean optical depth is 0.27, while the monthly value varied by ~20% with minima and maxima in winter and summer, respectively. Marquart et al. (2003) used a contrail parameterization in the ECHAM GCM to estimate future contrail coverage. Time slice simulations showed increase in the global annual mean contrail cover from 0.06% in 1992 to 0.14% in 2015 and to 0.22% in 2050. In the northern extratropics, the enhancement of contrail cover is mainly determined by aviation growth, but in the tropics, contrail cover appears to be affected by climate change.

Meyer et al. (2007) presented the contrail coverage over Thailand, Japan and the surrounding area through remote sensing observations. Locally received NOAA/AVHRR satellite data were analyzed by a fully automated contrail detection algorithm. The annual average of the daily mean contrail coverage is 0.13% and 0.25% for the Thailand and Japan regions, respectively, with a maximum value during spring for both regions. Travis et al. (2007) reported a contrail mid-season climatology for the coterminous United States (2000–2002) based on AVHRR data, US jet aircraft flight activity log, and NCEP-NCAR

reanalysis data at the tropopause level, and compared the frequencies with those previously reported for an earlier period (1977–1979) to determine spatial and seasonal contrail frequency changes.

- *Radiative forcing of contrails and cirrus clouds*

Meerkötter et al. (1999) used three different radiative transfer models and six model atmospheres (McClatchy et al. 1972) to study the instantaneous radiative impacts of contrails and found that a mean contrail cover of 0.1% with average optical depths of 0.2–0.5 would produce about 0.01–0.03 W m<sup>-2</sup> daily mean radiative forcings. Duda et al. (2001) used GOES data to study the evolution of solar and longwave radiative forcings in contrail clusters over Midwestern US, Eastern US, Atlantic Ocean, and Hawaii. They showed that observed radiative forcings are less than those from model simulations. Marquart et al. (2003) estimated increase in the global annual mean radiative forcing from 3.5 mW m<sup>-2</sup> in 1992 to 9.4 mW m<sup>-2</sup> in 2015 and to 14.8 mW m<sup>-2</sup> in 2050. Uncertainties in contrail radiative forcing mainly arise from uncertainties in the microphysical and optical properties such as particle size and shape and optical depth. Sausen et al. (2005) provided an estimate of the various contributions to radiative forcing (RF) from aviation based on results from the TRADEOFF project that was an update of the IPCC (1999). The new estimate of the total RF from aviation for 2000 is approximately the same as that of the IPCC's estimate for 1992 as a consequence of the reduced contrail RF that compensates for the RF increase due to increased aviation traffic from 1992 to 2000. The RF from other aviation-induced cirrus clouds might be as large as the present estimate of the total RF (without cirrus). However, our present knowledge on these aircraft-induced cirrus clouds is too limited to provide a reliable estimate of the associated RF.

Palikonda et al. (2005) derived longwave RF from NOAA-15 and NOAA-16 daytime AVHRR data over the CONUS, southern Canada, northern Mexico, and the surrounding oceans. The annual mean optical depth of 0.27 translated to a normalized contrail longwave RF of 15.5 W m<sup>-2</sup>. The overall daytime longwave RF for the domain is 0.11 W m<sup>-2</sup>. The normalized longwave RF peaked during summer, while the overall forcing was at a maximum during winter because of greater contrail coverage. Given the U.S. results and using mean contrail optical depths of 0.15 and 0.25, Minnis et al. (2004) estimated that the maximum contrail–cirrus global RF is 0.006–0.025 W m<sup>-2</sup>, depending on the radiative transfer model used in the calculations. Using contrail results simulated from a GCM, the cirrus trends over the United States are estimated to generate a tropospheric warming of 0.2°–0.3°C/decade. It is noted that the observed tropospheric temperature trend is 0.27°C/decade between 1975 and 1994. The magnitude of the estimated surface temperature change and the seasonal variation of the estimated temperature trends are in general agreement with observations.

#### **d. Present state of measurements and data analysis**

- *Contrail and cirrus climatology based on analyses of surface and satellite observations*

Minnis et al. (2004) demonstrated that global satellite remote sensing can provide long-term climatology datasets for contrails, contrail cirrus, and natural cirrus clouds. However, conventional sensors on the present NASA and NOAA satellites have had difficulty in detecting optically thin cirrus with an optical depth smaller than about 0.1 (Roskovensky and Liou 2003; 2005). A substantial amount of surface data for cloud classification near major airports exists. It appears that analysis of this data, albeit local, could be complementary to satellite observations. To support aviation operation and climate change, one can compile long-term cloud climatology similar to that shown in **Fig. 3** for contrails, contrail cirrus, and natural cirrus near major airport areas using current and future satellite data in combination with surface observations.

Duda et al. (2007) described a comprehensive data archive of surface contrail observations collected by the Global Learning and Observations to Benefit the Environment (GLOBE) program. A primary goal of the GLOBE program is to use detailed written protocols to enable student observers to provide scientifically valuable measurements of environmental parameters (Brooks and Mims 2001). In May 2003, GLOBE initiated a contrail observation protocol to classify observations of contrail occurrence and coverage throughout the CONUS from primary and secondary schools across the country. (See [www.globe.gov](http://www.globe.gov)). Over 18,500 observations were reported over the region between April 1, 2004 and June 27, 2005, including contrail coverage, contrail number, cloud coverage, cloud type and a classification of contrails into three categories: short-lived, non-spreading persistent contrails, and spreading persistent contrails.

- *Satellite remote sensing of contrails and cirrus clouds*

Satellite remote sensing of contrails can provide objective measures to determine the cloud cover induced by contrails globally. High resolution infrared satellite images often provide revealing patterns of contrails, while corresponding visible images are less clear (Joseph et al. 1975; Lee 1989). Carleton and Lamb (1986) showed that the occurrence of contrails can be determined by DMSP high-resolution visible bands (0.6 km) and infrared bands (1.0 km). From a pilot study, they found that contrails tend to occur frequently in association with natural cirrus clouds and tend to cluster in groups. Duda and Minnis (2002) reported GOES results for dissipating contrails over southeast Virginia and Chesapeake Bay. Duda et al. (2004) examined the development of widespread persistent contrails over the western Great Lakes on October 9, 2000 using the GOES data. Table 1 summarizes the current and future satellite observations that are relevant to the remote sensing of contrails and cirrus clouds. A more detailed description of each instrument follows.

(i) *Advanced Very High Resolution Radiometer (AVHRR)*. The AVHRR has been onboard NOAA polar-orbiting satellites for a number of years. It is a radiation-detection imager that can be used for remotely determining cloud cover and surface and cloud temperatures. The latest instrument version was the 6-channel AVHRR/3 on board NOAA-15 launched in May, 1998. The AVHRR/3 is an imaging system in which a small field-of-view (1.3 milliradians by 1.3 milliradians) is scanned across the Earth from one horizon to the other by a continuous 360 degree rotation of a flat scanning mirror. There are 1.362 samples per IFOV (instantaneous field-of-view). A total of 2048 samples are obtained per channel per Earth scan covering the area from the scan angles of  $\pm 55.4^\circ$  with reference to the nadir. The channel characteristics of AVHRR/3 are as follows: Ch.1 ( $\lambda = 0.58 - 0.68 \mu\text{m}$ , for daytime cloud and surface mapping), Ch.2 ( $\lambda = 0.725 - 1.00 \mu\text{m}$ , for characterizing land and water), Ch.3A ( $\lambda = 1.58 - 1.64 \mu\text{m}$ , operating only during daytime for detecting snow and ice); Ch.3B ( $\lambda = 3.55 - 3.93 \mu\text{m}$ , operating only during nighttime for nighttime cloud mapping and sea-surface temperature), Ch. 4 ( $\lambda = 10.3 - 11.3 \mu\text{m}$ , for nighttime cloud mapping and sea-surface temperature), and Ch.5 ( $\lambda = 11.5 - 12.5 \mu\text{m}$ , for sea-surface temperature).

(ii) *High Resolution Infrared Radiation Sounder (HIRS)*. The HIRS instrument has also been onboard NOAA polar-orbiting satellites and provides multispectral data from 1 visible channel (0.69  $\mu\text{m}$ ), 7 shortwave channels (3.7-4.6  $\mu\text{m}$ ) and 12 longwave channels (6.7-15  $\mu\text{m}$ ) using a single telescope and a rotating filter wheel containing 20 individual spectral filters. The IFOV for each channel is approximately  $0.7^\circ$  which, from a spacecraft altitude of 833 km, encompasses a circular area of 10 km at its nadir on the Earth. It is almost impossible for HIRS to detect contrails because of the large footprint, but the CO<sub>2</sub> slicing method applied to HIRS data appears to be capable of estimating the effective emissivity and temperature of cirrus clouds that are within the HIRS footprint.

(iii) *Geostationary Operational Environmental Satellites (GOES)/Imager*. GOES satellites are located around a fixed position above the Earth and provide continuous monitoring of about 1/3 of Earth's spherical surface. The geosynchronous plane is about 35,800 km (22,300 miles) above the Earth. The GOES I-M Imager is a 5-band (1 visible, 4 infrared) imaging radiometer designed to sense radiant and solar reflected energy from sampled areas of the Earth. The channel characteristics of GOES Imager are as follows: Ch.1 ( $\lambda = 0.55 - 0.75 \mu\text{m}$ , Instantaneous Geographic Field of View at nadir (IGFOV) = 1 km, for daytime cloud and surface mapping), Ch.2 ( $\lambda = 3.8 - 4 \mu\text{m}$ , IGFOV = 4 km, for characterizing land and water), Ch.3 ( $\lambda = 6.5 - 7 \mu\text{m}$ , IGFOV = 8 km, for measuring precipitable water); Ch. 4 ( $\lambda = 10.2 - 11.2 \mu\text{m}$ , IGFOV = 4 km, for nighttime cloud mapping and sea-surface temperature), and Ch.5 ( $\lambda = 11.5 - 12.5 \mu\text{m}$ , IGFOV = 4 km, for sea-surface temperature). Compared to AVHRR, the GOES IR Imager's spatial resolution is lower, and thus it is not ideal to detect fresh and short-lived contrails. As demonstrated by Minnis et al. (1998), however, this imager can be of some use for detecting persistent contrails and contrail-cirrus.

Table 1. Current and future satellite observations for remote sensing of contrails and cirrus clouds

Satellite Instrument	Measurements relevant to contrails and cirrus
NOAA/AVHRR	Detection of contrail and cirrus clouds, aerosol and cirrus cloud optical depths, ice crystal effective radius, cloud-top parameters
NOAA/HIRS	Detection of cirrus clouds, cloud effective emissivity and cloud-top pressure
GOES/Imager	Detection of contrail and cirrus clouds, aerosol and cirrus cloud optical depths, cloud-top parameters
Terra/Aqua/MODIS	Detection of contrail and cirrus clouds, aerosol and cirrus cloud optical depths, ice crystal effective radius, cloud-top parameters
CALIPSO	Aerosol and cloud vertical profiles
CloudSat	Vertical profile of IWC
IceSat/GLAS	Vertical Structure of Cloud
Terra/MISR	Aerosol optical depth and height
NPOESS (NPP)/VIIRS	Detection of contrails and cirrus clouds, Aerosol and cirrus cloud optical depths, ice crystal effective radius, cloud-top parameters
JMA/MTSAT-1R/Imager	Detection of contrails and cirrus clouds
EUMESAT/ESA/Meteosat-9/Imager	Detection of contrails and cirrus clouds
EUMESAT/ESA/Metop/AVHRR	Detection of contrail and cirrus clouds, aerosol and cirrus cloud optical depths, ice crystal effective radius, cloud-top parameters

(iv) *Moderate Resolution Imaging Spectroradiometer (MODIS)*. The MODIS has been on both Terra and Aqua satellites that were launched in December, 1999 and May, 2001, respectively. Both Terra and Aqua are in sun-synchronous polar orbits with daytime equator crossings at 10:30 am and 1:30 pm LTC, respectively. Aqua is the leading platform of the NASA A-Train, a constellation of polar-orbiting satellite platforms flying in formation. MODIS has a  $1 \text{ km}^2$  IFOV mapping to a swath of approximately 2330 km to achieve near complete global coverage every day. The MODIS cloud product contains both physical and radiative cloud properties, including cloud mask, cloud-particle phase (ice vs. water, clouds vs. snow), cloud-top temperature/pressure/height, effective cloud-particle radius, and cloud optical depth. Because of high spatial resolution and multi-spectral-band characteristics, MODIS can be effectively used to detect contrails and contrail cirrus. Terra/MODIS and Aqua/MODIS now have 8- and 5-year datasets, respectively, but a systematic compilation of contrail statistics using MODIS data has not yet been conducted.

(v) *CloudSat and Cloud-Aerosol Lidar and Infrared Pathfinder Satellite Observation (CALIPSO)*. Both CloudSat (Stephens et al. 2002) and CALIPSO (Winker et al. 2004) were launched on 28 April 2006. In the A-Train, CloudSat and CALIPSO lag Aqua by 1 to 2 minutes and are separated from each other by 10 to 15 seconds. The close proximity between these two platforms offers a unique opportunity for almost exact collocated and coincident observations of global cloudy areas. CloudSat's sensor consists of a 94 GHz radar referred to as the cloud profiling radar (CPR). With a sampling rate of 6 profiles/sec, the CPR generates a vertical profile for every 1.1 km along the flight track. Each profile has 125 vertical "bins", while each bin is about 240 m thick. The footprint covers a rectangular area of 1.4 km by 2.5 km. The backscattering reflectivity measurements from CloudSat/CPR provide the cloud liquid and ice water content profiles, with a 500-m vertical resolution from the surface to 30 km along with an effective FOV of  $1.4 \text{ (across track)} \times 3.5 \text{ (along track)} \text{ km}^2$ . The CALIPSO is equipped with a dual-wavelength (532 nm and 1064 nm) polarization sensitive lidar. Its vertical and horizontal resolutions are 30-60 m and 333 m, respectively. It will provide the vertically-resolved information on aerosol distribution, extinction coefficient, hydration state, and discrimination of large and small particles. It will also offer an improved cloud masking of aerosol data and the opportunity to assess possible aerosol biases in cirrus cloud detection. Because of the cross-track coverage of CALIPSO and CloudSat, search for contrails using both instruments would be limited.

(vi) *Ice, Cloud, and land Elevation Satellite (ICESat)/ Geoscience Laser Altimeter System (GLAS)*. ICESat is the benchmark Earth Observing System mission for measuring ice sheet mass balance, cloud and aerosol heights, as well as land topography and vegetation characteristics. The GLAS onboard ICESat is a diode-pumped Q-switched Nd:YAG laser operating in the near infrared (1064 nm) and visible (532 nm) wavelengths. It is a facility instrument designed to measure ice-sheet topography and associated temporal changes, as well as cloud and atmospheric properties. Dessler et al. (2006a, b) have used GLAS data to produce global statistics of thin cirrus and cloud-top height.

(vii) *Multi-angle Imaging SpectroRadiometer (MISR)*. The MISR sensor is aboard the Terra satellite. This instrument has the unique capability to determine the altitude of aerosol layers in the atmosphere. The MISR sensor uses nine cameras pointed at fixed angles to observe reflected and scattered sunlight. In each of the nine MISR cameras, images are obtained in four spectral bands corresponding to four different colors: blue, green, red, and near-infrared. The center wavelength of each of these bands is 446, 558, 672, and 867 nm. The FOV is  $17.6 \times 17.6 \text{ km}^2$  and the return period is 9 days. Validation of the MISR aerosol optical depth data over North America using AERONET has shown that the products from this instrument are of high quality and unbiased. The aerosol layer height can also be derived from MISR data. MISR aerosol products can be used for the quantitative detection of aerosol indirect effect on cirrus cloud formation.

(viii) *National Polar-orbiting Operational Environmental Satellite System (NPOESS)/Visible-Infrared Imager-Radiometer Suites (VIIRS)*. The VIIRS is being developed as a part of the NPOESS platform to satisfy the operational requirements for the global remote sensing of atmospheric and surface properties. Its design is similar to MODIS in terms of spectral characteristics, but has a smaller number of spectral image bands (16). One of the prime applications of VIIRS channels would be the remote sensing of cloud properties, including optical depth, particle size, cloud-top temperature, cloud cover/layers and cloud height, termed as cloud environmental data records. The first VIIRS onboard the NPOESS Preparatory Platform (NPP) is scheduled for launch in the 2009 time frame.

(ix) *Multi-functional Transport Satellite (MTSAT)*. The MTSAT-1R is a geostationary platform operated by the Japan Meteorological Agency to fulfill meteorological and aviation functions covering East Asia, Western Pacific Ocean, and Australia. The geosynchronous plane is about 35,800 km (22,300 miles) above the Earth at 135° E, 140° E (the operational position for meteorological function) or 145° E. The MTSAT-1R Imager is a 5-band (1 visible and 4 infrared) imaging radiometer designed to sense radiant and solar reflected energy from sampled areas of the Earth. The channel characteristics of GOES Imager are as follows: VIS ( $\lambda = 0.55 - 0.9 \mu\text{m}$ , Instantaneous Geographic Field of View at nadir (IGFOV) = 1 km), IR1 ( $\lambda = 10.3 - 11.3 \mu\text{m}$ , IGFOV = 4 km), IR2 ( $\lambda = 11.5 - 12.5 \mu\text{m}$ , IGFOV = 4 km); IR3 ( $\lambda = 6.5 - 7 \mu\text{m}$ , IGFOV = 4 km), and IR4 ( $\lambda = 3.5 - 12.5 \mu\text{m}$ , IGFOV = 4 km).

(x) *Meteosat-9*. The Meteosat Second Generation 2 (MSG-2) is a geostationary platform operated by the European Organisation for the Exploitation of Meteorological Satellites (EUMETSAT) and the European Space Agency, renamed as Meteosat-9 after its launch on 21 December 2005. Its purpose is to monitor the atmospheric and surface condition over Europe, Africa, and Eastern Atlantic Ocean. The geosynchronous plane is about 35,800 km (22,300 miles) above the Earth at 0° Longitude. The Meteosat-9 carries the Spinning Enhanced Visible and InfraRed Imager (SEVIRI), a 12-band spectro-radiometer imaging suite. The 12 bands are: 1 High Resolution Visible band, 3 visible bands ( $\lambda = 0.6, 0.8$  and  $1.6 \mu\text{m}$ ) and 11 IR bands ( $\lambda = 3.9, 6.2, 7.3, 8.7, 9.7, 10.8, 12.0$  and  $13.4 \mu\text{m}$ ).

(xi) *Metop-A*. This is the first of three satellites of the EUMETSAT Polar System (EPS), launched on 19 October 2006, and was operational on 15 May 2007. The Metop-A is a polar orbiter with the equator-crossing time at 0930 LTC. It carries the US-made AVHRR (see (i) for details).

- *Satellite remote sensing techniques applicable to contrails and cirrus clouds*

A number of satellite remote sensing techniques have been developed to detect the presence of contrails and cirrus clouds, and to retrieve their microphysical and optical properties. The detection/retrieval products can be further applied to determine the aerosol indirect effect on cirrus cloud formation. Table 2 summarizes these remote sensing techniques. A more detailed description of each instrument follows.

(i) *AVHRR Split-window Pattern Recognition*. Schumann and Wendling (1990) introduced a pattern recognition method for the detection of contrails using AVHRR split-window (10.7 and 12  $\mu\text{m}$  bands) data. Contrails have also been identified by their linear shape using images from visible reflectance and infrared brightness temperature (Palikonda et al. 2004). A drawback of this method is that natural cirrus with similar linear shape could be mistakenly identified as contrails.

(ii) *AVHRR Multi-Spectral Method*. Ou et al. (1996) developed a multi-spectral numerical scheme to identify pixels containing cirrus clouds overlapping low clouds using AVHRR channels based on their

spectral characteristics. This scheme has been applied to the AVHRR data collected over the FIRE-II IFO area during nine overpasses within seven observational dates. Results from the cloud typing program have been verified using the co-located and coincident ground-based radar and lidar return images, balloon-borne replicator data and the NCAR Cross-chain Loran Atmospheric Sounding System humidity soundings on a case-by-case basis.

**Table 2.** Satellite remote sensing techniques for detection and retrieval of contrails and cirrus clouds

<b>Satellite Remote Sensing Technique</b>	<b>Application to contrails and cirrus clouds</b>	<b>References</b>
AVHRR Split-window Pattern Recognition	Detection of line-shaped contrails	Schumann and Wendling (1990), Betancor-Gothe and Grassl (1993), Mannstein et al. (1999), Palikonda (2004)
AVHRR Multi-Spectral Method	Detection of cirrus clouds overlapping low clouds	Ou et al. (1996)
GOES Imager Detection Technique	Detection of persistent contrails and contrail cirrus	Minnis et al. (1998)
MODIS Cloud Mask/Phase Program	Detection of cirrus clouds	Ackerman et al. (2002), Platnick et al. (2003), King et al. (2004)
MODIS 1.38 $\mu\text{m}$ Detection Method	Detection of contrails and cirrus clouds	Roskovensky and Liou (2003) Gao et al. (1993), King et al. (1996), Hutchison and Choe (1996)
HIRS and MODIS CO <sub>2</sub> Slicing Method	Retrieval of cirrus cloud effective emissivity and cloud-top Pressure	Smith and Platt (1978), Menzel et al. (2002)
AVHRR Split-window Retrieval Method	Retrieval of cloud optical depths and ice crystal size of thin cirrus clouds and contrails	Parol et al. (1991), Betancor-Gothe and Grassl (1993), Duda and Spinhirne (1996), Duda et al. (1998)
AVHRR and NPOESS/VIIRS Thermal IR Window Retrieval Method	Retrieval of cloud optical depths, ice crystal size and cloud-top temperature of thin cirrus clouds and contrails	Ou et al. (1993, 1995, 1998a, b, 2002, 2003), Rao et al. (1995), Wong et al. (2007)
AVHRR, MODIS, and NPOESS/VIIRS Visible-Near-IR Window Retrieval Method	Retrieval of cloud optical depths, ice crystal size of thin cirrus clouds, and contrails	Hansen and Pollack (1970); Twomey and Cocks, (1982, 1989); Nakajima and King (1990), King et al. (1996, 1997), Ou et al. (1999, 2003), Rolland and Liou (2001), Rolland et al. (2000), Platnick et al. (2003), Roskovensky and Liou (2005, 2006)
AIRS Hyperspectral Retrieval Method	Retrieval of cloud optical depths and ice crystal size of cirrus clouds	Yue et al. (2007)

(iii) *GOES Imager Detection Technique.* Minnis et al. (1998) summarized a method for detecting contrails using GOES 0.65, 3.9, 11, and 12  $\mu\text{m}$  data. A contrail is detected either as a distinct or other

geometrical cold feature in the IR imagery or by using the BTD between thermal IR window bands. Once identified, a box is drawn around the contrail area and all pixels with brightness temperatures less than a threshold and  $BTD < 2K$  are flagged as contrails.

(iv) *MODIS Cloud Mask/Phase Program.* The MODIS cloud mask/phase programs use several cloud detection tests to indicate a level of confidence that the MODIS is observing a clear sky scene, and to assess the likelihood of a pixel being obstructed by clouds (Ackerman et al. 2002). Fourteen of the MODIS 36 spectral bands are utilized to maximize reliable cloud detection. Their products are generated globally for both daytime and nighttime overpasses with a 1 km-pixel resolution. Because cloud cover can occupy a pixel to varying extents, the MODIS Cloud mask program was designed to allow for varying degrees of clear sky confidence. The MODIS cloud mask/phase programs identify several conceptual domains according to surface type and solar illumination, including land, water, snow/ice, desert, and coast for both daytime and nighttime overpasses.

(v) *MODIS 1.38  $\mu\text{m}$  Detection Method.* The MODIS cloud mask products, which include data from the 1.38- $\mu\text{m}$  channel, have shown that the global cirrus-cloud coverage is less than that presented by Wylie et al. (1999). We note that MODIS products have not adequately utilized the 1.38- $\mu\text{m}$  channel reflectance. This channel is particularly useful for detecting thin cirrus due to its high sensitivity to upper tropospheric clouds and a nearly negligible sensitivity to low-level reflectance (Gao et al. 1993; King et al. 1996; Hutchison and Choe 1996). Specific 1.38- $\mu\text{m}$  reflectance threshold levels can be utilized to detect thin cirrus that has previously been undetectable by downward looking satellite imagery. Roskovensky and Liou (2003) developed a new cloud-detection scheme that utilizes 1.38- $\mu\text{m}$  reflectance to detect thin cirrus clouds. In this new method, the threshold is dependent on neighboring cloud type, water vapor concentration, and viewing geometry.

(vi) *HIRS and MODIS CO<sub>2</sub> Slicing Method.* The CO<sub>2</sub> slicing method is designed to determine the cloud-top pressure and the cloud effective emissivity based on the principle that the ratio of cloud signals (defined as the difference between cloudy and the clear radiances) for the two spectral bands is a function of cloud-top pressure only, which can then be evaluated by matching the ratio values derived from satellite measurements and from radiative transfer calculations using the cloud-top pressure and atmospheric temperature and humidity profiles. The CO<sub>2</sub> Slicing Method is most applicable to high-level clouds because of the strong sensitivity of the ratio value in the 15- $\mu\text{m}$  CO<sub>2</sub> band to cloud-top pressure at high altitudes.

(vii) *AVHRR Split-Window Retrieval Method.* This method was designed to determine the cloud optical depth and mean particle size based on the principle that correlation of the split-window BTD and Ch. 5 brightness temperature ( $T_5$ ) depends on both optical depth and mean particle size. For this method to work, it is necessary to know cloud-top and surface temperatures and pre-computed BTD and  $T_5$  based on a prescribed cloud microphysical model.

(viii) *AVHRR and NPOESS/VIIRS Thermal IR Window Retrieval Method.* Ou et al. (1993) developed a physical retrieval scheme using radiance data from AVHRR 3.7 $\mu\text{m}$  and 10.9 $\mu\text{m}$  bands to infer nighttime cirrus cloud parameters, including cloud temperature, optical depth, and mean effective ice crystal size based on the theory of radiative transfer and microphysics parameterizations. To apply this IR retrieval algorithm to daytime conditions, a numerical scheme to remove the solar component in the 3.7 $\mu\text{m}$  radiance has been developed (Rao et al., 1995). Analysis of the effects of error sources on retrieval results reveal that the maximum error in the 3.7 $\mu\text{m}$  solar component is less than 10 %.

(ix) *AVHRR, MODIS, and NPOESS/VIIRS Visible-Near-IR Look-Up Table Method.* This method was designed to determine cloud optical depth and mean particle size based on the principle that the reflection function of clouds at a non-absorbing band in the visible wavelength region is primarily a function of cloud optical depth, whereas the reflection function at a water (or ice) absorbing channel in the near-infrared (e.g., 1.61 $\mu\text{m}$  band) is primarily a function of cloud particle size (King *et al.* 1997). This principle was initially applied to the determination of water cloud optical depth and effective droplet radius during daytime. The approach has been discussed by Hansen and Pollack (1970), Twomey and Cocks (1982 and 1989), and Nakajima and King (1990) using visible and near-IR radiometers from an aircraft platform. Ou *et al.* (1999) applied this principle to the retrieval of cirrus cloud optical depth and mean particle size using AVHRR 0.67 and 3.7  $\mu\text{m}$  data. The same principle was applied to the MODIS Airborne Simulator (MAS) 0.657 and 1.609  $\mu\text{m}$  band reflectances by Rolland *et al.* (2000; 2002), to the MAS 0.657, 0.74, 0.86, and 1.87 $\mu\text{m}$  (surrogate of the MODIS 1.38  $\mu\text{m}$ ) band reflectances by Roskovensky and Liou (2005), and to the MODIS 0.65, 0.86, 1.38, and 1.64  $\mu\text{m}$  band reflectances by Roskovensky and Liou (2006) to evaluate cirrus cloud and aerosol parameters. This multi-channel technique has been incorporated into both the MODIS cloud retrieval program (King *et al.* 1997) and the NPOESS/VIIRS cloud optical property retrieval code (Ou *et al.* 2002; 2003).

(x) *AIRS Hyperspectral Thin Cirrus Retrieval Method.* This method was based on a thin cirrus cloud thermal infrared radiative transfer model constructed by combining the Optical Path Transmittance (OPTRAN, Mcmillin *et al.* 1995) model, developed for a speedy calculation of transmittances in clear atmospheres, and a thin cirrus cloud parameterization using a number of observed ice crystal size and shape distributions (Yue *et al.* 2007a). Numerical simulations show that cirrus cloudy radiances in the 800–1130  $\text{cm}^{-1}$  thermal infrared window are sufficiently sensitive to variations in cirrus optical depth and ice crystal size and shape if appropriate habit distribution models are selected *a priori* for analysis. The parameterization model has been applied to the Atmospheric Infrared Sounder (AIRS) on board the Aqua satellite to interpret clear and thin cirrus spectra observed in the thermal infrared window. Five clear and 29 thin cirrus cases at nighttime over and near the ARM program Tropical Western Pacific (TWP) Manus Island and Nauru Island sites have been chosen for this study. A  $\chi^2$ -minimization program was employed to infer the cirrus optical depth and ice crystal size and shape from the observed AIRS spectra. Independent validation shows that the AIRS-inferred cloud parameters are consistent with those determined by collocated ground-based millimeter-wave cloud radar measurements.

- *Ground-based remote sensing of contrails and cirrus*

Observations of contrails by lidar dated back as early as the late 80's. During the International Ice Experiment at German Bay (Raschke *et al.* 1990), a lidar developed by Morl *et al.* (1981) mounted on an aircraft was used to scan contrails from below (Schumann and Wendling, 1990). Later, Sassen *et al.* (1989a, 1989b), Freudenthaler *et al.* (1996b) and Gayet *et al.* (1996) used different lidar systems with a number of lidar wavelengths for detection and characterization of the contrail properties. Sassen (1997) presented a variety of persistent-contrail measurements employing polarization lidar and radiometric observations in Salt Lake City, Utah and gathered new information on contrails in a geographical area previously identified as being affected by relatively heavy air traffic. This dataset includes the hourly and monthly frequency of occurrence; the height, temperature, and relative humidity statistics; visible and infrared radiative impacts; the microphysical properties evaluated from *in situ* data, and the contrail optical phenomenon such as halos and coronas.

**Figure 8** presents an image of a 45-min old contrail generated by commercial jet aircraft flying in a flight corridor north of the ARM-SGP site on May 2, 1996 during SUCCESS. This image was obtained from a high-resolution (1.5 m by 0.1 sec) polarized diversity lidar deployed at Lamont, Oklahoma.

Contrail images, similar to the one shown in Fig. 8, contain abundant information regarding contrails' fine structure. It has been suggested that small particles typical of those in persistent contrails may favor albedo cooling over greenhouse warming, dependent on such factors as the geographic distribution and patterns of the day vs. night aircraft usage.

Atlas et al. (2006) discussed the morphology of contrails, their transition to cirrus uncinus, and their microphysical and radiative properties on the basis of the coincidental occurrence of a cluster of nearly parallel contrails, and the availability of collocated and concurrent observations by photography, satellite, automated ground-based lidar, and a freshly available database of aircraft flight tracks. Each contrail was observed sequentially by a lidar and tracked backward to the time and position of the originating aircraft track using the appropriate wind field. This lidar also provided particle fall speeds and estimated ice particle size, extinction coefficient, optical depth, and ice water path.

Systematic and continuous ground-based observations by lidar and other remote sensing instruments have been conducted by the Atmospheric Radiation Measurement (ARM) Program, a program established in 1989 that has been sponsored by the DOE Office of Science and managed by its Office of Biological and Environmental Research. One of the primary objectives of the ARM program is to improve scientific understanding of the fundamental physics governing the interaction between clouds and radiative feedback processes in the atmosphere. The ARM Program establishes and operates field research sites to study the effects of clouds on climate and climate change, and to improve their physical parameterization in GCMs. Three primary locations—the Southern Great Plains (SGP), Tropical Western Pacific (TWP), and North Slope of Alaska—were identified as representing the range of Earth's climate conditions. Each site has been heavily instrumented to gather a massive amount of climate data. Among these sites, the SGP site is particularly relevant to contrail observation because of its location near the flight corridors. Relevant instruments deployed at its Central Facility include the micropulse lidar (MPL), millimeter-wave cloud radar (MMCR), Raman lidar, total sky imager, Vaisala ceilometer, AERI, and various radiometers. Details of each instrument are given in the ARM website (<http://www.arm.gov/instruments/instclass.php?id=cloud>).

Among these instruments, the MPL is the most suitable for contrail and cirrus observation because of the strong sensitivity of the laser beam to small ice particles that are typical of contrails and thin cirrus. The MPL can detect cloud and aerosol signals between the ground level and 20 km with a vertical resolution of 0.03-0.3 km. The MMCR can detect cirrus clouds composed of particles with maximum dimensions larger than 100  $\mu\text{m}$ . The difference in cirrus detection between MPL and MMCR is illustrated by Comstock et al (2002), as shown in **Fig. 9**. Nevertheless, MMCR data collected at the ARM sites and during field campaigns in the past decade has been extensively used to study cirrus cloud characteristics (Mace et al. 1998a, 1998b, 2002, 2005) and to compile cirrus cloud climatology (Mace et al. 2006). MMCR can detect cloud signal between the ground level and 20 km with a vertical resolution of 0.05-0.1 km. For the retrieval of cirrus microphysical properties, several promising algorithms have been developed some of which can be applied to contrails. Matrosov et al. (1992) estimated layer-averaged ice cloud particle characteristic sizes and concentrations as well as the integrated ice water path from simultaneous ground-based radar and infrared radiometric measurements.

#### **e. Present state of modeling capability**

- *Parameterization of ice crystal microphysics properties in GCM*

A number of GCMs used temperature to determine ice crystal size (Donner et al., 1997; Kristjansson et al., 2005; Gu and Liou, 2006). This approach is rooted in earlier ice microphysics observations from

aircraft and attests to the fact that small and large ice crystals are related to cold and warm temperatures in cirrus cloud layers. Ou and Liou (1995) developed a parameterization equation relating cirrus temperature with a mean effective ice crystal size,  $D_e$ , based on a large number of midlatitude cirrus microphysics data presented by Heymsfield and Platt (1984). Ou et al. (1995) reduced large standard deviations in the size-temperature parameterization by incorporating a dimensional analysis between ice water content (IWC) and  $D_e$ . Using CEPEX data, McFarquhar et al. (2003) developed a  $D_e$  parameterization as a function of IWC for use in a single column model to understand the impact of tropical ice clouds on radiation fields.

Liou et al. (2007) recently analyzed the ice crystal size distribution data obtained from *in situ* aircraft measurements during a number of field experiments, including the ARM Intensive Cloud Observation Programs that were conducted over Oklahoma during April 1997 and March 2000, and the First ISCCP Regional Experiment (FIRE) II that was carried out over Kansas during November-December 1991 (Liou and Gu, 2006; Yue et al. 2007b). The IWC and  $D_e$  for radiation calculation are correlated on the basis of their mathematical definitions (Fu and Liou 1993). Excellent correlations between  $D_e$  and IWC have been found in the datasets by dividing the observed air temperature into two groups:  $-20^{\circ}\text{C}$  to  $-40^{\circ}\text{C}$  and  $-40^{\circ}\text{C}$  to  $-65^{\circ}\text{C}$  (Fig. 9). IWC and temperature are prognostic variables in most climate models. Thus, a corresponding  $D_e$  for radiation calculations can be determined using these correlations. Analysis also reveals that a Gamma distribution may be used to fit the observed ice crystal size distributions for calculating ice particle number concentration from the predicted IWC and temperature. These results are especially useful for evaluating ice cloud radiative effects in numerical simulations in which aerosol fields are not resolved. The empirical formulation allows us to calculate radiative transfer interactively with the ice microphysics used in numerical models, as well as to calculate effective ice crystal size in simulations where aerosol indirect effects are not explicitly considered.

- *Modeling optical properties for contrails for input into radiative transfer models*

Ice crystal size and shape in contrails and contrail cirrus are complex and intricate. Ice crystal images collected by the optical probe and replicator aboard aircraft during a limited number of field experiments have shown that contrails consist predominantly of bullet rosettes, columns, and plates with sizes ranging from about 1 to 100  $\mu\text{m}$ . Liou et al. (1998) presented four representative ice crystal size distributions in contrails and contrail cirrus clouds (**Fig. 10**). Ice crystal size distributions were obtained by FSSP onboard the University of North Dakota Citation aircraft flying over the ARM SGP site on April 18, 1994, re-penetrating its own 6-minute old contrail at a height of 13 km and a temperature of  $-65.9^{\circ}\text{C}$ . The sampled contrail contains a substantial number of small ice crystals on the order of 10  $\mu\text{m}$ . Ice crystal size distributions were also sampled over the ARM-SGP area by the Citation from near the top (13.4 km and  $-69.4^{\circ}\text{C}$ ) of an optically thin cirrus cloud that had contrails embedded in it. The two ice crystal size distributions over northeast Oklahoma on May 4, 1996 were measured by the replicator system developed by Arnott et al. (1994) mounted on the DC-8 aircraft, which tailed a Boeing 757 at a distance of 11.5 km and a time lag of 50 sec. The ambient temperature and dew point are  $-61.1^{\circ}\text{C}$  and  $-62.9^{\circ}\text{C}$ , respectively. Based on the SUCCESS replicator data, contrails contain a combination of bullet rosettes (50%), hollow columns (30%), and plates (20%). Using these shape factors, the mean effective sizes for the four ice crystal size distributions are 4.9, 9.8, 15.9, and 13.3  $\mu\text{m}$ .

To compare the ice crystal size distributions for contrails and natural cirrus clouds, **Figure 11** shows six representative distributions that were obtained from aircraft observations presented by Heymsfield and Platt (1984), Takano and Liou (1989) and the FIRE-IFO microphysical data. They are denoted as cold Ci,  $-60^{\circ}\text{C}$ , Cs, FIRE-I IFO 1 Nov, FIRE-I IFO 2 Nov, and Ci Uncinus. The ice crystal sizes span from about 5 to 2000  $\mu\text{m}$ , which is much wider than the range of contrail size distributions. The mean

effective sizes vary from 24 to 124  $\mu\text{m}$ , much larger than the contrail size distributions shown in the previous figure. Ice crystal shapes range from bullet rosettes, solid and hollow columns, and plates to aggregates, exhibiting a greater variety than contrail ice crystal shapes.

Using the four observed ice crystal size distributions as shown in Fig. 10, Liou et al. (1998) carried out the scattering and absorption calculations based on a unified theory for light scattering by ice crystals covering all sizes and shapes. The single-scattering parameters in terms of the phase function, single-scattering albedo, extinction coefficient, and asymmetry factor were computed for 200 solar wavelengths from 0.2 to 5  $\mu\text{m}$ . **Figures 12(a) and (b)** show the single-scattering phase functions for 0.46 and 3.5  $\mu\text{m}$ . Substantial differences in the backscattering part of the phase functions for the four mean effective sizes at the 3.5  $\mu\text{m}$  wavelength are noted. Because ice is a strong absorber at this wavelength, the scattered energy strongly depends on ice crystal size. For  $D_e = 4.9 \mu\text{m}$ , the halo and backscattering peaks are lower than those for other smaller sizes. **Figure 13** shows the extinction coefficient, single-scattering co-albedo and asymmetry factor based on a shape model of 50% bullet rosettes, 30% hollow columns, and 20% plates. The extinction coefficients show little variation, except for a minimum in the 2.85  $\mu\text{m}$  region, the so-called Christiansen effect. This effect occurs when the real part of the refractive index approaches 1, while the corresponding imaginary part is substantially larger, leading to the domination of absorption in light attenuation. This is particularly evident when ice particles are small. The single-scattering albedo also displays a strong minimum in the 2.85  $\mu\text{m}$  region with values much less than 0.5. When absorption is strong, the scattered energy is primarily contributed by diffraction in the forward directions. For this reason, maximum values of the asymmetry factor are noted around 3  $\mu\text{m}$ .

To compare the single-scattering properties between contrails and cirrus clouds, **Figures 14 (a) and (b)** show the phase functions for three representative size distributions involving cold Ci, cirrostratus, and cirrus uncinus for 0.672 and 3.7  $\mu\text{m}$  (Ou et al. 2002; 2003). For the non-absorbing 0.672  $\mu\text{m}$  wavelength, the overall phase function feature is not sensitive to variation in size distribution. The 22° and 46° halo features produced by two refracted rays are distinct in addition to the forward diffraction peak. Between about 150° and 160° scattering angles, there is another peak for all sizes produced by rays undergoing double internal reflections. Side-scattering is larger for smaller ice crystals. For the 3.7  $\mu\text{m}$  wavelength, the halos and backscattering peaks disappear due to strong absorption. Also, the strength of the forward scattering associated with diffraction varies with size distribution in this case. **Figure 15** shows the extinction coefficient, single-scattering co-albedo, and asymmetry factor for the three ice crystal size distributions and for wavelengths between 0.2 and 5  $\mu\text{m}$ . Extinction coefficients are nearly constant. Both the single-scattering co-albedo and asymmetry factor generally increase with increasing wavelengths and  $D_e$ .

- *Radiative transfer model for application to satellite remote sensing – LBLE model*

The LBLE radiative transfer model uses the adding-doubling method including full Stokes parameters developed by Takano and Liou (1989a, b) for vertically inhomogeneous atmospheres. The input parameters required to drive LBLE are generated by several pre-processors, including solar insolation, spectral band wavenumber, solar and viewing zenith angles, relative azimuthal angle, spectral surface albedo and emissivity, atmospheric temperature and humidity, and aerosol profiles. Input cloud configuration parameters include phase, base height, thickness, optical depth, and mean effective particle size.

The 1996/2000 HITRAN line-by-line absorption coefficients were used to develop the correlated k-distribution method for spectral radiative transfer. The correlated- $k$  coefficients for H<sub>2</sub>O covering the

spectral region from 2,000 to 21,000  $\text{cm}^{-1}$  (0.5-5  $\mu\text{m}$ ) were derived following a numerical approach in which efficient and accurate parameterizations for the calculation of pressure- and temperature-dependent absorption coefficients were developed on the basis of the theoretical values at three reference temperatures and 19 reference pressures. Absorption due to  $\text{O}_3$  and  $\text{O}_2$  bands follows Beer's law. In the original LBLE, the entire solar spectrum was divided into a total of 380 intervals with  $\Delta\lambda = 50 \text{ cm}^{-1}$ . For each spectral interval, the inverse of the cumulative probability function  $k(g)$  is evaluated at 30  $g$  values, where  $0 < g < 1$ . The model vertical domain was divided into 51 layers ( $\Delta p = 20 \text{ mb}$  for each layer, except for the bottom layer, where  $\Delta p = 13 \text{ mb}$ ). For wavelengths between 3.5 and 5  $\mu\text{m}$ , thermal emission contribution was accounted for in the solar flux transfer by adding the thermal emission component. Comparing the visible, near-IR and IR clear radiances computed from LBLE with those computed from MODTRAN shows differences within 10%, due to the different multiple-scattering treatment in the two models. Single-scattering parameters for ice clouds, which include the asymmetry factor ( $g$ ), the extinction coefficient ( $\beta_e$ ) and the absorption coefficient  $[(1-\omega)\beta_e]$ , were computed from the geometric ray-tracing method assuming randomly-oriented hexagonal ice crystals. The phase function values at discrete scattering angles were computed using a 200-term Legendre polynomial expansion of the phase function with the  $\delta$ -function transmission and diffraction-peak truncations. The resulting single-scattering parameters, cumulative  $k$ -distribution functions, phase functions, and other auxiliary data were combined and built into a radiative transfer program.

Using the preceding LBLE code, Liou et al. (1998) showed from spectral curves that cloud reflection increases as ice crystal sizes become smaller, but the cloud absorption increase is only evident for wavelengths longer than about 2.7  $\mu\text{m}$  (**Fig. 16**). The ice crystal shape has a substantial effect on cloud reflection and absorption for a given size. More complex ice particles reflect more solar radiation. For comparison, **Fig. 17** shows bidirectional reflectances for a number of representative ice crystal size distributions.

- *Radiative transfer model for radiative forcing calculations – Fu-Liou model*

Fu and Liou (1992; 1993) developed a state-of-the-art radiative transfer model that can be used for radiative forcing calculations associated with contrails and contrail-induced cirrus clouds. For the sake of computational efficiency and a high degree of accuracy, this radiation scheme was modified to use the  $\delta_4$ -stream approximation (Liou et al. 1988) for solar flux calculations, and the  $\delta_2/4$ -stream approximation (Fu et al. 1997) for IR flux calculations. The spectral integration has been carried out using the correlated  $k$ -distribution method developed by Fu and Liou (1992). The solar and IR spectra were divided into 12 and 6 bands, respectively according to the location of major gaseous absorption bands. Absorption due to water vapor, ozone, carbon dioxide and oxygen is accounted for in the solar spectrum. In the IR bands, absorption and emission included water vapor, ozone, carbon dioxide, methane, nitrogen oxide, and chlorofluorocarbons.

Calculations of the cloud radiative effects follow the procedure presented by Gu et al. (2003, 2006) in which the spectral extinction coefficient, the asymmetry factor, and the single-scattering albedo are determined in terms of cloud water content and the mean effective particle size for nonspherical ice crystals and liquid droplets. Calculations of the single-scattering properties of clouds require information about the particle shape and size distributions, and the indices of refraction as a function of wavelength. In typical GCM calculations, the mean effective radius of ice particles is prescribed with a constant value (e.g., 75  $\mu\text{m}$ ). The single-scattering properties for cirrus cloud particles were first parameterized based on 12 *in situ* measured composite ice crystal size distributions (Fu and Liou 1993). The extinction coefficient, single-scattering albedo, and asymmetry factor are dependent on wavelength and the cloud

position, and are parameterized in terms of IWC and mean effective ice crystal size. **Figure 18** shows the cirrus cloud radiative forcing as functions of ice water content for four different ice crystal sizes.

- *Global climate model – the UCLA AGCM*

The UCLA AGCM is a state-of-the-art grid-point model of the global atmosphere. The model prognostic variables are the horizontal wind, potential temperature, mixing ratios of water vapor, cloud liquid water and ice water, planetary boundary layer (PBL) depth, surface pressure, land surface temperature, and snow depth over land. The horizontal finite differencing of the primitive equations is based on a staggered Arakawa “C” grid scheme, while the vertical coordinate employed is the modified sigma coordinate developed by Suarez et al. (1983). For the time integration of prognostic variables, a leapfrog time-differencing scheme is used with a Matsuno step regularly inserted. The PBL is parameterized as a well-mixed layer of variable depth (Li et al. 2002). Parameterization of cumulus convection and its interaction with the PBL follows Arakawa and Schubert (1974). The geographical distribution of sea surface temperature (SST) is prescribed based on a 31-yr (1960–90) climatology corresponding to the Global Sea Ice and Sea Surface Temperature dataset (GISST) version 2.2. Daily values of the surface conditions are determined from the monthly mean values by linear interpolation. Ozone (O<sub>3</sub>) mixing ratios are prescribed as a function of latitude, height, and time based on the 1985–90 climatology (Li and Shine 1995). A low-resolution version of AGCM has been used by Gu et al. (2003), which is 4° (latitude) × 5° (longitude) with 15 layers from the earth’s surface to 1 hPa. Two cloud “types” are generated by the model. The first is free atmosphere clouds, whose main sources are grid-scale supersaturation and cumulus detrainment. In the current UCLA AGCM, a grid box of the free atmosphere is assumed to be entirely cloudy (i.e., the cloud fraction is 1) if the total cloud water mixing ratio is larger than 10<sup>-10</sup> kg kg<sup>-1</sup>. The second cloud type is the PBL clouds, which are generated at the PBL top when there are above the condensation level. PBL clouds are assigned a cloud fraction that increases linearly with pressure thickness to become 1 at and above 12.5 mb. A modified Fu-Liou radiative transfer code has been implemented in the UCLA AGCM in conjunction with the clouds that are formed in the model.

- *Global Contrail-Climate Model – the ECHAM4 GCM*

Version 4 of the European Center/Hamburg GCM (ECHAM4, Roeckner et al. 1996) has been specifically developed to simulate the climatic effects of contrail by Ponater et al. (2002). ECHAM4 has been applied to numerous climate sensitivity and climate change experiments (e.g., Feichter et al. 1997; Roeckner et al. 1999; Bengtsson et al. 1999). Following is a brief description of ECHAM4 with emphasis on parameterization for cirrus clouds and contrails. The ECHAM4 was a special version with 39 vertical layers that offer a vertical resolution of about 700 m in the upper troposphere and lower stratosphere where contrails occur. The horizontal resolution chosen was spectral T30 (about 670 km isotropically) with a time step of 30 min. The ECHAM4 cloud parameterization scheme was described in detail by Roeckner (1995), which sets the framework for parameterization of contrails. The scheme includes prognostic equations for water vapor and cloud water mixing ratios. It follows the original concept of Sundqvist (1978) who introduced a diagnostically determined fractional cloud cover as a function of relative humidity. Condensation and evaporation of cloud water, auto-conversion from cloud to rain, and evaporation of rain drops are parameterized. Parameterization of the contrail formation was based on the thermodynamic principle that predicts threshold values for contrail-forming temperature and humidity (Schumann 1996). Because only persistent contrails are assumed to contribute to climate change (Ponater et al. 1996), an environment that is supersaturated with respect to ice is required so that contrails may exist for a longer time, up to several hours, before they gradually transform into cirrus clouds or eventually disappear (e.g., Gierens and Jensen 1998; Minnis et al. 1998). Finally, the

dependency of actual contrail coverage on air traffic density was included by introducing the local amount of aircraft fuel consumption as a linear weighting factor to calculate the actual contrail coverage from contrail coverage (Sausen et al. 1998).

The radiative effect of clouds in the ECHAM4 is represented by the single-scattering albedo, the asymmetry factor, and the optical depth in the solar spectrum, and by the emissivity in the thermal infrared. These values were parameterized in terms of cloud water content and particle effective radius. For ice clouds, the calculation of solar radiative key parameters was based on the Lorenz-Mie theory assuming spherical ice particles (Rockel et al. 1991). The ice crystal effective radius was parameterized in terms of ice water content according to the data given in Heymsfield (1977) and McFarlane et al. (1992). The single-scattering albedo, asymmetry factor, and optical depth were fitted to the spectral radiation scheme, as documented in Boucher and Lohmann (1995). In order to account for the nonsphericity of ice particles, the asymmetry factor was empirically reduced by a factor of 0.91 (Roeckner 1995). Emissivity in the thermal infrared spectrum was approximated by an exponential function of ice water content and effective crystal radius developed by Stephens et al. (1990).

The optical properties of contrails were calculated exactly the same as those of natural cirrus clouds. However, known differences between the optical properties of cirrus and contrails are accounted for by making specific assumptions for contrail optical depth and particle size. Radiative fluxes and heating rates in the ECHAM4 were calculated using the radiation parameterizations developed by Fouquart and Bonnel (1980) and Morcrette (1991) for the solar and infrared spectrum, respectively. Evaluation of the cloud radiative effect in ECHAM4 has been reported by Lohmann and Roeckner (1996) and Chen and Roeckner (1996, 1997). Wild et al. (1998) indicated that the shortwave radiative budgets simulated by ECHAM4 are closer to observed values than those generated by other GCMs. However, this favorable result could be incidental rather than a result of a superior physical formulation.

- *Regional climate model – the WRF model*

The WRF model (Skamarock et al. 2005) is a next-generation mesoscale forecast model and data assimilation system that will advance both the understanding and prediction of mesoscale weather and accelerate the transfer of research advance into operation. It is designed to be a flexible, state-of-the-art, portable code efficient in a massively parallel computing environment. A modular single-source code is maintained that can be configured for both research and operation. It is a fully compressible, nonhydrostatic model and its vertical coordinate system is a terrain-following hydrostatic pressure coordinate. The grid staggering follows the Arakawa C-grid and the model uses the Runge-Kutta 2nd- and 3rd-order time integration schemes that offer numerous physics options. The principal components of WRF include data initialization, WRF-VAR (the data assimilation system), dynamic solvers, and physics packages. A version of the WRF, called the Advanced Research WRF (ARW), was developed at NCAR for research and development purposes. It has all the physical parameterizations required to produce simulation results.

Several cloud microphysics schemes have been implemented in WRF: (1) The Kessler scheme is a simple warm cloud scheme that includes water vapor, cloud water, and rain; (2) The Purdue Lin's scheme considers six classes of hydrometeors, including water vapor, cloud water, rain, cloud ice, snow, and graupel. All parameterization production terms are based on those developed by Lin et al. (1983) and Rutledge and Hobbs (1984) with modifications including saturation adjustment and ice sedimentation; (3) The NCEP simple ice scheme follows Hong et al. (1998) with a modification involving the ice sedimentation effect. Three categories of hydrometers are included: vapor, cloud water/ice, and rain/snow. The cloud ice and cloud water are considered to be in the same category but

distinguished by temperature; (4) The NCEP mixed phase scheme is similar to the NCEP simple ice scheme. However, rain and snow (cloud ice and cloud water) are in different categories. It allows supercooled water to exist and the gradual melting of snow as it falls (Hong et al. 1998); (5) The Eta microphysics scheme explicitly predicts the cloud water/ice mixing ratio. Liquid and frozen precipitations are derived diagnostically from cloud mixing ratio and are assumed to fall to the ground in a single time step. (6) The Eta grid-scale cloud and precipitation scheme predicts changes in water vapor and total condensate that are advected in the model. The density of precipitation ice is estimated from information on the total growth of ice by vapor deposition and accretion of liquid water. Sedimentation is treated by partitioning the time-averaged flux of precipitation into a grid box. The mean size of precipitation ice is assumed to be a function of temperature following the observational results. Mixed-phase physics are considered at temperatures warmer than  $-10^{\circ}\text{C}$ , whereas ice saturation is assumed for cloudy conditions at colder temperatures. (7) The Thompson et al. (2004) microphysical parameterization scheme includes six classes of moisture species, plus the ice number concentration as prognostic variables. Key improvements on the ice microphysics have been implemented in the primary ice nucleation and auto-conversion processes. Except for the Kessler scheme, all other schemes consider the ice-phase process.

For demonstration purposes, **Fig. 19** shows results from an illustration simulation corresponding to a specific dust storm and ice cloud case that occurred in the East Asia region. The model simulations were made with the current version (2.1.2) of WRF-ARW using the initial and boundary conditions from the GFS (Global Forecast System) "final analysis" product, which is a sequence of six hourly global gridded fields from the GFS data assimilation system. Seifert and Beheng's (2006) two-moment microphysics scheme was used that predicts mass content and number density for each of the five forms of condensed water: cloud droplets, ice crystals, snow, graupel and raindrops. The model simulations were started at 18Z on 19 March 2001, about 9 hours prior to the satellite overpass time.

#### **f. Current estimates of climatic impacts and uncertainties**

Radiative forcing by the line-shaped contrails has been estimated by Fahey et al. (1999). Rind et al. (2000) used a global circulation model coupled with a mixed-layer ocean model to show that a 1% increase in global cirrus cloud cover with an optical depth of 0.33 leads to a 0.43 K global warming. Ponater et al. (2005) found a smaller climate feedback from contrails than that from  $\text{CO}_2$  increase. In their global contrail-climate model, the equilibrium responses of surface temperature due to changes in radiative forcing are  $0.43\text{ K}/(\text{Wm}^{-2})$  and  $0.73\text{ K}/(\text{Wm}^{-2})$  for contrail and  $\text{CO}_2$  increases, respectively. For a scenario involving a global contrail-cover increase from 0.06% in 1992 to 0.15% in 2015, the mean radiative forcing increases from  $3.5\text{ mW}/\text{m}^2$  to  $9.8\text{ mW}/\text{m}^2$ . The computed transient global mean surface temperature increases by about 0.0005 K. According to Schumann (2005), the climatic impact of contrail cirrus could not be accurately estimated, because factors other than changes in the radiative forcing due to the presence of contrail and cirrus may also impact climate.

A much stronger climatic impact has been presented by Minnis et al. (2004) who analyzed the cirrus cloud cover trend over the continental U.S. between 1971 and 1995. The average 1%/yr increase in cirrus cloud cover is attributed exclusively to air traffic increase during this period. Assuming an optical depth of 0.25, this increase in high cloud cover results in a global mean radiative forcing of  $25\text{ mW}/\text{m}^2$  and a tropospheric temperature response of 0.2 to 0.3 K/decade in the region of the forcing, which would provide a practical explanation for the observed warming over this area between 1975 and 1994. However, Shine et al. (2005) and Ponater et al. (2005) pointed out several simplified assumptions employed in this study and reported temperature changes two orders of magnitude smaller.

In response to Shine et al. (2005), Minnis (2005) noted that the regional, non-equilibrium responses in climate models are highly uncertain and the estimated tropospheric response is comparable to the instantaneous changes expected in the presence of contrails. Since Minnis et al. (2004) used the contrail temperature response efficacy given by Rind et al. (2000) for the GISS climate model used by Hansen et al. (2005), the GISS model must have changed in the interval between the two model studies. In addition to questionable regional responses, many uncertainties exist in the treatment of high clouds in global models. For example, the GISS model substantially underestimates high cloud coverage in the midlatitude (Zhang et al., 2005) and significantly overestimates ice water path (Waliser et al. 2007). These types of uncertainties suggest that none of the current studies of contrail climate impact are conclusive and more definitive observations and models are needed. Specific information summarizing the needs and how research could be coordinated, funded and integrated should be important action items for future discussion.

Travis et al. (2001) claimed observable increases in the daily temperature range (DTR) due to reduced contrails in the three-day period of 11–14 September 2001, when air traffic over parts of the U.S. was reduced. They reported that DTR was 1 K above the 30-year average for the grounding period, which was interpreted as evidence that jet aircraft do have an impact on the radiation budget over the USA. However, the statistical significance of the data may not be strong enough to conclude that the above-than-average DTR is solely caused by missing contrails, since for unknown reasons, the DTR in 1982 was also nearly 1 K above the average (Travis et al. 2002). Hence, Travis et al. (2004) further analyzed the spatial variations of the DTR and of minimum and maximum temperatures, and estimated the contrail cover that would have occurred under normal traffic conditions. The potential contrail cover appears to be related to the observed variation in DTR. However, a quantitative model which relates the DTR to the change in contrail cloud cover is not provided, and other reasons may be responsible for the observed DTR variations. Kalkstein and Balling (2004) analyzed the air-mass and weather conditions in relation to the observed temperature range over the USA for a short period after 9 September 2001. They too, found a higher-than-average DTR.

Long-term responses to aviation-induced contrails and contrail cirrus have been estimated by inserting small percentages of cirrus into a general circulation model (GCM) at various time steps along the air traffic fly routes, and then letting the model run until equilibrium (Rind et al. 2000). The GCM results account for many of the feedbacks and the redistribution of the radiative energy in the system. Gu et al. (2004) used the UCLA atmospheric GCM to study the effects of cirrus cloud inhomogeneity on the atmospheric thermal structure with an interactive cirrus cloud parameterization. It is not clear at this point whether the regional climatic effects of contrails and contrail cirrus can be captured by GCMs, an area, which requires intensive literature survey and research.

The radiative and climatic effects, though small on a global scale, could be significant on a regional scale. A regional study by Strauss et al. (1997) shows that a 1% increase in local cirrus cloud cover (optical thickness 0.28) leads to a local surface temperature increase of about 0.1 K. Wang et al. (2001) studied effects of contrails on the radiative forcing and climate impact around Taiwan using the State University of New York at Albany regional climate model. The effects are calculated based on the contrail coverage, radiative properties as functions of particle effective radius, and solar and infrared optical depths as simulated from the National Taiwan University contrail model (Chen et al. 2001). Both short-lived and persistent contrails are considered. For persistent contrails with diurnal variation, the daily mean solar and infrared radiative forcings at the top of atmosphere are calculated to be 5.8 and 2.1  $\text{W m}^{-2}$ , respectively, while the radiative forcings at surface are 4.9 and 0.19  $\text{W m}^{-2}$ . Radiative forcings for short-lived contrails are much smaller than those for persistent contrails.

Overall, it is difficult to determine the net warming effect on climate caused by the presence of contrails and cirrus clouds. The extent of feedbacks between ice cloud microphysics and radiation is also not well understood, leading to numerous uncertainties and gaps, some of which are described below.

#### **g. Interconnectivity with other SSWP theme areas**

- *Formation, evolution, and persistence for contrails and contrail cirrus*

Duda et al. (2007) evaluated the use of high-resolution meteorological data from two operational numerical weather analyses (NWA) to diagnose and predict contrail formation using a variety of contrail observation database. Monthly contrail coverage statistics derived from surface and satellite observations were compared to the NWA-derived humidity, vertical velocity, wind shear, and atmospheric stability. The relationship between contrail occurrence and the NWA-derived statistics was analyzed to determine the atmospheric conditions under which persistent contrail formation is favored. Humidity is the most important factor that determines whether contrails are short-lived or persistent. Persistent contrails are more likely to appear when vertical velocities are positive and to spread when the atmosphere is less stable. Although artificial upper limits on the upper tropospheric humidity within NWA prevent a quantitative agreement of the model data with the contrail formation theory, logistic regression or similar statistical methods may improve the prediction of contrail occurrence.

The study by Duda et al. (2007) and other recent investigations showed that for common periods, surface and satellite data agree in the general direction of the trends but not in magnitude. Ensuring that the trends are due to air traffic requires knowledge of the concomitant trends in upper tropospheric humidity (UTH), a parameter that has not been measured either adequately or consistently for any length of time. Recent efforts to separate natural humidity effects and anthropogenic impacts have had limited success. Furthermore, confidence in the results remains tepid because of uncertainties in humidity record and differences between surface and satellite observations. The humidity issue has been skirted, to a certain degree, by focusing on the relationship between cirrus trends or amounts and upper tropospheric air traffic. Such studies generally agree that cirrus coverage is greater in areas where air traffic occurs, but they do not answer the question regarding the suppression of cirrus in other areas. Definitive answers to these questions would depend on understanding humidity variability in both areas with special emphasis on ice supersaturated regions.

- *Contrails and contrail cirrus specific microphysics*

After initial homogeneous and/or heterogeneous nucleation involving suitable aerosol particles and atmospheric conditions, ice crystal growth is governed by diffusion processes and the subsequent actions by means of collision and coalescence. These physical processes are complicated by the nature of the ice crystal's hexagonal and irregular shape. For cirrus clouds, nucleation of ice particles can occur via the heterogeneous process involving insoluble IN. At temperatures below about  $-38^{\circ}\text{C}$ , nucleation occurs by the homogeneous freezing of liquid solution droplets. For cirrus forming *in situ*, homogeneous freezing occurs in increasingly concentrated solution droplets as temperature decreases below  $-36^{\circ}\text{C}$ . Heterogeneous ice nucleation in particles that are partially or fully soluble can potentially cause cirrus formation at warmer temperatures and, for temperatures below  $-38^{\circ}\text{C}$ , lower RH. Heterogeneous ice-nucleation mechanisms (modes) most relevant to UTLS conditions include immersion freezing (ice nucleation induced by an IN previously immersed in a liquid aerosol droplet), contact freezing "inside-out" (freezing initiated when a solid IN immersed in a liquid aerosol particle collides with the drop surface from the inside), and deposition nucleation (direct nucleation of ice from vapor at a solid particle surface), which may occur in rare cases when IN reach the upper troposphere in a dry state. Recent

research demonstrates the relevance of organics in heterogeneous ice nucleation (Zuberi et al., 2001; Zobrist et al., 2006; Shilling et al., 2006). Not all of these modes have been shown to operate efficiently at cold temperatures. The concentration and nucleation relative RH of IN mainly determines their impact on cirrus cloud properties (DeMott et al., 1997; Kärcher and Lohmann, 2003).

Based on *in situ* observations of the microphysical properties of upper-tropospheric contrails and cirrus clouds by FSSP and replicator during more than 15 airborne missions over central Europe, Shröder et al.(2000) investigated the development of contrails into cirrus clouds on the timescale of 1 hour in terms of a representative set of number densities, size distributions and surface area distributions of aerosols and cloud elements, with special emphasis on small ice crystals (diameter, 20  $\mu\text{m}$ ). They found that contrails are dominated by high concentrations ( $\sim 100 \text{ cm}^{-3}$ ) of nearly spherical ice crystals with mean diameters in the range 1–10  $\mu\text{m}$ . Young cirrus clouds, which mostly contain small regularly shaped ice crystals in the range of 10–20  $\mu\text{m}$  diameter and typical concentrations of 2–5  $\text{cm}^{-3}$ , have been observed. Measurement results are compared to simple parcel model calculations to identify parameters relevant to the contrail–cirrus transition. Observations and model estimates suggest that contrail growth is only weakly, if at all, affected by preexisting cirrus clouds.

The basic uncertainty associated with ice nucleation processes is that they occur within short time scales (often only within seconds) and are rather localized (in sufficiently supersaturated patches of air). For this reason, it is extremely difficult to determine their relative importance in *in situ* measurements, or to even determine the basic nucleation mode. It is possible to isolate different ice nucleation pathways in the laboratory, but the question arises whether the employed IN particles are representative of atmospheric particles, an issue particularly important for aircraft because real engine soot and its processing cannot easily be represented in laboratory measurements.

Past studies of IN compositions have identified clay particles and mineral dust as important atmospheric IN. Lidar studies have documented the strong cloud-glaciating effect of dust particles from both Asian and Saharan sources. Laboratory studies using surrogates for airborne crystal and mineral dust particles predict the strong ice-nucleation efficiency of such particles throughout cirrus cloud forming temperatures.

Aircraft soot particles must compete with efficient IN in dust layers, but dust aerosols are highly variable in time and space and it remains uncertain how many dust particles are actually present in aircraft flight corridors. In the absence of dust, measurements in aging aircraft plumes face the difficulty of distinguishing between soot particles from aircraft exhaust and those from other sources (biomass burning, forest fires). Recent findings that certain organics might cause precipitation of ice-nucleating crystalline solids in liquid particles render efforts to disentangle the roles of various particle types in ice formation even more complicated.

### **3. Outstanding limitations, gaps and issues that need improvement**

#### **a. Science**

- *Long-term trends in contrail cirrus and cirrus*

Four primary sources of data can be used to estimate the long-term trends in contrail-cirrus and cirrus clouds: surface observations of cloud cover, meteorological sounding of humidity profiles, ground-based active remote sensors, and satellite observations. Each source has its limit. Surface observations suffer from inaccuracy problems, humidity soundings have large uncertainty for high-

altitude measurements, ground-based remote sensing is restricted in geographical coverage, and polar-orbiting and geostationary satellite remote sensing is limited by temporal and spatial resolution, respectively.

- *Aerosol-cirrus and contrail-cirrus indirect effects*

The aerosol and contrail indirect effects on the microphysical and radiative properties of cirrus clouds are critical, but these effects are complex and difficult to quantify by either *in situ* observations or modeling approach. Extensive and systematic *in situ* measurements of contrail and contrail cirrus have been extremely limited because of the requirement of high flying aircraft and the development of accurate and durable sampling instruments. Modeling approaches, on the other hand, are limited by an insufficient understanding of the physical and chemical processes that control the ice formation in the presence of aerosols. Satellite remote sensing is a viable alternative to capture the indirect effects, but research in this area is in its embryonic stage.

- *Microphysical and radiative properties on contrails and cirrus*

Because of the lack of *in situ* measurements, contrails' microphysical and radiative properties are largely unknown. Large-scale field campaigns like SUCCESS did provide microphysical observations of contrails, but it is not known how representative these observations are. It is quite clear that a selection of a number of representative *in situ* observations similar to SUCCESS must be conducted in order to obtain necessary and sufficient understanding and knowledge on contrail properties for climate impact assessment.

- *Radiative forcing of contrails*

The global average value of the radiative forcing has been increased from  $0.02 \text{ Wm}^{-2}$  in 1992 to  $0.03 \text{ Wm}^{-2}$  in 2000. However, uncertainty associated with these average values is two to three times greater. For regional radiative forcing, particularly near air traffic corridors, the range of radiative forcing is between  $-0.15$  and  $0.7 \text{ Wm}^{-2}$  based on contrail coverage of 0.5%. Model simulation of the contrail radiative forcing using 100% contrail coverage produces a range of  $-30$  to  $70 \text{ Wm}^{-2}$ . Further studies are clearly needed to narrow down the uncertainty range.

- *Climatic impacts of contrails and contrail cirrus*

It is well recognized based on physical principle that contrails and contrail cirrus could cause the global temperature to increase, as discussed above. However, many disagreed on the magnitude of this warming. The global average value of temperature increase due to an increase in contrail coverage is between near 0 K/decade (Ponater et al. 2005) to 0.2 – 0.3 K/decade (Minnis et al. 2004). For regional temperature, Struass et al. (1997) showed that a 1% increase in local cirrus cover can lead to about 0.1 K local temperature rise.

## **b. Measurements and analyses**

- *Satellite remote sensing*

Satellite remote sensing of contrails is limited by both spatial resolution and coverage as well as observation frequency. The polar-orbiting satellites visit the same local spot once or twice a day. For the scanning radiometer on board a satellite, the viewing zenith angle may be too far from the nadir,

rendering observations useless. Moreover, because polar-orbiting satellites are usually 700 – 900 km above the Earth, the sensor coverage for one sweep is only about 2000 – 3000 km. The geostationary platform is equipped with spin-scan sensors and can scan the same spot every 30 minutes. However, the sensor can only cover about 1/3 of the Earth's surface. Further, because the geostationary satellite is located about 40,000 km away from the Earth, the sensor pixel resolution is on the order of 4 km, too large to detect the narrow contrails.

For the reasons stated above, it has been extremely difficult to detect freshly formed and young contrails that are narrow by low-spatial-resolution space-borne sensors, including NOAA/HIRS, Aqua/AIRS, and GOES/Imager/IR-bands. Before 2000, NOAA/AVHRR and DMSP/OLS were the only space-borne meteorological satellite instruments that could detect contrails with linear shape. As mentioned above, the contrail detection algorithms using AVHRR split-window bands suffer from a drawback that cirrus clouds with similar linear shape can be misidentified as contrails. With the launch of high-spatial-resolution sensors such as Aqua/MODIS and future NPOESS/VIIRS, the detection of contrails is expected to be improved in view of a better image resolving power. Still, an effective contrail detection algorithm remains to be developed for the accurate and effective determination of contrail coverage. In light of the preceding discussion, the remote sensing of microphysical and optical properties of contrails is still in its embryonic stage. It is quite clear that a coordinated *in situ* observation of the microphysical and single-scattering properties is needed to narrow down numerous uncertainties presented above.

- *Ground-based remote sensing*

The ground-based remote sensing by lidar and radar is limited to spatial density of the instrument deployed and the areas that the lidar pulse and radar emission cover. Thus, it would be difficult to use them to detect freshly formed and young contrails that are geometrically narrow. If a lidar can capture a contrail, then it can determine its vertical extent as it drifts over the observation site. However, radar would be unable to detect freshly formed or young contrails containing small particle sizes.

### c. **Modeling capability**

- *Modeling the optical properties for contrails and cirrus for radiative transfer calculations*

Because of limitations in the *in situ* observation of contrails and the lack of understanding of their microphysics properties, it has been difficult to construct representative models for their microphysical and optical properties for the purpose of radiative transfer calculations. Further concerted observation and model analysis research on the contrail properties must be carried out to improve our current understanding.

- *Radiative transfer model*

In addition to uncertainties in the microphysical and optical models, the spatial inhomogeneity of the contrail composition is another source of error in radiative transfer calculations for remote sensing and radiative forcing applications. However, Gounou and Hogan (2007) found that the 3D inhomogeneity effect of contrails is not important.

- *Global and regional climate modeling*

Process studies of the evolution of aerosols and their role as INs will be required in order to produce effective emission indices for input to global models because the characteristics of emitted particles may have changed significantly by the time emissions have been placed onto global model grid scales. In this regard, global models and contrail/cirrus studies need to establish the essential parameters that can properly incorporate aviation aerosols and their effects into atmospheric calculations.

Most climate models have not been capable of predicting supersaturation in the UT/LS region. Saturation adjustment schemes are normally employed to remove excess water vapor above saturation obtained within one time step due to cooling or ice water transport. This type of approach is well justified for warm (liquid phase) clouds. However, ice cloud formation requires tens of percent of ice supersaturation. An accurate knowledge of ice supersaturation is crucial to quantify both the direct and indirect effects of aviation on cirrus cloudiness. High-resolution regional models are needed to accomplish this important task.

Many cloud schemes in GCMs compute cloud fraction based on an empirical function of grid-mean RH that may not be applicable to stratiform cirrus clouds. These clouds are known to be long-lived and can be transported over many grid boxes of a large-scale model during their lifetime. For cirrus and long-lived contrail-cirrus, a prognostic description of its cloud cover would appear to be more appropriate. In many cases, only ice water mass is predicted in global models. This hampers the introduction of physically-based links to ice crystal nucleation to distinguish between many different types of cirrus and to track the indirect effect of aircraft-produced aerosols. Also, in most global models cirrus is treated as one class of clouds in terms of their radiative properties. However, contrail-cirrus are composed of a large number of small (diameter  $\sim 10\text{-}30\ \mu\text{m}$ ) ice crystals as compared to particle sizes that have been observed in natural cirrus clouds.

It would be very difficult to provide reliable global real-time forecasts of contrail-cirrus to support control strategies or to project with some confidence the impact of aviation-induced cloudiness in future climate change scenarios without resolving some of the first order problems. While some progress has been made in the past 10 years to deal with ice supersaturation and to parameterize ice crystal nucleation in cirrus clouds, coordinated interdisciplinary research commitment must be made to gather a suitable set of dynamical, microphysical, and radiative components related to cirrus clouds in global models. This must be carried out in concert with laboratory, *in situ*, and remote sensing data analyses that can provide guidance in developing the parameterization schemes of subgrid-scale processes for use in GCMs.

- *Global distribution and properties of supersaturation, aerosols, and thin cirrus.*

Even if the degree and frequency of occurrence of supersaturation and the composition and size distributions of aerosol and cirrus cloud particles can be simulated in GCMs, it would be a difficult task to validate these parameters. We have previously addressed the problems of detecting and verifying ice supersaturation measurements from satellites. The global inventory is not available to yield quantitative information about the aerosol budget in the UTLS region particularly for soot-containing aerosols. Current global model aerosol validation exercises (e.g., the AEROCOM initiative) strongly focus on lower tropospheric aerosols. Cloud climatology such as those presented by ISCCP does not include high clouds with optical depths less than about 0.2, but such thin cirrus clouds are common in regions where aircraft activities occur. Stratospheric aerosol and subvisual cloud climatology, especially those from the Stratospheric Aerosol and Gas Experiment (SAGE) and the Halogen Occultation Experiment (HALOE), have limited observations in the upper troposphere region.

#### d. Interconnectivity with other SSWP theme areas

- *Detection and prediction of ice supersaturation*

Recent studies have shown that for the same period, the surface and satellite data agree in the general direction of trends but not in magnitude. Ensuring that trends are due to air traffic requires knowledge of the concomitant trends in upper tropospheric humidity (UTH), a parameter that has not been measured either adequately or consistently for any length of time. The humidity issue has been skirted, to certain degree, by focusing on the relationships between cirrus trends or amounts and upper tropospheric air traffic. Such studies generally agree that cirrus coverage is greater in areas where air traffic occurs, but they do not answer the question regarding the suppression of cirrus in other areas. Answers to these questions appear dependent on understanding humidity variability in both areas, with special emphasis on ice supersaturated regions. While it is not possible to return to the past and reconstruct a more accurate UTH record, it is recommended that improved methods for measuring UTH and supersaturation be standardized and applied consistently on a global basis in the future. Development of innovative methods to unscramble the natural and anthropogenic effects should be continued. Furthermore, both surface and satellite observations should be sustained in order to detect cirrus changes as air traffic patterns evolve over the coming years.

Contrails and the expansion of contrails into cirrus clouds occur in a supersaturated environment. However, global distributions of supersaturation in the upper troposphere where aviation-produced cirrus is likely to occur are not well known. MLS (Microwave Limb Sounder), AIRS (Atmospheric Infrared Sounder) and TOVS (TIROS Operational Vertical Sounder) observations may provide improved data for supersaturation analysis in the upper troposphere. However, current retrievals that are adequate for water vapor and temperature measurements under sub-saturated conditions may not be sufficient for supersaturated cases. Existing satellites do not have the horizontal or vertical resolution to accurately define the frequency and extent of supersaturated regions. Required in the future is a remote sounding instrument that measures both temperature and humidity with good vertical resolution and/or can detect RH directly.

- *Chemistry within emission plumes*

Current global models have treated aircraft emissions as well mixed within the grid box, but ignoring the plume processing of emissions. The effects of nonlinear plume processes (both chemical and microphysical) have not been evaluated in depth in the context of global chemical transport models. None of the currently available emission inventories considers the effect of plume processing on species or particle mixing ratios (e.g., NO<sub>x</sub> to NO<sub>y</sub> repartitioning, volatile and soot aerosol number concentrations and size) that eventually enter global simulations. Two types of aerosols are known to exist in aircraft plumes: the first is associated with soot particle emission and has a number emission index of  $\sim 10^{14}$ - $10^{15}$  /kg-fuel; the second is due to the formation of volatile particles induced by chemions (e.g., Eichkorn et al. 2002) and has a number emission index of  $\sim 10^{16}$ - $10^{17}$ /kg-fuel. The aviation-generated particles may perturb the abundance and properties of climate-relevant particles in the upper troposphere. To properly assess this perturbation and the associated climatic effect, further research is needed to understand the properties, transformation, and fate of aircraft-generated particles. Aviation aerosols are composed of water, sulfuric acid, organics, and soot. The composition of particles may affect their role to act as IN. In this regard, it is necessary to characterize the dependence of particle composition on engine operation conditions and fuel properties as well as the relative contribution of organics versus sulfur to the mass of particles of different sizes as a function of time in dispersing aircraft plumes. The aircraft-generated particles interact with background aerosols through coagulation

and mixing, and will eventually become part of ambient aerosols. In addition, photochemistry will provide additional condensable material (e.g., sulfuric acid from emitted SO<sub>2</sub>).

Research is lacking on how the properties (number concentration, surface area, composition, and mixing state) of ambient aerosols are perturbed at the presence of jet engine emissions under various conditions. In this regard, a detailed investigation of the microphysical (condensation and coagulation) and chemical processes (oxidation of precursor gases) governing the evolution of aviation aerosols in the time scale of days to weeks after emission is required. Research is also needed to define the abundance and properties of ambient aerosols as well as gaseous aerosol precursor concentrations in the troposphere. Both theoretical modeling and in situ measurements are needed to advance our knowledge about the perturbation of climate-relevant particles in the upper troposphere by aviation emissions.

- *Contrail-cirrus development*

The development of cirrus clouds from contrails and the resulting radiative effects are poorly characterized in current climate models and have been studied only on a limited basis from satellites and detailed cloud-scale models. The role of wake dynamics in determining immediate contrail ice particle concentrations has not been fully explored. For example, the interactions between the wakes of four versus two engines could, perhaps, dissipate young contrails through induced subsidence, even in nominally super-saturated conditions. Otherwise, once a contrail forms in supersaturated conditions, it will continue to grow and spread. However, knowledge of the impact of the type and numbers of primary and secondary emission particles on the number of ice crystals and hence particle growth potential and precipitation is inadequate. Such factors, along with wind shear, local vertical humidity profiles, and wake turbulence will determine how contrails grow vertically and horizontally and whether they dissipate in a few minutes or hours. The resulting vertical distribution of particles and their sizes determine the contrail-cirrus optical depth and effective particle size that govern their radiative effects.

A number of modeling studies have examined the transformation of young contrails to cirrus clouds and its sensitivity to the number of nucleating particles and wind shear, but the effects of realistic emission particle distributions, induced turbulence, radiation interactions, and the mesoscale environment have not yet been examined in a meaningful way. Such modeling studies are clearly needed but will remain theoretical exercises until relevant variables can be measured simultaneously. While early field campaigns have been conducted to accomplish that goal, the amount of useful data is insufficient to confidently model and understand the processes determining the microphysical and optical properties of contrails and contrail-cirrus in a wide range of atmospheric conditions.

Cloud-to-regional scale measurements and modeling are necessary steps in building a dependable set of tools to determine the contrail-cirrus impacts on climate. They form the basis for modeling the effects on global scale. However, knowledge of the global distribution of contrail-cirrus optical properties and coverage still remains uncertain. To date, satellite-based estimates of contrail particle sizes, optical depths, altitudes, and coverage are confined to only a few regions, seasons, and years. The most studied area is Western Europe followed by the United States. A more comprehensive climatology of aircraft-induced cirrus properties and radiative effects is needed, at least, for those areas where air traffic is significant or will become increasingly significant in the near future, e.g., eastern and southern Asia. The climatology should include several years that differ in upper tropospheric humidity in order to determine variability over the actual range of conditions that occur over time scales greater than a decade. A database of this type will serve as the basis for understanding the direct impact of contrails and contrail-cirrus and for guiding and validating global climate models that include this new class of ice clouds.

- *In situ measurements of aerosol composition and small ice crystals*

It is difficult to make *in situ* measurements of both the aerosol composition and small ice crystals. The low mass loading of particles provides a challenge to instrumentation even if they can adequately measure particle composition at lower altitudes. Mass spectrometric data indicates that at least in some regions, a majority of the particle mass in the upper troposphere is carbonaceous (e.g., include organic and elemental carbon). These data do not extend to the most numerous small particles below ~100 nm in diameter, nor is there information on the type of organic molecules. These organics could significantly change the freezing behavior of particles, affecting the evolution of contrail-cirrus and cirrus.

Significant problems exist with the measurement of small ice particles. Cirrus ice crystals can range from a few to hundreds of  $\mu\text{m}$  or more in diameter. Measuring this range requires several instruments and the agreement between them in the same size range has not always been good. Although the basic size modes in cirrus are not in as much question as for mixed phase clouds, it appears questionable whether any of the existing probes can obtain accurate ice crystal sizes and shapes that are both important for evaluating cloud radiative properties. Existing instrumentation appears difficult to measure the shape of very small (diameter  $<20 \mu\text{m}$ ) crystals that have often been found in contrails and contrail cirrus clouds. Ice can form much more easily on some particles in the atmosphere. The measurement of these ice nuclei in both contrail-cirrus and the background atmosphere is crucial to understanding how particles emitted from aircraft compete with background particles in the formation of new or modification existing cirrus. There are many fewer IN than other aerosol particles that requires improved instrumentation to measure their number and properties. The radiative properties of cirrus clouds and contrail-cirrus also depend on the vertical distribution of their microphysical properties. An examination of those radiative properties using remote sensing instruments (e.g., lidar, radar, radiometers, and interferometers) is often obscured by the presence of lower level clouds.

- *Properties of heterogeneous ice nuclei from natural and anthropogenic sources*

The formation of cirrus clouds is characterized by a competition between freezing particles for the available water vapor. Because of this competition, the ice-nucleating behavior of particles from aviation depends on the ice nucleation properties of particles from other anthropogenic and natural sources. The chemical composition of IN in the free troposphere is important to understand both the details of their freezing behavior and sources. A special case is elemental or soot-like carbon. The available data indicate that their ice nucleating behavior depends on source and processing in the atmosphere such as the addition of sulfate or organics. For example, elemental carbon from biomass burning probably has different ice-nucleating properties than aviation soot. None of the laboratory studies of ice nucleation has used authentic aviation soot. Sulfates and organics have been shown to affect ice nucleation ability, but the role of organics that condense in the plume behind a jet engine has not been studied in cruise conditions.

Measurements carried out in wave clouds have shown that at temperatures close to  $-38^{\circ}\text{C}$ , certain aerosol particles can nucleate ice at lower supersaturations (Field et al. 2001). This preconditioning effect is neither theoretically understood nor well explored experimentally. Short-lived contrails that form in sub-saturated air could lead to pre-conditioning of exhaust soot particles, as it is known that contrail ice crystals mainly form on emitted soot particles. After sublimation, these modified soot particles could facilitate ice formation in the atmosphere, increasing the relative importance of indirect effect. Conversely, if the soot is not so transformed by this conditioning, it may never be as effective as ambient IN, even though these soot particles previously served as nuclei for contrail particles. Whether

or not soot particles are effective IN and to what extent contrail processing changes their properties is an important question.

#### 4. Prioritization of research needs for tackling outstanding issues

##### a. Airborne *in situ* and remote observations and ground-based remote sensing of contrail cirrus and aircraft emission plumes

- *Impacts*

Airborne *in situ* observations and ground-based remote sensing of contrail, contrail-cirrus, and aircraft emission plumes are needed. As mentioned in Section 3, the aerosol and contrail indirect effects on the microphysical and radiative properties of cirrus clouds are critical in the analysis of climatic impacts of contrails, but these effects are difficult to quantify by *in situ* measurements. Nevertheless, with the availability of high-flying aircraft and accurate and durable sampling instruments, ice crystal and aerosol properties can be obtained to gain further understanding of ice cloud and aerosol interaction.

Measurements of the basic ice crystal properties can also help to build up the microphysical and radiative properties models for contrails. In fact, a comprehensive archive of ice crystal microphysical and spectral radiative properties models for cirrus clouds has been constructed based on *in situ* microphysics measurements collected during several field campaigns, including FIRE-I, FIRE-II, ARM-Cloud-IOP-2000, TRMM, CRYSTAL-FACE (Baum et al. 2005a,b; 2007; Young et al. 2000; 2005). Prototype models have been developed by Liou et al. (1998), as shown in Fig. 13. Similar procedures can be followed for contrails and contrail-cirrus.

Further measurements of ice crystal microphysics properties can also assist in the development of parameterization of ice crystal single-scattering properties in terms of ice crystal size parameters and ice water content for incorporation into a radiative transfer model for radiative forcing calculations. Preliminary parameterizations between ice crystal mean effective size and ice water content have been developed by Liou et al. (2007) based on limited *in situ* measurements of ice crystal size distributions as shown in Fig. 9.

- *Uncertainty reduction in climate impact estimate*

A direct measurement of the optical properties for ice crystal clouds can help to reduce uncertainty in current models and parameterizations. Advanced instrument design (e.g., the nephelometer developed by Barkey et al. 2002) can be used to validate the light scattering properties computed from theoretical models. In addition, the airborne and remote broadband and narrow-band radiometric measurements combined with collocated and coincident ice crystal *in situ* observations can be used to validate atmospheric and surface contrail radiative forcings computed by radiative transfer models. Such validation efforts have been made by Ou et al (1995).

- *Practical application and achievability*

Following the suggestion of JPDO and PARTNER (2006), a series of coordinated regional-scale campaigns need to be carefully designed and executed to measure appropriate variables governing the formation and dissipation of contrail and contrail-cirrus. Because the properties and life times of contrails and contrail-cirrus clouds are highly variable, a large number of flights must be executed for measurement in order to gather statistically meaningful samples. These regional-scale experiments

would preferably be conducted over long-term ground-based measurement sites and aircraft sampling flights should be coordinated with the overpasses of satellite platforms listed in Table 1.

- *Estimated cost and timeline*

Estimated cost and timeline for coordinated research efforts depend on the number of participants, instruments, and platforms involved. Based on past experiences, a regional-scale field campaign involving a large number of participants (more than 100), instruments, and multiple aircraft platforms (e.g., SUCCESS) have been very costly. Thus, it is necessary to achieve an optimal balance between scientific objective and cost. The timeline from the start of scientific and logistic planning, instrument development, and to the field deployment and operation could stretch over several years.

- *Prioritization*

A coordinated research effort involving *in situ* and ground-based observations of contrails and contrail cirrus is needed to reduce uncertainty in the assessment of climatic impacts of contrails and contrail-cirrus produced by aviation effects and is theoretically ranked “high priority”. However, considering the possible cost and time involved and the intricate scientific and logistic planning, we must add a “low priority” tag to such an effort.

## **b. Global and regional model studies addressing contrail direct and indirect effects**

- *Impacts*

In recent years, development in cloud modeling has included prognostic equations for the prediction of IWC for high-level clouds formed in GCMs and climate models. This is a milestone accomplishment from the standpoint of incorporating a physically-based cloud microphysics scheme in these models, and at the same time, it is also essential from the prospective of studying cloud-radiation interactions. For the study of contrails and contrail cirrus, it is also necessary to develop prognostic equations for computing IWC in contrails.

Cloud particle size is also an independent parameter that affects radiation transfer. For example, for a given IWC in clouds, smaller particles would reflect more sunlight than larger counterparts, an effect that has been recognized by Twomey et al. (1984) and Liou and Ou (1989) in conjunction with aerosol-cloud indirect effects. Incorporating a fully interactive ice microphysics based on the first principle in a GCM appears to be a challenging but an extremely difficult computational task. Innovative ice crystal size parameterization based on theory and observation must be developed for GCM applications.

Global and regional model studies addressing contrail direct and indirect effects have been limited by insufficient understanding of the physical and chemical processes that control the ice formation in the presence of aerosols. As pointed out by Kärcher et al. (2007), the inclusion of indirect aerosol effects in global models is at its infancy. At present, simplified parametric models of indirect effects of soot and dust aerosols using simplified assumptions of ice nucleation thresholds appear feasible for global model studies. A better grasp of the basic mechanism for ice crystal formation is required to improve the parameterization of heterogeneous ice nucleation rates. Data collected from coordinated atmospheric *in situ* measurements of the ice crystal and aerosol properties would help in the development of physical parameterization so that the contrail direct and indirect effects in global models can be physically simulated.

- *Practical use and achievability*

Following the suggestion of JPDO and PARTNER (2006), the direct effects of persistent contrails on cirrus cloud cover and radiative forcing can be studied even in the framework of conventional climate models, if appropriate parameterizations can be developed to separate contrail cirrus as a distinct class of ice clouds in a manner that is consistent with the built-in physics in GCMs. Even without explicit calculation of ice supersaturation, such studies will be more realistic than existing GCM estimates and lead to improved prediction of the hitherto poorly quantified global contrail climate impact.

- *Estimated cost and timeline*

The estimated cost for modeling efforts is much smaller than the efforts involving in situ measurements. The former timeline would also be shorter, perhaps on the order of one to two years.

- *Prioritization*

Because of the important potential impact and the potential benefit of uncertainty reduction in the estimate of climatic impact of contrails and contrail cirrus and because of its practical applications in the study of aviation effects on climate change, the need for global and regional model studies addressing contrail direct and indirect effects is ranked “high priority”. Such studies are also less expensive and require less time than coordinated efforts for in situ measurements.

### **c. Synergistic satellite remote sensing of contrails and contrail cirrus**

- *Impacts*

A combination use of satellite observations listed in Table 1 will improve the dependability of the estimate of long-term trends in contrails and contrail cirrus. As mentioned in Section 3, there are limits in the capability of the four primary sources of data: surface observations, meteorological soundings, ground-based remote sensing, and satellite observation. Only satellite observations cover the whole Earth. However, polar-orbiting and geostationary satellite measurements are limited by temporal and spatial resolutions, respectively. Therefore, it is recommended that a concerted effort be carried out to gather data from currently operating polar-orbiting and five geostationary satellites and integrated these datasets to establish the global long-term estimates of contrails and contrail cirrus with high resolutions in both space and time.

In addition, integrated satellite observations making use of an extensive suite of space-based instruments currently in operation, assisted by collocated and coincident *in situ* measurements, can also be used in the study of aerosol-cirrus indirect effect. These observations contain rich and valuable information that can be used to investigate the relationship between aerosol and ice cloud formation. Meaningful statistical and physically based methodologies need to be developed to systematically quantify the indirect effect.

Integrated satellite observations can also be used to assist in the investigation of radiative forcing due to contrails and contrail cirrus in two aspects. First, the radiative flux measurements from research-grade broadband radiometric sensor, such as CERES/Aqua, may be used to directly evaluate contrail radiative forcing, provide that contrail areas can be reliably detected by using collocated imager data. Second, contrail radiative forcing can also be computed using a radiative transfer model with the

ingestion of satellite-retrieved ice crystal microphysical properties. Both approaches are expected to improve our estimates of contrail radiative forcing.

- *Uncertainty reduction in climate impact estimate*

Integrated satellite observations can be combined with collocated surface observations, meteorological soundings and ground-based remote sensing measurements to further improve the accuracy of the detection of contrails and contrail cirrus. This improvement will add reliability to the satellite-estimated long-term trends in contrails and contrail-cirrus.

Integrated satellite observations can also be used to determine improved parameterizations of aerosol indirect effects and combined with model-derived parameterizations for incorporation into GCM studies.

- *Practical application and achievability*

Following the suggestion of JPDO and PARTNER (2006), synergistic satellite observation would be a high priority to determine the optical and microphysical properties of contrails and contrail-cirrus, including the cloud-top temperature/height, optical depth and effective particle size, three basic cloud parameters that are essential to the study of cloud radiative forcing. The space-borne polar-orbiting and geostationary radiometric measurements facilitate a unique approach to investigate the characteristics of the global distribution and temporal evolution of contrails, respectively. In particular, the passive sensors (e.g. MODIS) and active sensors (CALIPSO/CALIOP and CloudSat/CPR) in the A-Train constellation offer unprecedented opportunity to explore aviation-induced and modified high-level contrails and contrail-cirrus. The research objective would be to systematically analyze the characteristics of the global and temporal distributions of contrails and contrails-cirrus. To achieve this goal, robust and efficient new analysis programs must be developed to detect contrails and contrail cirrus and to retrieve their microphysical and optical properties.

- *Estimated cost and timeline*

Along the line of modeling study efforts, the estimated cost on the basis of *per annum* for analyzing synergistic satellite observations is much smaller than the coordinated efforts of *in situ* field measurements. The timeline for long-term estimates can stretch into decades. Other analysis efforts, including the detection of indirect effects and uncertainty reduction require only 3 to 5 years.

- *Prioritization*

For uncertainty reduction in the assessment of climatic impact of contrails and contrail-cirrus and for understanding of the aviation effects on climate change, fusion of the current and future satellite data containing contrails and contrail-cirrus is ranked “high priority”. Such an approach is also less expensive and requires less time than coordinated efforts for *in situ* field measurements. Note that success of this effort relies upon innovative developments involving reliable and effective contrail detection programs.

## **5. Recommendations for best use of current tools for modeling and data analysis**

- *Long-term trends in the coverage and frequency of contrail-cirrus and cirrus occurrence*

In conjunction with the modeling study, it is necessary to have global contrail and cirrus data sets for validation and analysis. Satellite derived cirrus cloud parameters that have the best quality in terms of

spatial resolution and reliability have been the MODIS cloud mask and products and along with AVHRR and GOES imager data, they can be used to study long-term trends in the coverage and frequency of contrail-cirrus and cirrus occurrence. The MODIS products are available from 2000 for Terra and from 2002 for Aqua. Another potential dataset for estimating contrail long-term trends is the CALIPSO/CALIOP cloud mask products, which are recently made available for the period since its launch in April, 2006. However, it is difficult for CALIPSO/CALIOP to intercept contrails given the fact that the lidar aboard has no cross track scanning capability. To match the CALIPSO/CALIOP track with MODIS pixels requires labor-intensive search. Once the collocation is done, CALIPSO/CALIOP observations can be used to validate MODIS contrail detection results.

- *Aerosol-cirrus and contrail-cirrus indirect effects*

In view of various problems encountered in the quantification of aerosol indirect effects solely through direct *in situ* observations, an alternative approach to study the aerosol-cirrus and contrail-cirrus indirect effects would be through the satellite observation of ice clouds and aerosols. In this conjunction, MODIS cloud retrieval products can be used to study long-term trends in the coverage and frequency of contrail-cirrus and cirrus occurrence. Parameterizations of aerosol-cloud processes can be derived by using the correlations between MODIS retrieved cloud and aerosol microphysical and radiative properties.

- *Climatic impacts of contrails and contrail cirrus*

The global climatic effect of contrails and contrail cirrus has been estimated to be relatively small. However, their regional climatic impact could be substantial and significant. A regional climate model including a physically-based radiative transfer model interactive with ice microphysics must be developed to understand radiative forcing issues and provide assessment on this important area. It appears that the best regional model that has been developed so far is the WRF model. We suggest that this model coupled with a spectral radiative transfer and ice microphysics parameterizations be used for simulating the formation, evolution, and dissipation of contrails and contrail cirrus using input of the flight track and jet fuel consumption information, and that the simulation results be compared with the independent remote sensing results determined from MODIS and other satellite cloud products.

## References

- Ackerman, S., K. Strabala, P. Menzel, R. Frey, C. Moeller, L. Gumley, B. Baum, S. W. Seeman, and H. Zhang, 2002: Discriminating clear-sky from cloud with MODIS. *MODIS Algorithm Theoretical Basis Document (MOD35)*, 115pp.
- Ackerman, T. P., K. N. Liou, F. P. J. Valero, and L. Pfister, 1988: Heating rates in tropical anvils. *J. Atmos. Sci.*, **45**, 1606 – 1623.
- Appleman, H., 1953: The formation of exhaust contrails by jet aircraft. *Bull. Amer. Meteor. Soc.*, **34**, 14-20.
- Arakawa, A. and W. H. Schubert, 1974: Interaction of a cumulus cloud ensemble with the large-scale environment, Part I. *J. Atmos. Sci.*, **31**, 674–701.
- Archuleta, C. M., P. J. DeMott, and S. M. Kreidenweis, 2005: Ice nucleation by surrogates for atmospheric mineral dust and mineral dust/sulfate particles at cirrus temperatures. *Atmos. Chem. Phys.*, **5**, 2617-2634.
- Arnott, W. P., Y. Y., Dong, and J. Hallett, 1994: Role of small ice crystals in radiative properties of cirrus: A case study, FIRE II, November 22, 1991. *J. Geophys. Res.*, **99**, 1371- 1381.
- Atlas, D., Z. Wang, and D. P. Duda, 2006: Contrails to cirrus – morphology, microphysics and radiative properties. *J. Appl. Meteor. Clim.*, **45**, 5-19.
- Bakan, S., M. Betancor, V. Gayler and H. Grassl, 1994: Contrail frequency over Europe from NOAA-satellite images. *Anna. Geophys. Atmos. Hydro. and Space Sci.*, **12**, 962-968.
- Barkey, B., M. Bailey, K. N. Liou, and J. Hallett, 2002: Light-scattering properties of plate and column ice crystals generated in a laboratory cold chamber. *Appl. Opt.*, **41**, 5792-5796.
- Baum, B. A., A. J. Heymsfield, P. Yang, S. T. Bedka 2005a: Bulk scattering properties for the remote sensing of ice clouds. Part I: Microphysical data and models. *J. Appl. Meteor.*, **44**, 1885–1895.
- Baum, B. A., P. Yang, A. J. Heymsfield, S. Platnick, M. D. King, Y.-X. Hu, and S. T. Bedka, 2005b: Bulk scattering properties for the remote sensing of ice clouds, Part II: Narrowband Models. *J. Appl. Meteor.*, **44**, 1896–1911.
- Baum, B. A., P. Yang, S. L. Nasiri, A. K. Heidinger, A. J. Heymsfield, and J. Li, 2007: Bulk scattering properties for the remote sensing of ice clouds. Part III: High resolution spectral models from 100 to 3250  $\text{cm}^{-1}$ . *J. Appl. Meteor. Clim.*, **46**, 423–1350 434.
- Baumgardner, D., J. E. Dye, B. Gandrud, R. G. Knollenberg, 1995: The multi-angle aerosol spectrometer probe: a new instrument for airborne particle research. AMS 9<sup>th</sup> Symposium on Meteorological Observations and Instrumentation, March 27-31, 1995, Charlotte, N. C., 1995.
- Bengtsson, L., E. Roeckner, and M. Stendel, 1999: Why is the global warming proceeding much slower than expected? *J. Geophys. Res.*, **104**, 3865–3876, 1999.
- Betancor-Gothe, M., and H. Grassl, 1993: Satellite remote sensing of the optical depth and mean crystal size of thin cirrus and contrails. *Theo. Appl. Clim.*, **48**, 101-113.
- Boucher, O., 1999: Influence of air traffic on cirrus occurrence. *Nature*, **397**, 30-31.
- Boucher, O. and U. Lohmann, 1995: The sulfate-CCN-cloud albedo effect: A sensitivity study with two general circulation models. *Tellus*, **47B**, 281-300.
- Bows, A., P. Upham, and K. Anderson, 2005: Growth Scenarios for EU and UK Aviation: Contradictions with climate policy. *Report for Friends of the Earth Trust Ltd.* Tyndall Center for Climate Change (North), University of Manchester. 91pp.
- Brasseur, G., R. Cox, D. Hauglustaine, I. Isaksen, J. Lelieveld, D. Lister, R. Sausen, U. Schumann, A. Wahner, P. Wiesen, 1998: European scientific assessment of the atmospheric effect of aircraft emissions. *Atmospheric Environment*, **32**, 2329–2418.
- Brooks, D. R., and F. M. Mims III, 2001: Development of an inexpensive handheld LED-based Sun photometer for the GLOBE program, *J. Geophys. Res.*, **106**, 4733-4740.

- Cantrell, W., and A.J. Heymsfield, 2005: Production of ice in tropospheric clouds: A review. *Bull. Amer. Meteor. Soc.*, **86**, 795-807.
- Carleton, A. M., and P. J. Lamb, 1986: Jet contrails and cirrus clouds: a feasibility study employing high-resolution satellite imagery. *Bull. Amer. Meteor. Soc.*, **67**, 301-309.
- Changnon, S. A., R. G. Semonin, and W. M. Wendland, 1980: *Effects of contrail cirrus on surface weather conditions in the Midwest – Phase I*. Final Report to National Science Foundation, Illinois Institute of Natural Resources, and University of Illinois, 141pp.
- Changnon, S. A., Jr., 1981: Midwestern cloud, sunshine and temperature trends since 1901: Possible evidence of jet contrail effects. *J. Appl. Meteor.*, **20**, 496-508.
- Chen, C.-T., and E. Roeckner, 1996: Validation of the Earth radiation budget as simulated by the Max Planck Institute for Meteorology general circulation model ECHAM4 using satellite observations of the Earth radiation budget experiment. *J. Geophys. Res.*, **101**, 4269–4287.
- Chen, C.-T., and E. Roeckner, 1997: Cloud simulations with the Max Planck Institute for Meteorology general circulation model ECHAM4 and comparison with observations. *J. Geophys. Res.*, **102**, 9335– 9350.
- Chen, J.-P., W.-H. Lin, and R.-F. Lin, 2001: Estimation of contrail frequency and radiative effects over the Taiwan area. *Terr. Atmos. Oceanic Sci.*, **12**, 155-178.
- Chýlek, P. et al., 2006: Aerosol indirect effect over the Indian Ocean. *Geophys. Res. Lett.*, **33**, L06806, doi:10.1029/2005GL025397.
- Comstock, J. M., T. P. Ackerman, and G. G. Mace, 2002: Ground-based lidar and radar remote sensing of tropical cirrus clouds at Nauru Island: Cloud statistics and radiative impacts. *J. Geophys. Res.*, **107**, D23, 4714, doi:10.1029/2002JD002203.
- DeMott, P. J., 1990: An exploratory study of ice nucleation by soot aerosols. *J. Appl. Meteorol.*, **29**, 1072-1079.
- DeMott, P. J., D. C. Rogers, S.M. Kreidenweis, 1997: The susceptibility of ice formation in upper tropospheric clouds to insoluble aerosol components. *J. Geophys. Res.*, **102**, 19,575-19,584.
- DeMott, P. J., Y. Chen, S. M. Kreidenweis, D. C. Roger, and D. E. Shermann, 1999: Ice formation by BC particles. *Geophys. Res. Lett.*, **26**, 2429-2432.
- Dessler, A. E., S. P. Palm, W. D. Hart, and J. D. Spinhirne, 2006a: Tropopause-level thin cirrus coverage revealed by ICESat/Geoscience Laser Altimeter System. *J. Geophys. Res.*, **111**, D08203, doi:10.1029/2005JD006586.
- Dessler, A. E., S. P. Palm, W. D. Hart, and J. D. Spinhirne, 2006b: Tropical cloud-top height distributions revealed by the Ice, Cloud, and land elevation Satellite (ICESat)/Geoscience Laser Altimeter System. *J. Geophys. Res.*, **111**, D12215, doi:10.1029/2005JD006705.
- Donner, L., C. J. Seman, B. J. Soden, R. S. Hemler, J. C. Warren, J. Ström, and K. N. Liou, 1997: Large-scale ice clouds in the GFDL SKYHI general circulation model. *J. Geophys. Res.*, **102**, doi: 10.1029/97JD01488, 21745-21768.
- Duda , D. P., and J. D. Spinhirne, 1996: Split window retrieval of particle size and optical depth in contrails located above horizontally inhomogeneous ice clouds. *Geophys. Res. Lett.*, **23**, 3711- 3714.
- Duda, D. P. and P. Minnis, 2002: Observations of Aircraft Dissipation Trails from GOES. *Mon. Wea. Rev.*, **130**, 398-406.
- Duda , D. P., P. Minnis, and L. Nguyen, 2001: Estimates of cloud radiative forcing in contrail clusters using GOES imagery. *J. Geophys. Res.*, **106**, 4927 – 4937.
- Duda, D. P., P. Minnis, P. K. Costulis, R. Palikonda, 2003: CONUS contrail frequency estimated from RUC and flight track data. *Proceedings of European Conference on Aviation, Atmosphere, and Climate*.
- Duda, D. P., P. Minnis, L. Nguyen, and R. Palikonda, 2004: A Case Study of the Development of Contrail Clusters over The Great Lakes. *J. Atmos. Sci.*, **61**, 1132-1146.

- Duda, D. P., P. Minnis, D. P. Garber, and R. Palikonda, 2005: CONUS contrail frequency and coverage estimated from RUC and flight track data. *Meteorol. Z.*, **14**, 537-548.
- Duda, D. P., R. Palikonda, and P. Minnis, 2008: Relating satellite and surface detection of contrails to numerical weather output. *Geophys. Res. Lett.* (in press).
- Eichkorn, S., K.-H. Wohlfrom, and F. Arnold, 2002: Massive positive and negative chemiions in the exhaust of an aircraft jet engine at ground level: Mass distribution measurements and implications of aerosol formation. *Atmospheric Environment*, **36**, 11, 1821-1825.
- Fahey, D. W., U. Schumann, S. Ackerman, P. Artaxo, O. Boucher, M.Y. Danilin, B. Kärcher, P. Minnis, T. Nakajima, O.B. Toon, 1999: Aviation produced aerosols and cloudiness, in: J.E. Penner, D.H. Lister, D.J. Griggs, D.J. Dokken, M. McFarland (Eds.), *Aviation and the Global Atmosphere, A Special Report of IPCC (Intergovernmental Panel on Climate Change)*, Cambridge Univ. Press, Cambridge, UK, , pp. 65–120.
- Feichter, J., U. Lohmann, and I. Schult, 1997: The atmospheric sulfur cycle and its impact on the shortwave radiation. *Clim. Dyn.*, **13**, 235– 246.
- Forster, P., V. Ramaswamy, P. Artaxo, T. Berntsen, R. Betts, D.W. Fahey, J. Haywood, J. Lean, D.C. Lowe, G. Myhre, J. Nganga, R. Prinn, G. Raga, M. Schulz and R. Van Dorland, 2007: Changes in Atmospheric Constituents and in Radiative Forcing. In: *Climate Change 2007: The Physical Science Basis. Contribution of Working Group I to the Fourth Assessment Report of the Intergovernmental Panel on Climate Change* [Solomon, S., D. Qin, M. Manning, Z. Chen, M. Marquis, K.B. Averyt, M.Tignor and H.L. Miller (eds.)]. Cambridge University Press, Cambridge, United Kingdom and New York, NY, USA.
- Fortuin, J. P., F. R. Van Dorland, W. M. F. Wauben, and H. Kelder, 1995: Greenhouse effects of aircraft emissions as calculated by a radiative transfer model. *Ann. Geophys.*, **13**, 413-418.
- Fouquart, Y., and B. Bonnel, 1980: Computations of solar heating of the Earth's atmosphere: A new parameterization. *Beitr. Phys. Atmos.*, **53**, 35 – 62.
- Frankel, D., K. N. Liou, S. C. Ou, D. P. Wylie, and P. Menzel, 1997: Observations of cirrus cloud extent and their impacts to climate, *Proceedings for the Ninth Conference on Atmospheric Radiation. Amer. Meteor. Soc.*, February 2-7, 1997, Long Beach, CA, pp 414 – 417.
- Freeman, K. P., and K. N. Liou, 1979: Climate effects of cirrus clouds. *Adv. Geophys.*, **21**, 231-287.
- Freudenthaler, V., F. Homburg, and H. Jager, 1996a: Contrail observations by ground-based scanning lidar: Cross-sectional growth. *Geophys. Res. Lett.*, **22**, 3501 – 3504.
- Freudenthaler, V., F. Homburg, and H. Jager, 1996b: Optical parameters of contrails from lidar measurements: Linear depolarization. *Geophys. Res. Lett.*, **23**, 3715 – 3718.
- Fu, Q., and K. N. Liou, 1992: On the correlated  $k$ -distribution method for radiative transfer in non-homogeneous atmospheres. *J. Atmos. Sci.*, **49**, 2139 – 2156.
- Fu, Q., and K. N. Liou, 1993: Parameterization of the radiative properties of cirrus clouds. *J. Atmos. Sci.*, **50**, 2008-2025.
- Fu, Q., K.N. Liou, M. Cribb, T.P. Charlock, and A. Grossman, 1997: Multiple scattering in thermal infrared radiative transfer. *J. Atmos. Sci.*, **54**, 2799-2812.
- Gao, B.-C., A. F. H. Goetz, and W. J. Wiscombe, 1993: Cirrus cloud detection from airborne imaging spectrometer data using the 1.38- $\mu\text{m}$  water vapor band. *Geophys. Res. Lett.*, **20**, 301–304.
- Gayet, J. F., G. Febvre, G. Brogniez, H. Chepfer, W. Renger, and P. Wendling, 1996: Microphysical and optical properties of cirrus and contrails: Cloud field study on 13 October 1989. *J. Atmos. Sci.*, **53**, 126-138.
- Gierens, K., and E. Jensen, 1998: A numerical study of the contrail to cirrus transition. *Geophys. Res. Lett.*, **25**, 4341–4344.
- Goodman, J., R. F. Pueschel, E. J. Jensen, S. Verma, G. V. Ferry, S. D. Howard, S. A. Kinne, and D. Baumgardner, 1998: Shape and size of contrails ice particles. *Geophys. Res. Lett.*, **25**, 1327-1330.

- Gorbunov, B., A. Baklanov, N. Kakutkina, H. L. Windsor, and R. Toumi, 2001: Ice nucleation on soot particles. *J. Aerosol Sci.*, **32**(2), 199-215.
- Gounou, A., and R. J. Hogan, 2007: A sensitivity study of the effect of horizontal photon transport on the radiative forcing of contrails. *J. Atmos. Sci.*, **64**, 1706-1716.
- Grassl, H., 1990: Possible climatic effects of contrails and additional water vapor. In *Air Traffic and the Environment Background, Tendencies and Potential Global Atmospheric Effects*. U. Schumann (ed), Springer-Verlag, Berlin, pp 124-137.
- Gu, Yu, and K. N. Liou, 2006: Cirrus cloud horizontal and vertical inhomogeneity effects in a GCM. *Meteor. Atmos. Phys.*, **91**, 223-235.
- Gu, Y., J. Farrara, K. N. Liou, and C. R. Mechoso, 2003: Parameterization of cloud/radiation processes in the UCLA general circulation model. *J. Climate*, **16**, 3357-3370.
- Gu, Y., K. N. Liou, Y. Xue, C. R. Mechoso, W. Li, and Y. Luo, 2006: Climatic effects of different aerosol types in China simulated by the UCLA general circulation model. *J. Geophys. Res.*, **111**, D15201, doi:10.1029/2005JD006312.
- Gulberg, A., 2003: A study of contrails in a general circulation model. Proceeding of the AAC-Conference, June 30 to July 3, 2003, Friedrichshafen, Germany, 261 – 265.
- Hansen, J. E., and J. B. Pollack, 1970: Near-Infrared light scattering by terrestrial clouds. *J. Atmos. Sci.*, **27**, 265-281.
- Hansen, J., Mki. Sato, R. Ruedy, L. Nazarenko, A. Lacis, G.A. Schmidt, G. Russell, I. Aleinov, M. Bauer, S. Bauer, N. Bell, B. Cairns, V. Canuto, M. Chandler, Y. Cheng, A. Del Genio, G. Faluvegi, E. Fleming, A. Friend, T. Hall, C. Jackman, M. Kelley, N. Kiang, D. Koch, J. Lean, J. Lerner, K. Lo, S. Menon, R. Miller, P. Minnis, T. Novakov, V. Oinas, Ja. Perlwitz, Ju. Perlwitz, D. Rind, A. Romanou, D. Shindell, P. Stone, S. Sun, N. Tausnev, D. Thresher, B. Wielicki, T. Wong, M. Yao, and S. Zhang, 2005: Efficacy of climate forcings. *J. Geophys. Res.* **110**, D18104, doi:10.1029/2005JD005776.
- Heymsfield, A. J., 1977: Precipitation development in stratiform ice clouds: A microphysical and dynamical study. *J. Atmos. Sci.*, **34**, 367-381.
- Heymsfield, A. J., and G. M. McFarquhar, 1996: On the high albedos of anvil cirrus in the tropical Pacific warm pool: Microphysical interpretations from CEPEX and from Kwajalein, Marshall Islands. *J. Atmos. Sci.*, **53**, 2424-2451.
- Heymsfield, A. J., and C. M. R. Platt, 1984: A parameterization of the particle size spectrum of ice clouds in terms of the ambient temperature and the ice water content. *J. Atmos. Sci.*, **41**, 846-855.
- Heymsfield, A. J., R. P. Lawson, and G. W. Sachse, 1998: Growth of ice crystals in a precipitating contrail. *Geophys. Res. Lett.*, **25**, 1335-1338.
- Hong, S.-Y., H.-M. H. Juang, and Q. Zhao, 1998: Implementation of prognostic cloud scheme for a regional spectral model. *Mon. Wea. Rev.*, **126**, 2621-2639.
- Hutchison, K. D., and N. J. Choe, 1996: Application of 1.38  $\mu\text{m}$  imagery for thin cirrus detection in daytime imagery collected over land surfaces. *Int. J. Remote Sens.*, **17**, 3325-3342.
- IPCC, 1999: *Aviation and the Global Atmosphere*. Penner et al., eds., Ch. 3, *Aviation-Produced Aerosols and Cloudiness*. D. W. Fahey and U. Schumann, eds. pp. 63-120. Cambridge Univ. Press, Cambridge, U.K.
- Jensen, E. J., O. B. Toon, S. Kinne, G. W. Sachse, B. E. Anderson, K. R. Chan, C. H. Twohy, B. Gandrud, A. Heymsfield, and R. Miake-Lye, 1998a: Environmental conditions required for contrail formation and persistence. *J. Geophys. Res.* **103**, 3929-3936.
- Jensen, E. J., O. B. Toon, A. tabazadeh, G. W. Sachse, B. E. Anderson, K. R. Chan, C. W. Twohy, B. Gandrud, S. M. Aulenbach, A. Heymsfield, J. Hallet, and B. Gary, 1998b: Ice nucleation processes in upper tropospheric wave-clouds observed during SUCCESS. *Geophys. Res. Lett.*, **25**, 1363 – 1366.

- Jensen, E. J., A. S. Ackerman, D. E. Stevens, O. B. Toon, P. Minnis, 1998c: Spreading and growth of contrails in a sheared environment. *J. Geophys. Res.* **103**, 31557 - 31567.
- Joint Planning and Development Office and Partnership for AiR Transportation Noise and Emissions Reduction, 2006: *A Report of Findings and Recommendations for workshop on the Impacts of Aviation on Climate change*, June 7-9, 2006, Boston, MA., 63pp.
- Joseph, J. H., Z. Levin, Y. Mekler, G. Ohring, and dJ. Otterman, 1975: Study of contrails observed from the ERST-1 satellite imagery. *J. Geophys. Res.*, **80**, 366-372.
- Jones, A., D.L. Roberts, and A. Slingo, 1994: A climate model study of the indirect radiative forcing by anthropogenic sulphate aerosols. *Nature*, **370**, 450-453.
- Kalkstein, A. J., and R.C. Balling, Jr, 2004: Impact of unusually clear weather on United States daily temperature range following 9/11/2001. *Climate Res.*, **26**, 1-4.
- Kärcher, B. and U. Lohmann, 2002: A parameterization of cirrus cloud formation: Homogeneous freezing of supercooled aerosols. *J. Geophys. Res.* **107**, doi: 10.1029/2001JD000470.
- Kärcher, B. and U. Lohmann, 2003: A parameterization of cirrus cloud formation: Heterogeneous freezing. *J. Geophys. Res.* **108**, doi: 10.1029/2002JD003220.
- Kärcher, B. , R. Busen, A. Petzold, F. P. Schroder, U. Schumann, and E. Jensen, 1998: Physicochemistry of aircraft-generated liquid aerosols, soot, and ice particles, 2, Comparison with observations and sensitivity studies. *J. Geophys. Res.*, **103**, 17129-17147.
- Kärcher, B., J. Hendricks, and U. Lohmann, 2006: Physically based parameterization of cirrus cloud formation for use in global atmospheric models. *J. Geophys. Res.*, **111**, D01205, doi: 10.1029/2005JD006219.
- Kärcher, B., O. Möhler, P. J. DeMott, S. Pechtl, and F. Yu, 2007: Insights into the role of soot aerosols in cirrus cloud formation. *Atmos. Chem. Phys.*, **7**, 4203-4227.
- King, M. D., W. P. Menzel, P. S. Grant, J. S. Myers, G. T. Arnold, S. E. Platnick, L. E. Gumley, S. C. Tsay, C. C. Moeller, M. Fitzgerald, K. S. Brown, and F. G. Osterwisch, 1996: Airborne scanning spectrometer for remote sensing of cloud, aerosol, water vapor and surface properties. *J. Atmos. Oceanic Technology*, **13**, 777-794.
- King, M. D., S.-C. Tsay, S. E. Platnick, M. Wang, and K. N. Liou, 1997: Cloud retrieval algorithms for MODIS: Optical thickness, effective particle radius, and thermodynamic phase. *MODIS Algorithm Theoretical Basis Document, No. ATBD-MOD-05*, MOD-06-Cloud Product, version 5, 79pp. ([http://modis.gsfc.nasa.gov/data/atbd/atbd\\_mod05.pdf](http://modis.gsfc.nasa.gov/data/atbd/atbd_mod05.pdf)).
- King, M. D., S. Platnick, P. Yang, G. T. Arnold, M. A. Gray, J. C. Riedi, S. A. Ackerman, and K. N. Liou, 2004: Remote Sensing of Liquid Water and Ice Cloud Optical Thickness and Effective Radius in the Arctic: Application of Airborne Multispectral MAS Data. *J. Atmos. Oceanic Technol.*, **21**, 857- 875.
- Knollenberg, R. G., 1972: Measurements of the growth of the ice budget in a persisting contrail. *J. Atmos. Sci.*, **29**, 1367-1374.
- Konrad, T. G., and J. C. Howard, 1974: Multiple contrail streamers observed by radar. *J. Appl. Meteor.*, **13**, 563-572.
- Kristjánsson, J. E., T. Iversen, A. Kirkevåg, Ø. Seland, and J. Debernard, 2005: Response of the climate system to aerosol direct and indirect forcing: Role of cloud feedbacks. *J. Geophys. Res.*, **110**, D24206, doi:10.1029/2005JD006299.
- Kuhn, P. M., 1970: Airborne observations of contrail effectson the thermal radiation budget. *J. Atmos. Sci.*, **27**, 937 - 942.
- Lawson, R. P., A. J. Heymsfield, T. L. Jensen, and S. M. Aulenbach, 1998: Shapes, sizes, and light scattering properties of ice crystals in cirrus and a persistent contrail during SUCCESS. *Geophys. Res. Lett.*, **25**, 1331-1334.

- Lee, T. F., 1989: Jet contrail identification using the AVHRR infrared split window. *Journal of Applied Meteorology*, **28**, 993-999.
- Li, D.-M., and K. P. Shine, 1995: A 4-dimensional ozone climatology for UGAMP models. UGAMP Internal Rep. 35.
- Li, J.-L. F., M. Köhler, J. D. Farrara, and C. R. Mechoso, 2002: The impact of stratocumulus cloud radiative properties on surface heat fluxes simulated with a general circulation model. *Mon. Wea. Rev.*, **130**, 1433–1441.
- Liepert, B., P. Fabian, and H. Grassl, 1994: Solar radiation in Germany – observed trends and an assessment of their causes. I. regional approach. *Beitrage zur Physik der Atmosphäre*, **67**, 15-29.
- Liepert, B., 1997: Recent changes in solar radiation under cloudy conditions. *Int. J. Climatology*, **17**, 1581-1593.
- Lin, Y.-L., R. D. Farley, and H. D. Orville, 1983: Bulk parameterization of the snow field in a cloud model. *J. Clim. Appl. Meteor.*, **22**, 1065 – 1092.
- Liou, K. N., 1986: The influence of cirrus on climate processes: a global perspective. *Mon. Wea. Rev.*, **114**, 1167-1199.
- Liou, K. N., 2005: Cirrus clouds and climate. *McGraw-Hill 2005 Yearbook of Science & Technology*, 51 – 53.
- Liou, K. N., and S. C. Ou, 1981: Parameterization of infrared radiation transfer in cloudy atmospheres. *J. Atmos. Sci.*, **38**, 2707-2716.
- Liou, K. N., and K. L. Gebhart, 1982: Numerical experiments on the thermal equilibrium temperature in cirrus cloudy atmospheres. *J. Meteor. Soc. Japan*, **60**, 570-582.
- Liou, K.N., and S.C. Ou, 1983: Theory of equilibrium temperatures in radiative-turbulent atmospheres. *J. Atmos. Sci.*, **40**, 214-229.
- Liou, K. N., and S.C. Ou, 1989: The role of cloud microphysical processes in climate: An assessment from a one-dimensional perspective. *J. Geophys. Res.*, **94**, 8599–8607.
- Liou, K. N. and Y. Gu, 2006: Radiative transfer in cirrus clouds: Some thought on its connection to climate and general circulation models (*INVITED*). *2006 AGU Fall Meeting*, San Francisco, California.
- Liou, K. N., S. C. Ou, and P. J. Lu, 1985: Interactive cloud formation and climatic temperature perturbations. *J. Atmos. Sci.*, **42**, 1969 – 1981.
- Liou, K. N., Q. Fu, and T. P. Ackerman, 1988: A simple formulation of the delta-four-stream approximation for radiative transfer parameterizations. *J. Atmos. Sci.*, **45**, 1940-1947.
- Liou, K. N., S. C. Ou, and G. Koenig, 1990: An investigation on the climatic effect of contrail cirrus. In *Air Traffic and the Environment Background, Tendencies and Potential Global Atmospheric Effects*. U. Schumann (ed), Springer-Verlag, Berlin, pp 154-169.
- Liou, K. N., P. Yang, Y. Takano, K. Sassen, T. Charlock, and W. Arnott, 1998: On the radiative properties of contrail cirrus. *Geophys. Res. Lett.*, **25**, 1161-1164.
- Liou, K. N., Y. Que, Y. Gu, and G. MacFarguhar, 2007: On the correlation between ice water content and ice crystal size and its application to radiative transfer and general circulation models (Submitted to *Geophys. Res. Lett.*).
- Liu, X. and J. E. Penner, 2005: Ice nucleation parameterization for global models. *Meteorol. Z.*, **14**, 499-514.
- Lohmann, U., and E. Roeckner, 1996: Design and performance of a new cloud microphysics scheme developed for the ECHAM4 general circulation model. *Clim. Dyn.*, **12**, 557– 572.
- Mace, G. G., C. Jakob, and K. P. Moran, 1998a: Validation of hydrometeor prediction from the ECMWF model during winter season 1997 using millimeter wave radar data. *Geophys. Res. Lett.*, **25**, 1645– 1648.

- Mace, G. G., T. P. Ackerman, P. Minnis, and D. F. Young, 1998b: Cirrus layer microphysical properties derived from surface-based millimeter radar and infrared interferometer data. *J. Geophys. Res.*, **103**, 23,207 – 23,216.
- Mace, G. G., E. E. Clothiaux, and T. P. Ackerman, 2001: The composite characteristics of cirrus clouds: Bulk properties revealed by 1-year of continuous cloud radar data. *J. Clim.*, **14**, 2185–2203.
- Mace, G. G., A. J. Heymsfield, and M. R. Poellot, 2002: On retrieving the microphysical properties of cirrus clouds using the moments of the millimeter-wavelength Doppler spectrum. *J. Geophys. Res.*, **107**, doi:10.1029/2001JD001308.
- Mace, G. G., Y. Zhang, S. Platnick, M. D. King, P. Minnis, and P. Yang, 2005: Evaluation of cirrus cloud properties derived from MODIS data using cloud properties derived from ground-based observations collected at the ARM SGP site. *J. Appl. Meteor.*, **44**, 221 - 240.
- Mace, G. G., S. Benson, and E. Vernon, 2006: Cirrus clouds and the Large-scale atmospheric State: Relationship revealed by six years of ground-based data. *J. Clim.*, **19**, 3257–3278.
- Machta, L., and T. Carpenter, 1971: Trends in high cloudiness at Denver and Salt Lake City. In *Man's Impact on the Climate*, W. H. Matthews, W. W. Kellogg, and G. D. Robinson, eds., MIT Press, Boston, pp. 410-415.
- Mannstein, H., R. Meyer, and P. Wendling, 1999: Operational detection of contrails from NOAA-AVHRR data. *Int. J. Rem. Sens.*, **20**, 1641-1660.
- Marquart, S., M. Ponater, F. Mager, and R. Sausen, 2003: Future development of contrail cover, optical depth, and radiative forcing: Impacts of increasing air traffic and climate change. *J. Climate*, **16**, 2890–2904.
- Matrosov, S. Y., T. Uttal, J. B. Snider, and R. A. Kropfli, 1992: Estimates of ice cloud parameters from ground-based infrared radiometer and radar measurements. *J. Geophys. Res.*, **97**, 11,567–11,574.
- McClatchy, R. A., R. W. Fenn, J. E. A. Selby, F. E. Volz, and J. S. Garing, 1972: *Optical Properties of the Atmosphere*. Air Force Cambridge Research Laboratories. Bedford, MA. 80pp.
- McFarlane, N. A., G. J. Boer, J.-P. Blanchet, and M. Lazare, 1992: The Canadian Climate Centre second-generation general circulation model and its equilibrium climate. *J. Clim.*, **5**, 1013– 1044.
- McFarquhar, G. M., S. Iacobellis, and R. Somerville, 2003: SCM simulations of tropical ice clouds using observationally based parameterizations of microphysics. *J. Climate*, **16**, 1643-1664.
- McMillin, L. M., L. J. Crone, M. D. Goldberg, and T. J. Kleespies, 1995: Atmospheric transmittance of an absorbing gas. 4. OPTRAN: a computationally fast and accurate transmittance model for absorbing gases with variable mixing ratios at variable viewing angles. *Appl. Opt.*, **34**, 6269–6274.
- Meerkötter, R., U. Schumann, D. R. Doelling, P. Minnis, T. Nakajima, Y. Tsushima, 1999: Radiative forcing by contrails. *Ann. Geophys.*, **17**, 1080-1094.
- Menzel, W. P., B. A. Baum, K. I. Strabala and R. A. Frey, 2002: Cloud top properties and cloud phase algorithm theoretical basis document, *Algorithm theoretical basis document, ATBD\_MOD\_04, NASA GSFC*. ([http://modis.gsfc.nasa.gov/data/atbd/atbd\\_mod04.pdf](http://modis.gsfc.nasa.gov/data/atbd/atbd_mod04.pdf)).
- Meyer, R., R. Buell, C. Leiter, H. Mannstein, S. Pechtl, T. Oki, and P. Wendling, 2007: Contrail observations over Southern and Eastern Asia in NOAA/AVHRR data and comparisons to contrail simulations in a GCM. *Int. J. Remote Sens.*, **28**, 2049-2069, doi:10.1080/01431160600641707, 2007.
- Minnis, P., 2002: Contrails. *Encyclopedia of Atmospheric Sciences*, Academic Press, London, J. Holton, J. Pyle, and J. Curry, Editors, pp. 509-520.
- Minnis, P., 2005: Reply. *J. Clim.*, **18**, 2783-2784.
- Minnis, P., D. F. Young, D. P. Garber, L. Nguyen, W. L. Smith, Jr., and R. Palikonda, 1998: Transformation of contrails into cirrus during SUCCESS. *Geophys. Res. Lett.*, **25**, 1157-1160.
- Minnis, P., U. Schumann, D. R. Doelling, K. M. Gierens, and D. W. Fahey, 1999: Global distribution of contrail radiative forcing. *Geophys. Res. Lett.*, **26**, 1853 – 1856.
- Minnis, P., J. K. Ayers, M. L. Nordeen, and S. P. Weaver, 2003: Contrail frequency over the United States from surface observations. *J. Climate*, **16**, 3447 – 3462.

- Minnis, P., J. K. Ayers, R. Palikonda, and D. Phan, 2004: Contrails, cirrus trends, and climate. *J. Climate*, **17**, 1671-1685.
- Minnis, P., R. Palikonda, B. J. Walter, J. K. Ayers, and H. Mannstein, 2005: Contrail properties over the eastern North Pacific from AVHRR data. *Meteorol. Z.*, **14**, 515-523.
- Morcrette, J.-J., 1991: Radiation and cloud radiative properties in the European Centre for Medium Range Weather Forecasts forecasting system. *J. Geophys. Res.*, **96**, 9121–9132.
- Morl, P., M. E. Reinhardt, E. Renger, and R. Schellhase, 1981: The use of the airborne lidar system “ALEX F 1” for aerosol tracing in the lower atmosphere. *Beitr. Phys. Atmos.*, **54**, 403-410.
- Murcray, W. B., 1970: On the possibility of weather modification by aircraft contrails. *Mon. Wea. Rev.*, **98**, 745 – 748.
- Nakajima, T. and M. D. King, 1990: Determination of the optical thickness and effective particle radius of clouds from reflected solar radiation measurements. Part I: Theory. *J. Atmos. Sci.*, **47**, 1878-1893.
- Next Generation Air Transportation System, 2004: *Federal Aviation Administration report to the US Congress*.
- Ou, S. C., and K. N. Liou, 1984: A two-dimensional radiation-turbulence climate model: I. Sensitivity to cirrus radiative properties. *J. Atmos. Sci.*, **41**, 2289-2309.
- Ou, S. C., and K. N. Liou, 1995: Ice microphysics and climatic temperature perturbations. *Atmos. Res.*, **35**, 127–138.
- Ou, S. C., K. N. Liou, W. M. Gooch, and Y. Takano, 1993: Remote sensing of cirrus clouds parameters using AVHRR 3.7 and 10.9  $\mu\text{m}$  channels. *Appl. Opt.*, **32**, 2171-2180.
- Ou, S. C., K. N. Liou, and Coauthors, 1995: Remote sounding of cirrus cloud optical depths and ice crystal sizes from AVHRR data: Verification using FIRE-II-IFO measurements. *J. Atmos. Sci.*, **52**, 4143-4158.
- Ou, S. C., K. N. Liou, and B. A. Baum, 1996: Detection of multilayer cirrus cloud systems using AVHRR data: Verification based on FIRE-II-IFO composite measurements. *J. Appl. Meteor.*, **35**, 178-191.
- Ou, S. C., K. N. Liou, and T. R. Caudill, 1998a: Remote sounding of multilayer cirrus cloud systems using AVHRR Data collected during FIRE-II-IFO. *J. Appl. Meteor.*, **37**, 241-254.
- Ou, S. C., K. N. Liou, P. Yang, P. Rolland, T. R. Caudill, J. Lisowski, and B. Morrison, 1998b: Airborne retrieval of cirrus cloud optical and microphysical properties using ARES 5.1-5.3 and 3.7  $\mu\text{m}$  channel data. *J. Geophys. Res.*, **103**, 23231-23242.
- Ou, S. C., K. N. Liou, M. D. King, and S. C. Tsay, 1999: Remote sensing of cirrus cloud parameters based on a 0.63-3.7  $\mu\text{m}$  radiance correlation technique applied to AVHRR data. *Geophys. Res. Lett.*, **26**, 2439-2440.
- Ou, S. C., K. N. Liou, and Y. Takano, G. J. Higgins, A. George, and R. Slonaker, 2002: *VIIRS cloud effective particle size and cloud optical depth algorithm theoretical basis document*. Algorithm Theoretical Basis Document, Version 5, Raytheon, Lanham, MD, .176pp.
- Ou, S. C., Y. Takano, K. N. Liou, G. J. Higgins, A. George and R. L. Slonaker, 2003: Remote sensing of cirrus cloud optical thickness and effective particle size for the National Polar-orbiting Operational Environmental Satellite System Visible/Infrared Imager Radiometer Suite: sensitivity to instrument noise and uncertainties in environmental parameters. *Appl. Opt.*, **42**, 7202-7214.
- Palikonda, P., D. N. Phan, V. Chakrapani, and P. Minnis, 2004: Contrail coverage over the USA from MODIS and AVHRR data. *Preprints, European Conf. on Aviation, Atmosphere, and Climate*. Friedrichshafen at Lake Constance, Germany, Institut für Physik der Atmosphäre, DLR.
- Palikonda, R., P. Minnis, D. P. Duda, and H. Mannstein, 2005: Contrail coverage derived from 2001 AVHRR data over the continental United States of America and surrounding areas. *Meteorol. Z.*, **14**, 525-536.
- Parol, F., J. C. Buriez, G. Brognies, and Y. Fouquart, 1991: Information content of AVHRR channels 4 and 5 with respect to particle size. *J. Appl. Meteor.*, **30**, 973-984.

- Platnick, S., M. D. King, S. A. Ackerman, W. P. Menzel, B. A. Baum, J. C. Riedi, R. A. Frey, 2003: The MODIS cloud products: algorithms and examples from Terra. *IEEE Trans. Geos. Rem. Sens.*, **41**, 459-473.
- Ponater, M., S. Brinkop, R. Sausen, and U. Schumann, 1996: Simulating the global atmospheric response to aircraft water vapour emissions and contrails—a first approach using a GCM. *Annales Geophysicae*, **14**, 941-960.
- Ponater, M. S. Marquart, and R. Sausen, 2002: Contrails in a comprehensive global climate model: Parameterization and radiative forcing results. *J. Geophys. Res.*, **107**, D13,4164, doi:10.1029/2001JD000429.
- Ponater, M., S. Marquart, R. Sausen, and U. Schumann, 2005: On contrail climate sensitivity. *Geophys. Res. Lett.*, **32**, L10706, 10.1029/2005GL022580.
- Ramaswamy, V., O. Boucher, J. Haigh, D.A. Hauglustaine, J. Haywood, G. Myhre, T. Nakajima, G.Y. Shi, S. Solomon, 2001: Radiative forcing of climate change. In: Houghton, J.T., et al. (Eds.), *Climate Change 2001: The Scientific Basis Intergovernmental Panel on Climate Change*. Cambridge University Press, Cambridge, New York, 349–416.
- Rao, N. X., S. C. Ou, and K. N. Liou, 1995: Removal of solar component in the AVHRR 3.7  $\mu\text{m}$  radiances for the retrieval of cirrus cloud parameters. *J. Appl. Meteor.*, **34**, 482-499.
- Raschke, E. J., J. Schmetz, J. Heintenberg, R. Kandel, and R. W. Saunders, 1990: The international Cirrus Experiment (ICE) – A joint European effort. *ESA J.*, **14**, 193 -199.
- Rebetez, M., and M. Beniston, 1998: Changes in sunshine duration are correlated with changes in daily temperature range this century : an analysis of Swiss climatology data. *Geophys. Res. Lett.*, **25**, 3611-3613.
- Rind, D., P. Lonergan, and K. Shah, 1996: Climatic effect of water vapor release in the upper troposphere. *J. Geophys. Res.*, **101**, 29395-29406
- Rind, D., P. Lonergan, K. Shah, 2000: Modeled impact of cirrus cloud increases along aircraft flight paths. *J. Geophys. Res.*, **105**, 19927–19940.
- Rockel, B., E. Raschke, and B. Weyres, 1991: A parameterization of broad-band radiative transfer properties of water, ice and mixed clouds. *Beitr. Phys. Atmos.*, **64**, 1– 12.
- Roeckner, E., 1995: Parameterization of cloud radiative properties in the ECHAM4 model. In *World Climate Research Program Workshop Proceedings, WMO/TD 713*, World Meteorol. Org., Geneva, 105–116.
- Roeckner, E., K. Arpe, L. Bengtsson, M. Christoph, M. Claussen, L. Dümenil, M. Esch, M. Giorgetta, U. Schlese, and U. Schulzweida, 1996: The atmospheric general circulation model ECHAM-4: Model description and simulation of present-day climate. *Report No. 218, Max-Planck-Institut für Meteorologie*, Hamburg, Germany, 90pp.
- Roeckner, E., L. Bengtsson, J. Feichter, J. Lelieveld, and H. Rodhe, 1999: Transient climate change simulations with a coupled atmosphere-ocean GCM including the tropospheric sulfur cycle. *J. Clim.*, **12**, 3004– 3032.
- Rolland, P., and K. N. Liou, 2001: Surface variability effects on the remote sensing of thin cirrus optical and microphysical properties. *J. Geophys. Res.*, **106**, 22965-22977.
- Rolland, P., K. N. Liou, M. D. King, S.-C. Tsay, and G. M. McFarquhar, 2000: Remote sensing of optical and microphysical properties of cirrus clouds using Moderate-Resolution Imaging Spectroradiometer channels: Methodology and sensitivity to physical assumptions. *J. Geophys. Res.*, **105**, 11721–11738.
- Roskovensky, J. K., and K. N. Liou, 2003: Detection of thin cirrus from 1.38  $\mu\text{m}$ /0.65  $\mu\text{m}$  reflectance ratio combined with 8.6–11  $\mu\text{m}$  brightness temperature difference. *Geophys. Res. Lett.*, **30**, 1985, doi:10.1029/2003GL018135.
- Roskovensky, J. K., and K. N. Liou, 2005: Differentiating airborne dust from cirrus clouds using MODIS data. *Geophys. Res. Lett.*, **32**, L12809, doi:10.1029/2005GL022798.

- Roskovensky, J. K., and K. N. Liou, 2006: Simultaneous determination of aerosol and thin cirrus optical depths over oceans from MODIS Data: Some Case Studies. *J. Atmos. Sci.*, **63**, 2307-2323.
- Rossow, W. B., and R. A. Schiffer, 1999: Advances in understanding clouds from ISCCP. *Bull. Am. Meteor. Soc.*, **80**, 2261-2287
- Rutledge, S. A., and P. V. Hobbs, 1984: The mesoscale and microscale structure and organization of clouds and precipitation in midlatitude cyclones. XII: A diagnostic modeling study of precipitation development in narrow cloud-frontal rainbands. *J. Atmos. Sci.*, **20**, 2949–2972.
- Sassen, K. 1997: Contrail-cirrus and their potential for regional climate change. *Bull. Amer. Meteor. Soc.*, **78**, 1885 – 1903.
- Sassen, K., and C. Hsueh, 1998: Contrail properties derived from high-resolution polarization lidar studies during SUCCESS. *Geophys. Res. Lett.*, **25**, 1165-1168.
- Sassen, K., D. O’C Starr, and T. Uttal, 1989a: Mesoscale and microscale structure of cirrus clouds: Three case studies. *J. Atmos. Sci.*, **46**, 371 – 396.
- Sassen, K. M. Griffin, and G. C. Dodd, 1989b: Optical scattering and microphysical properties of subvisual cirrus clouds, and climatic implications. *J. Appl. Meteor.*, **28**, 91-98.
- Sausen, R., K. Gierens, M. Ponater, and U. Schumann, 1998: A diagnostic study of the global distribution of contrails, part I, Present day climate. *Theor. Appl. Climatol.*, **61**, 127– 141.
- Sausen, R. and U. Schumann, 2007: Climate Impact of Aviation. *ASD Focus*, **1**, 4-5.
- Sausen, R. and Co-Authors, 2005: Aviation radiative forcing in 2000: An update on IPCC (1999). *Meteorol. Z.*, **14**, No. 4, 555-561.
- Schröder, F., B. Kärcher, C. Durore, J. Ström, A. Petzold, J.-F. Gayet, B. Strauss, P. Wendling, and A. Thomas, 2000: On the transition of contrails into cirrus clouds. *J. Atmos. Sci.*, **57**, 464 – 480.
- Schumann, U., 1996: On conditions for contrail formation from aircraft exhausts. *Meteor. Z.*, **5**, 4-23.
- Schumann, U., 2001: Climate sensitivity to contrails for increasing propulsion efficiency. In: Schumann, U., and Amanatidis, G.T. (Eds.), *Aviation, Aerosols, Contrails and Cirrus Clouds (A2C3)*. European Commission, Brussels, 271–274pp.
- Schumann, U., 2002: Contrail cirrus. In: *Cirrus*, D. K. Lynch, K. Sassen, D. O’C. Starr, G. Stephens (Eds.), Oxford Univ. Press, Oxford, UK., 231-255.
- Schumann, U., 2005: Formation, properties and climatic effects of contrails. *C. R. Physique*, **6**, 549–565.
- Schumann, U., and Wendling, 1990: Determination of contrails from satellite data and observational results. In *Air Traffic and the Environment Background, Tendencies and Potential Global Atmospheric Effects*. U. Schumann (Ed), Springer-Verlag, Berlin, pp 138-153.
- Schumann, U., H. Schlager, F. Arnold, J. Ovarlez, H. Kelder, Ø. Hov, G. Hayman, I. S. A. Isaksen, J. Staehelin, and P. D. Whitefield, 2000: Pollution from aircraft emissions in the North Atlantic flight corridor: Overview on the POLINAT projects. *J. Geophys. Res.*, **105**, 3605 – 3631.
- Seaver, W. L., and J. E. Lee, 1987: A statistical examination of sky cover changes in contiguous United States. *J. Climate Appl. Meteor.*, **26**, 88-95.
- Seifert, A., and K. D. Beheng, 2006: A two moment cloud microphysics parameterization for mixed-phase clouds. Part I: Model description. *Meteor. Atmos. Phys.*, **92**, 46-66.
- Seinfeld, J. H., 1998: Clouds, contrails, and climate. *Nature*, **391**, 837-838.
- Shilling, J.E., T.J. Fortin, M.A. Tolbert, 2006: Depositional ice nucleation on crystalline organic and inorganic solids. *J. Geophys. Res.*, 111, D12204, doi:10.1029/2005JD006664.
- Shine, K.P., R.G. Derwent, D.J. Wuebbles, J.-J. Morcrette, 1990: Radiative forcing of climate. In: Houghton, J. T., et al. (Eds.), *Climate change: The IPCC Scientific Assessment*. Cambridge University Press, Cambridge, New York, pp. 41–68.
- Shine, K. P. 2005: Comments on “Contrails, Cirrus Trends, and Climate. *J. Clim.*, **18**, 2781-2782.
- Skamarock, W. C., J. B. Klemp, J. Dudhia, D. O. Gill, D. M. Barker, W. Wang, and J. G. Powers, 2005: *A Description of the Advanced Research WRF Version 2*, NCAR Technical Note, NCAR/TN-468+STR., NCAR, Boulder, Colorado, 88pp.

- Smith, W. L., and C. M. Platt, 1978: Comparison of satellite-deduced cloud heights with indications from radiosonde and ground-based laser measurements. *J. Appl. Meteor.*, **17**, 1796-1802.
- Stevens, D. E., and C. S. Bretherton, 1996: A forward-in-time advection scheme and adaptive multilevel flow solver for nearly incompressible atmospheric flow. *J. Comput. Phys.*, **129**, 284-295.
- Stephens, G. L., S. Tsay, P. W. Stackhouse Jr., and P. J. Flatau, 1990: The relevance of the microphysical and radiative properties of cirrus clouds to climate and climate feedback. *J. Atmos. Sci.*, **42**, 2682-2694.
- Stephens, G. L., D. G. Vane, R. J. Boain, G. G. Mace, K. Sassen, Z. Wang, A. J. Illingworth, E. J. O'Connor, W. B. Rossow, S. L. Durden, S. D. Miller, R. T. Austin, A. Benedetti, C. Mitrescu, and the CloudSat Science Team, 2002: The CloudSat mission and the A-Train. *Bull. Amer. Meteor. Soc.*, **83**, 1771-1790.
- Strauss, B., R. Meerkotter, B. Wissinger, P. Wendling, and M. Hess, 1997: On the regional climatic impact of contrails: microphysical and radiative properties of contrails and natural cirrus clouds. *Ann. Geophysicae*, **15**, 1457-1467.
- Study on Man's Impact on Climate, 1971: *Inadvertent Climate Modification*. MIT Press, 308 pp.
- Suarez, M. J., A. Arakawa, and D. A. Randall, 1983: The parameterization of the planetary boundary layer in the UCLA general circulation model: Formulation and results. *Mon. Wea. Rev.*, **111**, 2224-2243.
- Sundqvist, H., 1978: A parameterization scheme for non-convective condensation including prediction of cloud water content. *Q. J. R. Meteorol. Soc.*, **104**, 677-690.
- Takano, Y., and K. N. Liou, 1989a: Solar radiative transfer in cirrus clouds. Part I. Single-scattering and optical properties of hexagonal ice crystals. *J. Atmos. Sci.*, **46**, 3-19.
- Takano, Y., and K. N. Liou, 1989b: Solar radiative transfer in cirrus clouds. Part II. Theory and computation of multiple scattering in an aniso-tropic medium. *J. Atmos. Sci.*, **46**, 20-36.
- Takano, Y. and K.N. Liou, 1995: Radiative transfer in cirrus clouds. III. Light scattering by irregular ice crystals. *J. Atmos. Sci.*, **52**, 818-837.
- Thompson, G., R. M. Rasmussen, and K. Manning, 2004: Explicit forecasts of winter precipitation using an improved bulk microphysics scheme. Part I: Description and sensitivity analysis. *Mon. Wea. Rev.*, **132**, 519-542.
- Toon, O. B., and R. C. Miake-Lye, 1998: Subsonic aircraft: Contrail and cloud effects special study. *Geophys. Res. Lett.*, **25**, 1109 - 1112.
- Twomey, S.A., M. Piepgrass, and T. Wolfe, 1984: An assessment of the impact of pollution on global cloud albedo. *Tellus*, **36B**, 356-366.
- Travis, D. J., A.M. Carleton, and R.G. Lauritsen, 2001: Jet aircraft contrails: Surface temperature variations during the aircraft groundings of September 11-13, 2001. In: *10th Conference on Aviation, Range & Aerospace Meteorology, 13-16 May 2002, Portland, Oregon*, American Meteorological Society, paper J1.1.
- Travis, D. J., A. M. Carleton, R.G. Lauritsen, 2002: Contrails reduce daily temperature range, brief communications. *Nature*, **418**, 601.
- Travis, D. J., A. M. Carleton, R.G. Lauritsen, 2004: Regional variations in U.S. diurnal temperature range for the 11-14 September 2001 aircraft groundings: Evidence of jet contrail influence on climate. *J. Clim.*, **17**, 1123-1134.
- Travis, D. J., A. M. Carleton, J. S. Johnson, and J. Q. DeGrand, 2007: US jet contrail frequency changes: influences of jet aircraft flight activity and atmospheric conditions. *Int. J. Clim.*, **27**, 621-632.
- Twomey, S. and T. Cocks (1982). Spectral reflectance of clouds in the near-infrared: Comparison of measurements and calculations. *J. Meteor. Soc. Japan*, **60**, 583-592.
- Twomey, S, and T. Cocks (1989). Remote sensing of cloud parameters from spectral reflectance in the near-infrared. *Beitr. Phys. Atmos.*, **62**, 172-179.

- Waitz, I., J. Townsend, J. Cutcher-Gershenfeld, E. Greitzer, and J. Kerrebrock, 2004: *Report to the United States Congress: aviation and Environment, A National Vision, Framework for Goals and Recommended Actions*. PARTNER, MIT, Cambridge, MA. 52pp.
- Waliser D., Li F., Jiang J., Wu D., Stephens G., Vane D., Tompkins A., Chern J., Khairoutdinov M., Woods C., 2007: Exploiting MLS and CloudSat Data to Support Weather and Climate Model Development and Validation: Applications to Upper Tropospheric Cloud Processes, A-Train Lille 2007 Symposium, Lille, France, October 22-25, 006.
- Wang, W.-C., W. Gong, and J.-P. Chen, 2001: SUNYA Regional Model simulation of radiative forcing and climate impact due to contrails over regions around Taiwan. *Terr. Atmos. Oceanic Sci.*, **12**, 179-194.
- Wang, Z., and K. Sassen, 2002a: Cirrus cloud microphysical property retrieval using lidar and radar measurements. Part I: Algorithm description and comparison with in-situ data. *J. Appl. Meteor.*, **41**, 218-229.
- Wang, Z., and K. Sassen, 2002b: Cirrus cloud microphysical property retrieval using lidar and radar measurements. Part II: Midlatitude cirrus microphysical and radiative properties. *J. Atmos. Sci.*, **59**, 2291-2302.
- Wild, M., A. Ohmura, H. Gilgen, E. Roeckner, M. Giorgetta, and J.-J. Morcrette, 1998: The disposition of radiative energy in the global climate system: GCM calculated versus observational estimates. *Clim. Dyn.*, **14**, 853– 869.
- Winker, D. M., W. H. Hunt, and C. A. Hostetler, 2004: Status and Performance of the CALIOP lidar. *Proc. SPIE*, **5575**, 8-15.
- Wong, E., K. Hutchison, S. C. Ou, and K. N. Liou, 2007: Cirrus cloud top temperatures retrieved from radiances in the National Polar-Orbiting Operational Environmental Satellite System - Visible Infrared Imager Radiometer Suite 8.55 and 12.0  $\mu\text{m}$  bandpasses. *Appl. Opt.*, **46**, 1316-1325.
- Wylie, D., W. P. Menzel, and K. I. Strabala, 1994: Four years of global cirrus cloud statistics using HIRS. *J. Climate*, **7**, 1972–1986.
- Wylie, D. P., and W. P. Menzel, 1999: Eight years of high cloud statistics using HIRS. *J. Climate*, **12**, 170–184.
- Wylie, D., D. L. Jackson, W. P. Menzel, and J. J. Bates, 2005: Trends in global cloud cover in two decades of HIRS observations. *J. Climate*, **18**, 3021-3031.
- Yang, P., and K. N. Liou, 1996a: Finite-difference time domain method for light scattering by small ice crystals in three-dimensional space. *J. Opt. Soc. Amer.*, **A13**, 2072-2085.
- Yang, P., and K. N. Liou, 1996b: Geometric-optics-integral-equation method for light scattering by nonspherical ice crystals. *Appl. Opt.*, **35**, 6568-6584.
- Yang, P., H. Wei, H.-L. Huang, B. A. Baum, Y. X. Hu, G. 1640 W. Kattawar, M. I. Mishchenko, and Q. Fu, 2005: Scattering and absorption property database for nonspherical ice particles in the near-through far-infrared spectral region. *Appl. Opt.*, **44**, 5512–5523.
- Yue, Q., K. N. Liou, S. C. Ou, B. H. Kahn, P. Yang, and G. G. Mace, 2007a: Interpretation of AIRS data in thin cirrus atmospheres based on a fast radiative transfer model. *J. Atmos. Sci.*, **64**, 3827-3842.
- Yue, Q., K. N. Liou, and Yu Gu, 2007b: Investigation of the radiative forcings of thin cirrus in the tropical atmosphere using AIRS/ARM data. *2007 ARM Science Team Meeting*, March 26-30, 2007, Monterey, California.
- Zhang, M. H., W. Y. Lin, S. A. Klein, J. T. Bacmeister, S. Bony, R. T. Cederwall, A. D. Del Genio, J. J. Hack, N. G. Loeb, U. Lohmann, P. Minnis, I. Musat, R. Pincus, P. Stier, M. J. Suarez, M. J. Webb, J. B. Wu, S. C. Xie, M.-S. Yao, and J. H. Zhang, 2005: Comparing clouds and their seasonal variations in 10 atmospheric general circulation models with satellite measurements. *J. Geophys. Res.*, **110**, 10.1029/2004JD005021.
- Zerefos, C. S., K. Eleftheratos, D. S. Balis, P. Zanis, G. Tselioudis, C. Meleti, 2003: Evidence of impact of aviation on cirrus cloud formation. *Atmos. Chem. Phys.*, **3**, 1633 – 1644.

- Zobrist, B. , Marcolli, C., Koop, T., Luo, B. P., Murphy, D. M., Lohmann, U., Zardini, A., Krieger, U. K., Corti, T., Cziczo, D. J., Fueglistaler, S., Hudson, P. K., Thomson, D. S. and Peter, T., 2006: Oxalic acid as a heterogeneous ice nucleus in the upper troposphere and its indirect aerosol effect. *Atmos. Chem. and Phys. Disc.*, **6**, 3571-3609.
- Zuberi, B., A.K. Bertram, T. Koop, L.T. Molina, and M.J. Molina, 2001: Heterogeneous freezing of aqueous particles induced by crystallized (NH<sub>4</sub>)<sub>2</sub>SO<sub>4</sub>, ice, and letovicite. *J. Phys. Chem. A*, **105**, 6458-6464.



**Fig. 1** (a) Short-lived contrails and (b) Persistent contrails and contrail cirrus (after Minnis 2002).

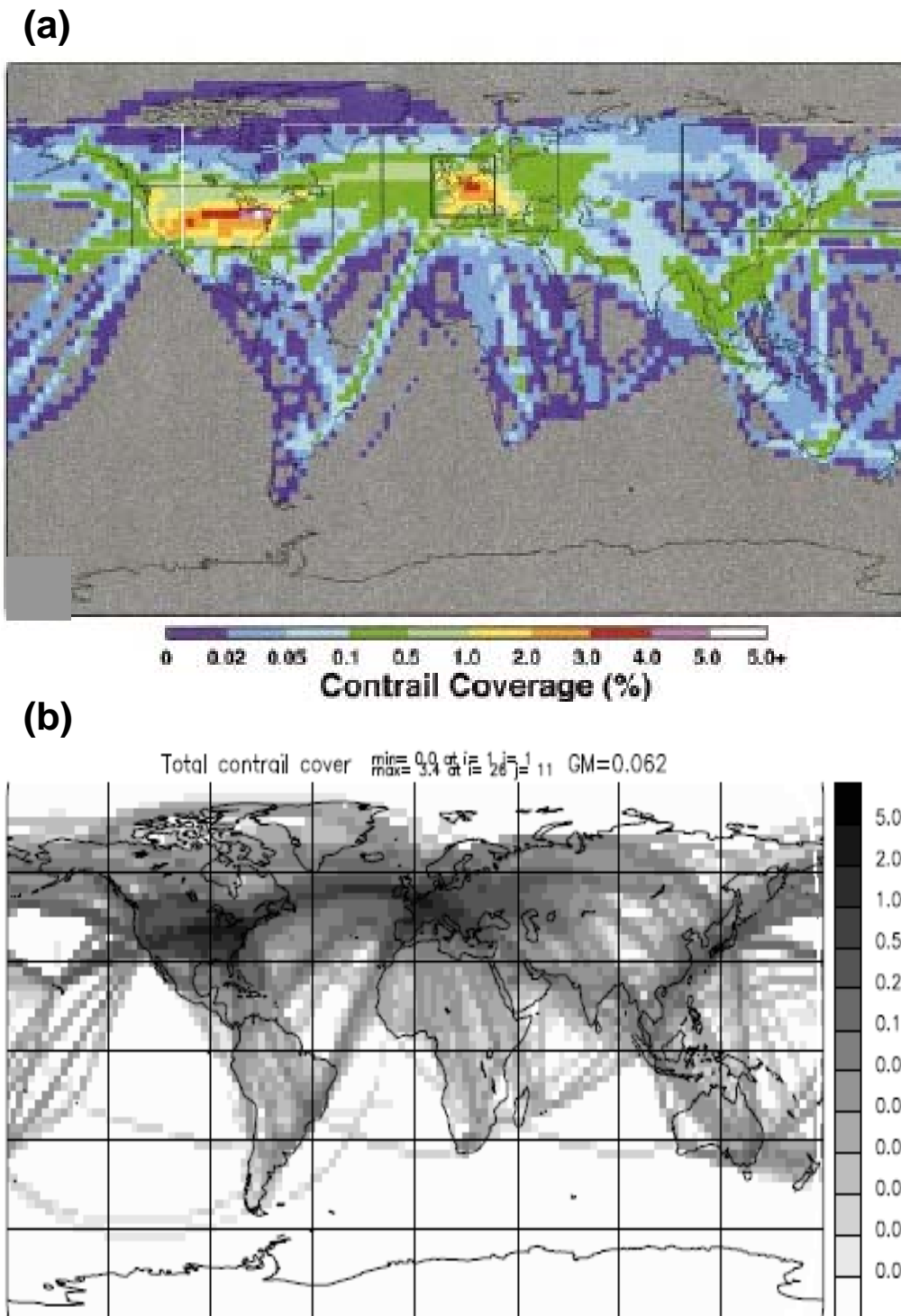


**Fig. 2** (a) Estimated linear contrail coverage based on a  $2.8^\circ$  grid resolution and a parameterization of contrail formation adjusted to match satellite observations of linear contrails using air traffic data from 1992 and applied to 10 years of global numerical weather analyses of relative humidity and temperatures at selected pressure levels (Sausen et al. 1998 and Minnis et al. 2004). Black and white boxes determine the boundaries for the land and ocean air traffic regions, respectively. (b) Total contrail cover simulated by IFSHAM model (after Gulberg 2003).

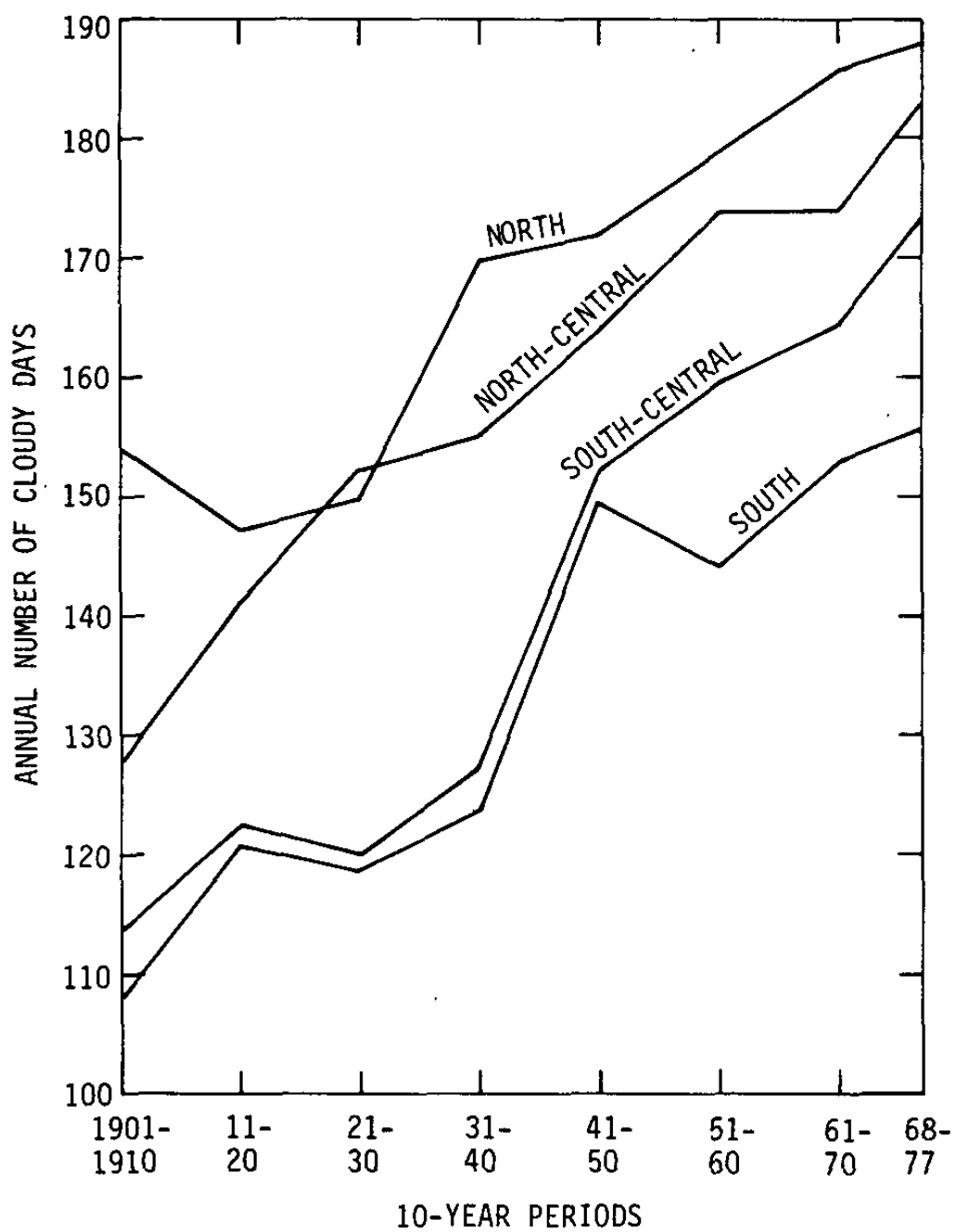


**Fig. 3** Area mean 10-year values of cloudy days (after Changnon 1981).

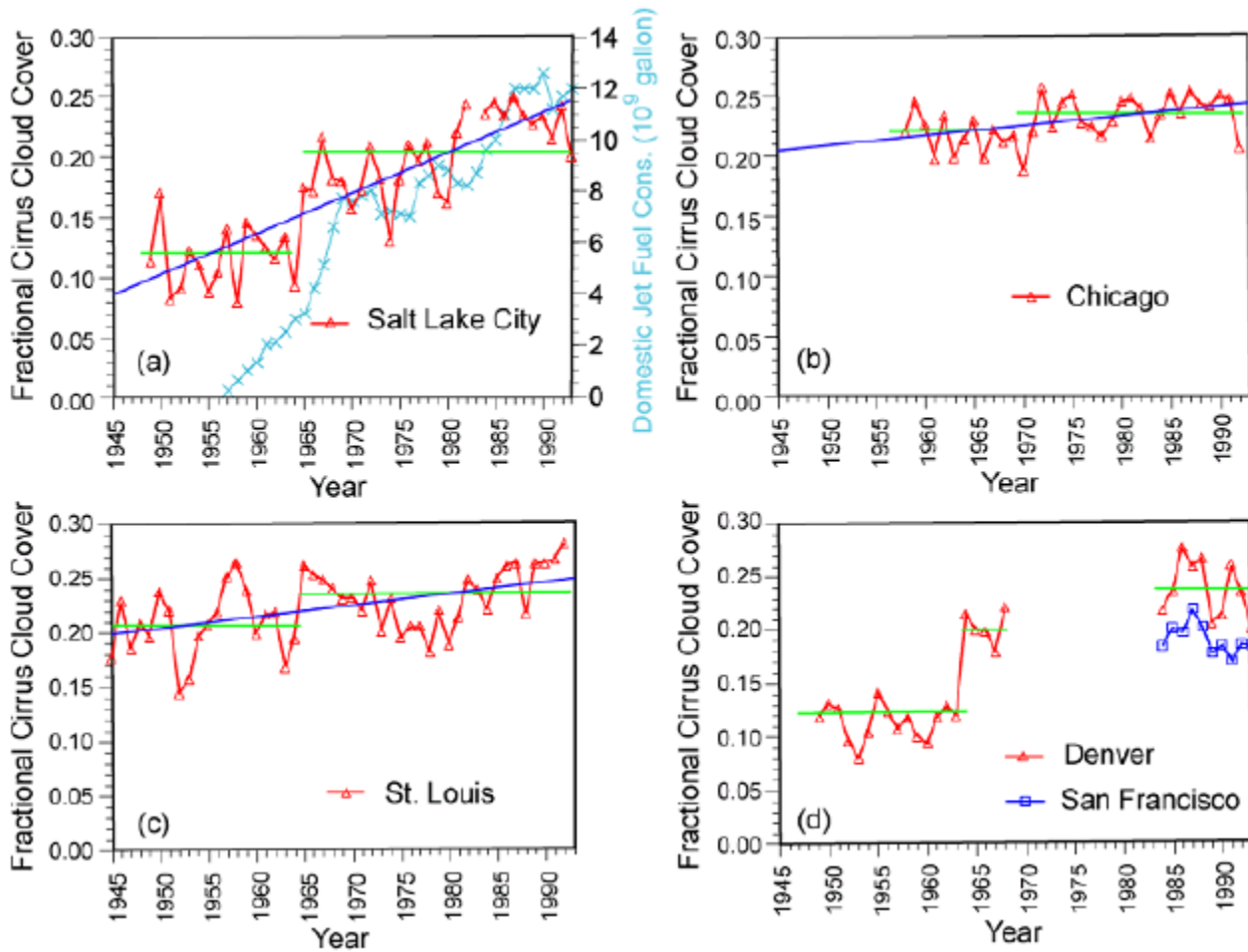


**Fig. 4** Mean annual high cloud cover over Salt Lake City from 1948 to 1992 and domestic jet fuel consumption (after Liou et al. 1990; Frankel et al. 1997). The two solid lines are the statistical fitting curves for high cloud cover for 1948-1964 and 1965-1992. The statistical fitting curve for the entire period is denoted by the heavy line. Also shown are cirrus cloud covers for several midlatitude cities from 1945 to 1992.

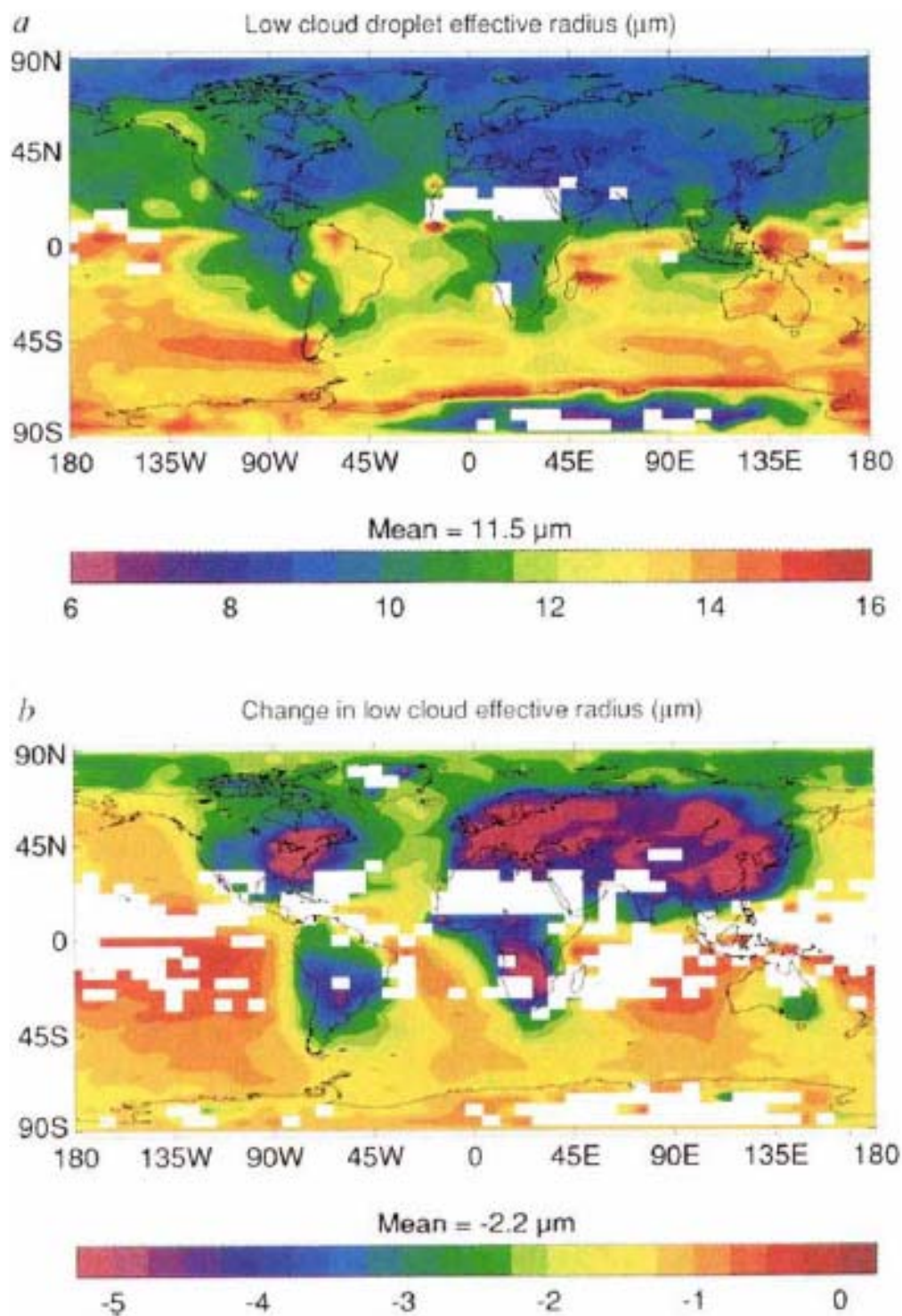


**Fig. 5** (a) A simulation of annual mean distribution of low-level cloud droplet effective radius at cloud top. The blank areas indicate regions where there were no low clouds during the integration. (b) annual-mean composite of the instantaneous change in low cloud droplet effective radius due to changing from natural-only to total aerosol concentration. The blank areas indicate regions where there were no low clouds during any of the sampling periods (after Jones et al. 1994).

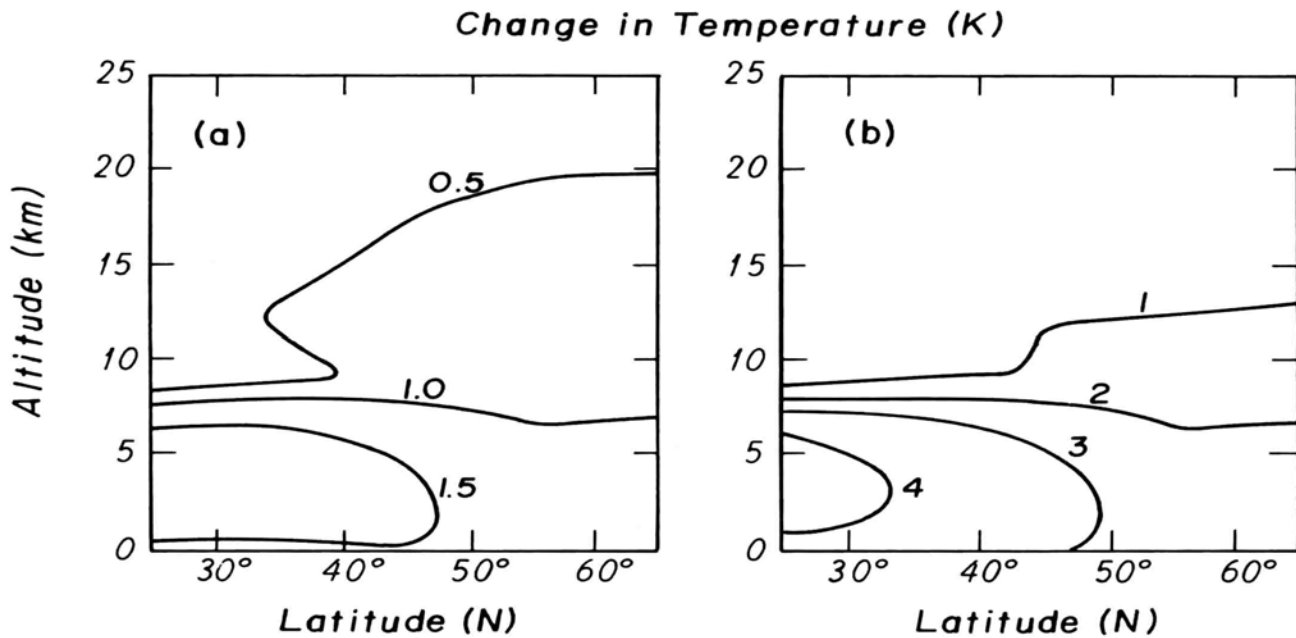


**Fig. 6** Changes in zonally mean atmospheric and surface temperatures subject to thermal equilibrium due to increases in high cloud cover of (a) 5%, and (b) 10% subject to interaction between humidity and cloud cover, as simulated by the two-dimensional energy balance climate model (after Liou et al 1990).

## High Clouds

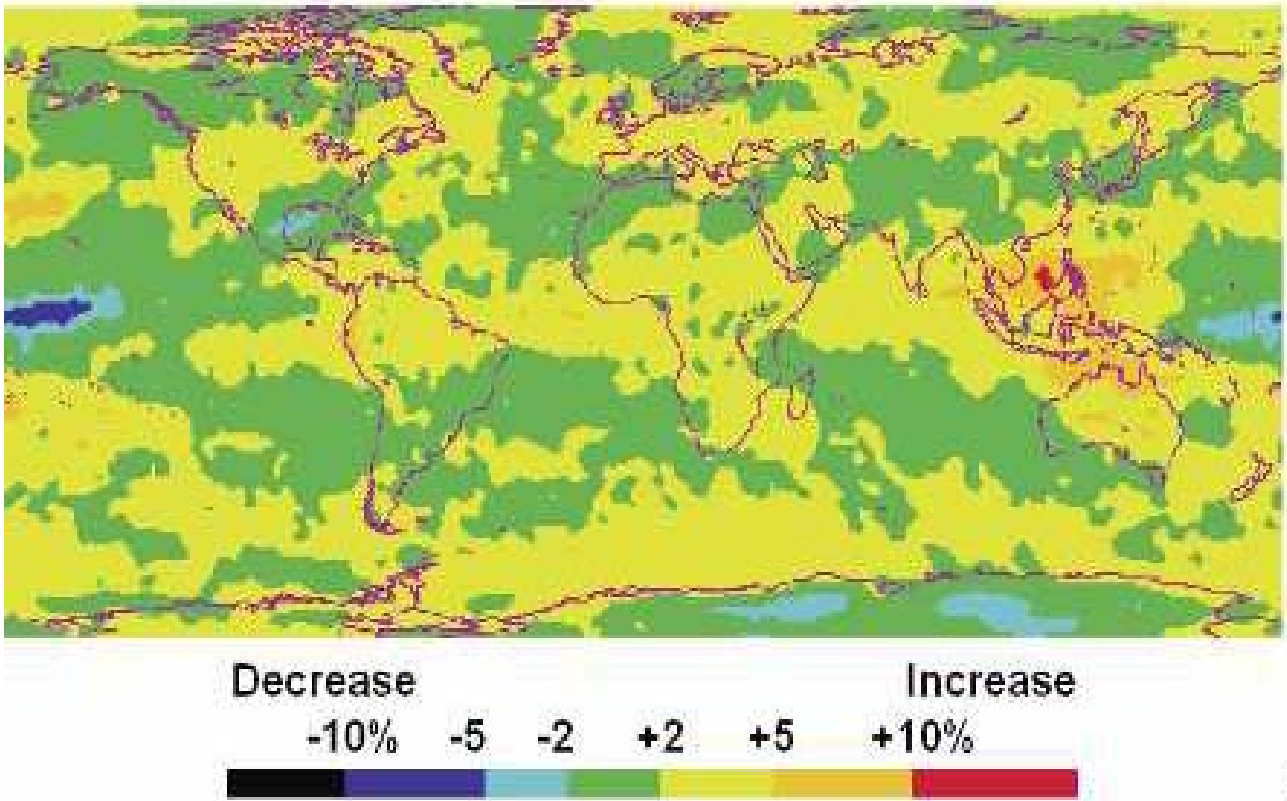


**Fig. 7** The geographical locations of changes in high-cloud frequency between the 1994-2001 and 1985-1992 periods (after Wylie et al. 2005).

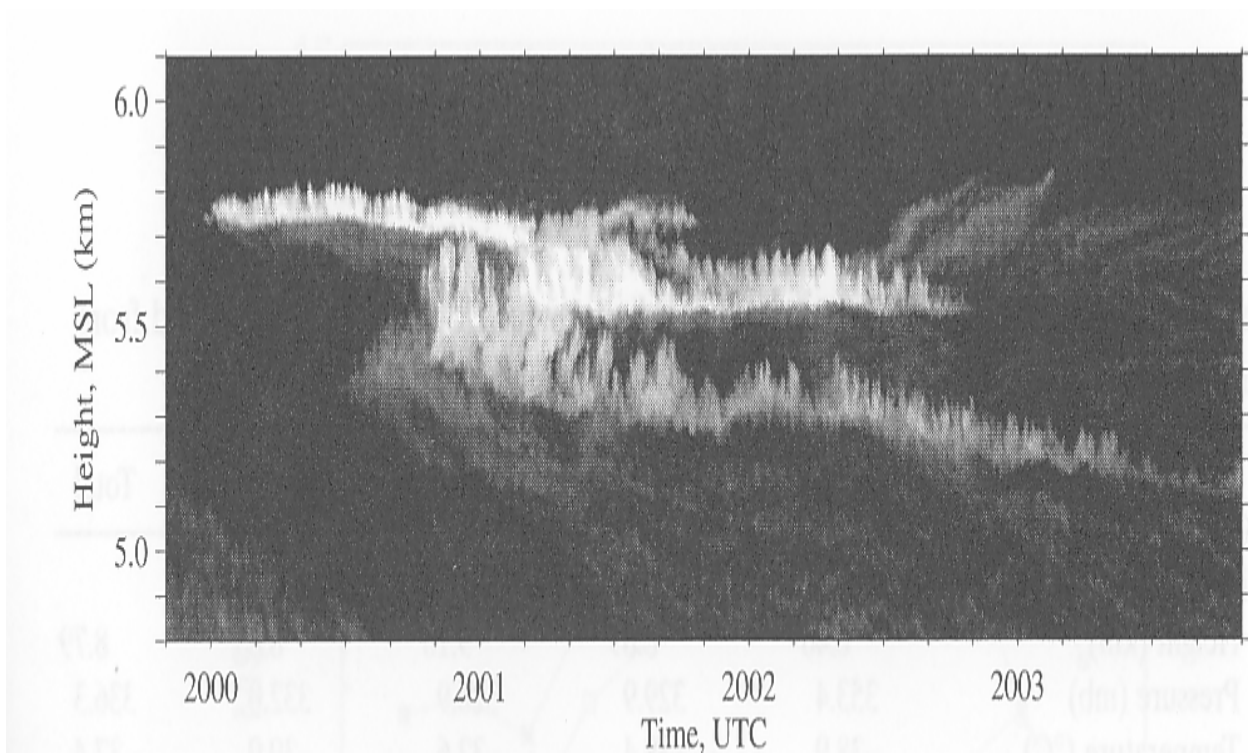


**Fig. 8** High-resolution image of spreading contrails, resembling cirrocumulus and natural cirrus probed in the 1.06mm polarization diversity lidar channel at the ARM-SGP site on May 2, 1996 during SUCCESS field experiment (after Sassen 1997).

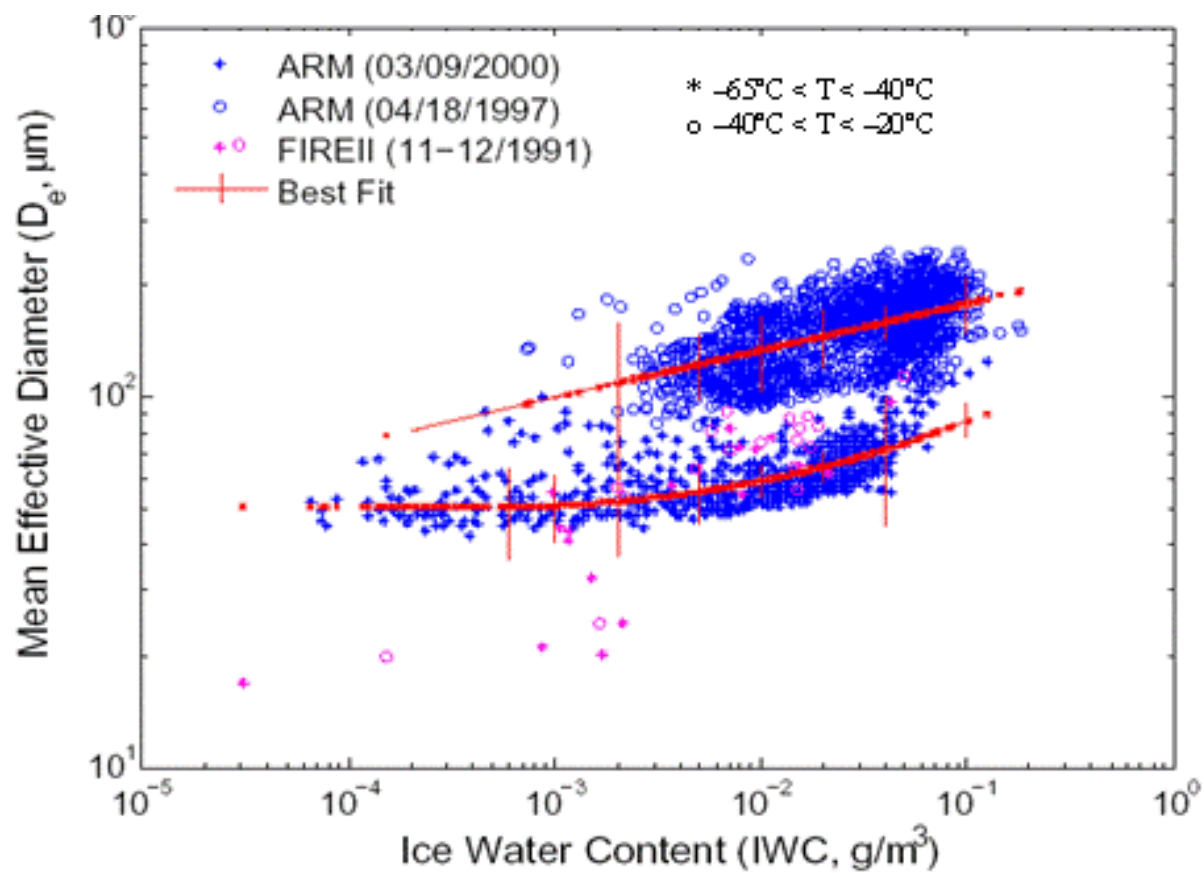


**Fig. 9** The IWC and mean effective size correlation for midlatitudes cirrus based on 4066 aircraft observations during ARM and FIRE intensive cirrus cloud field campaigns. The solid curves denote the best fitting with vertical bar representing standard deviations.

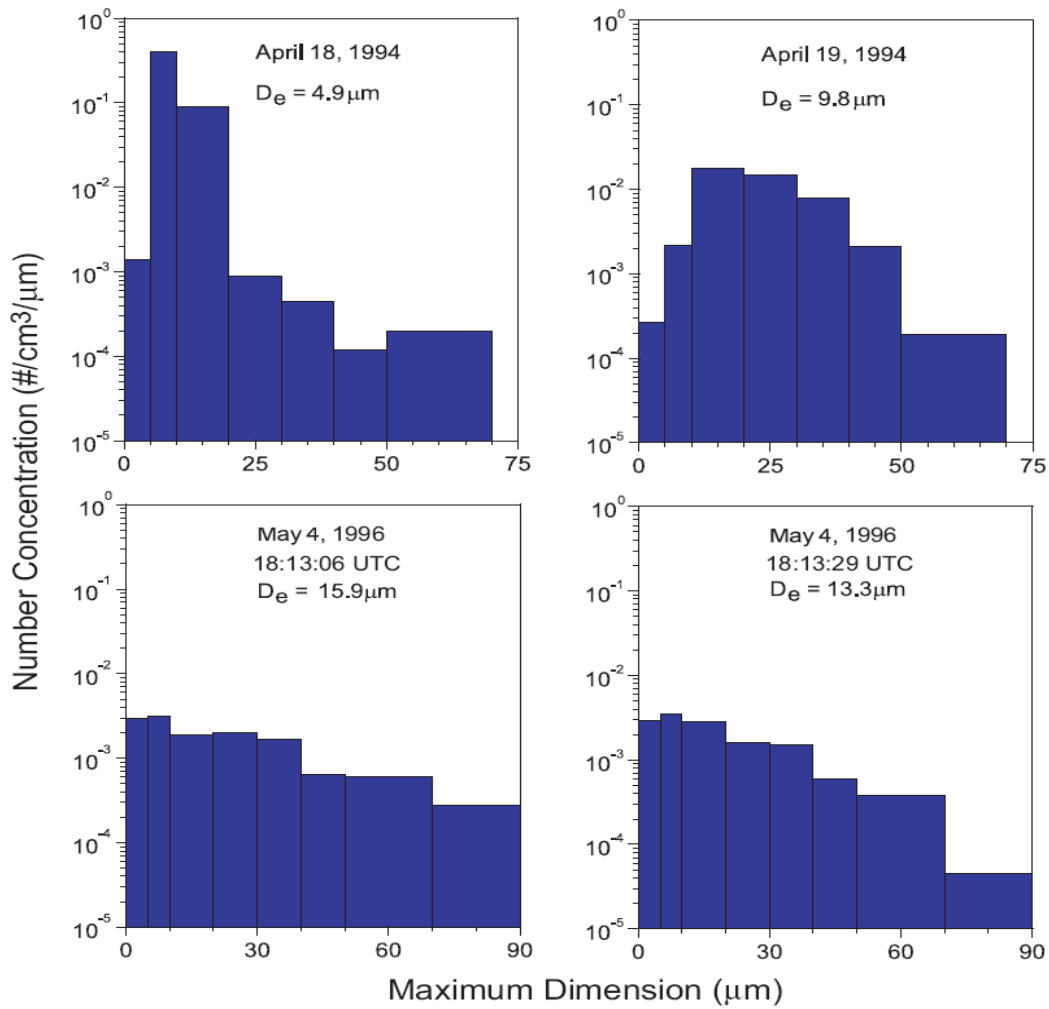


**Fig. 10** Discretized ice crystal size distributions for a contrail and a cold cirrus (~ 6 min duration) measured by FSSP on board the University of North Dakota Citation on April 18 and 19, 1994 (upper panels); and for contrail cirrus (~ 50 sec duration) measured by the replicator system mounted on the NASA's DC-8 that tailed a Boeing 757 during SUCCESS on May 4, 1996 (after Liou et al. 1998).

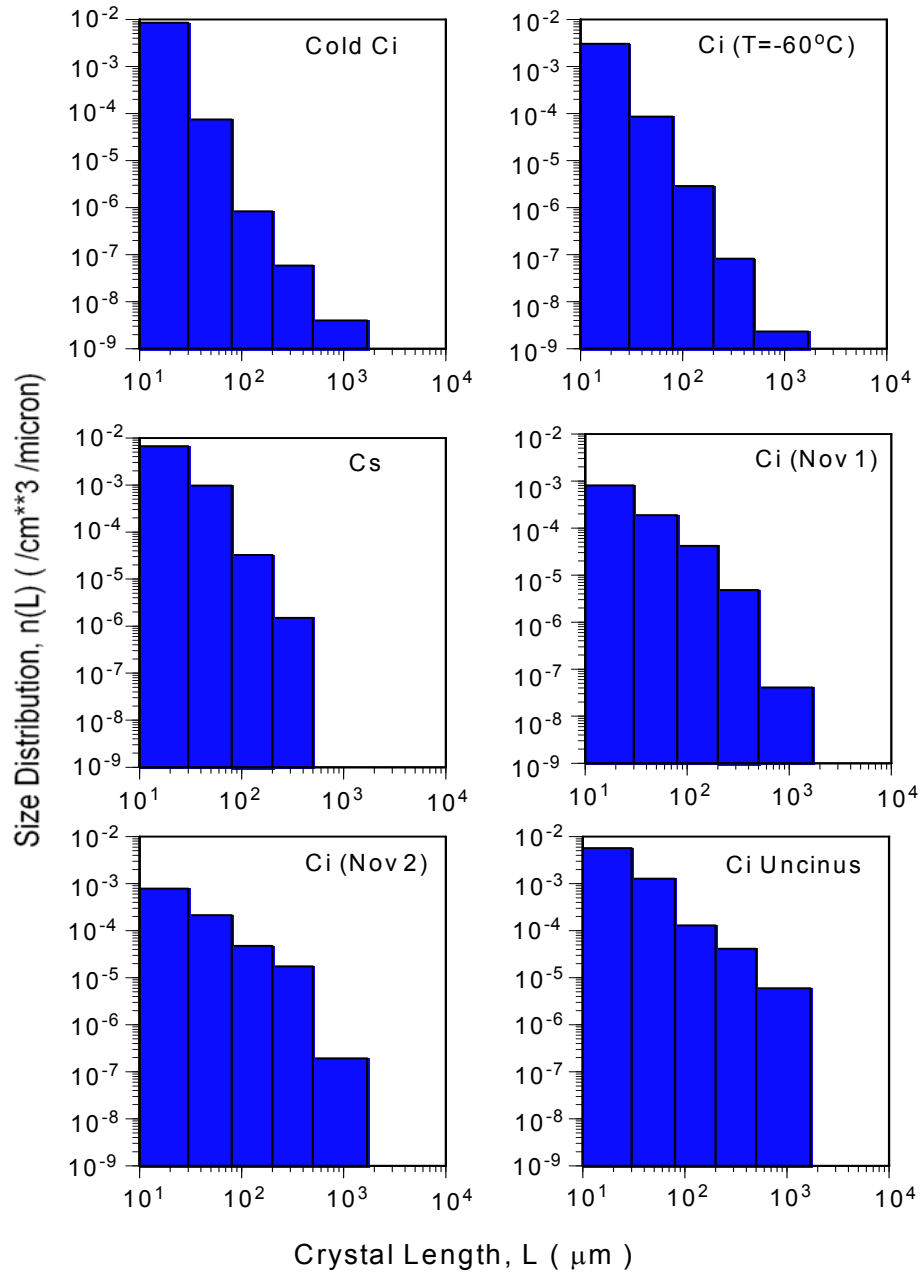


**Fig. 11** Six discretized ice crystal size distributions (after Ou et al. 2002).

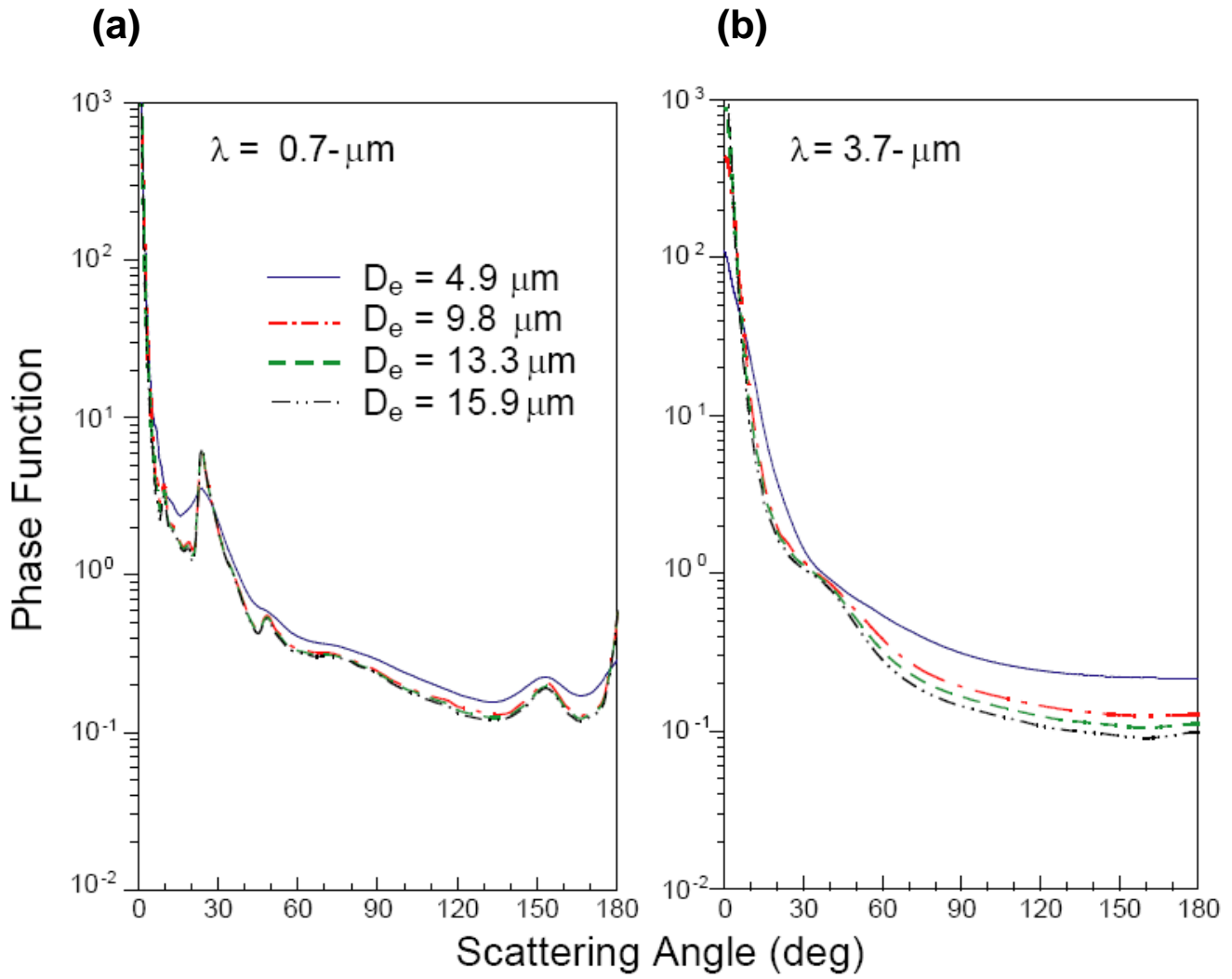


**Fig. 12** Phase functions for (a)  $0.7\text{ }\mu\text{m}$  and (b)  $3.7\text{ }\mu\text{m}$  wavelengths using a contrail cirrus model consisting of 50% bullet rosettes, 30% hollow columns, and 20% plates (after Liou et al. 1998).

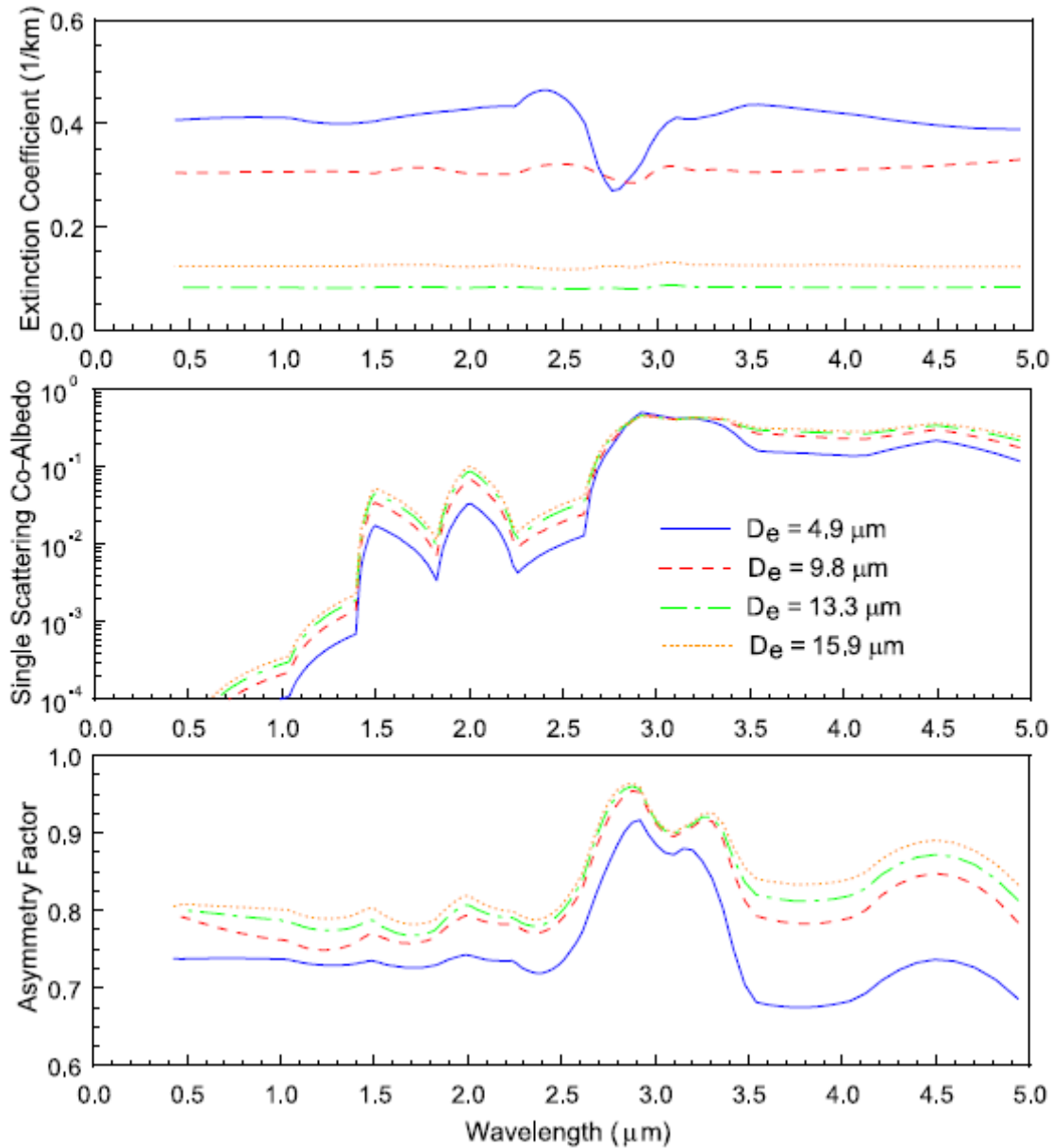


**Fig. 13** Extinction coefficient (top), single-scattering co-albedo ( $1 - \omega$ , middle), and asymmetry factor (bottom) as functions of wavelength from 0.2 to 5  $\mu\text{m}$ . The minima for the extinction coefficient and the maxima for single-scattering co-albedo and asymmetry factor located at 2.85  $\mu\text{m}$  are due to the well-known Christiansen effect (after Liou et al. 1998).

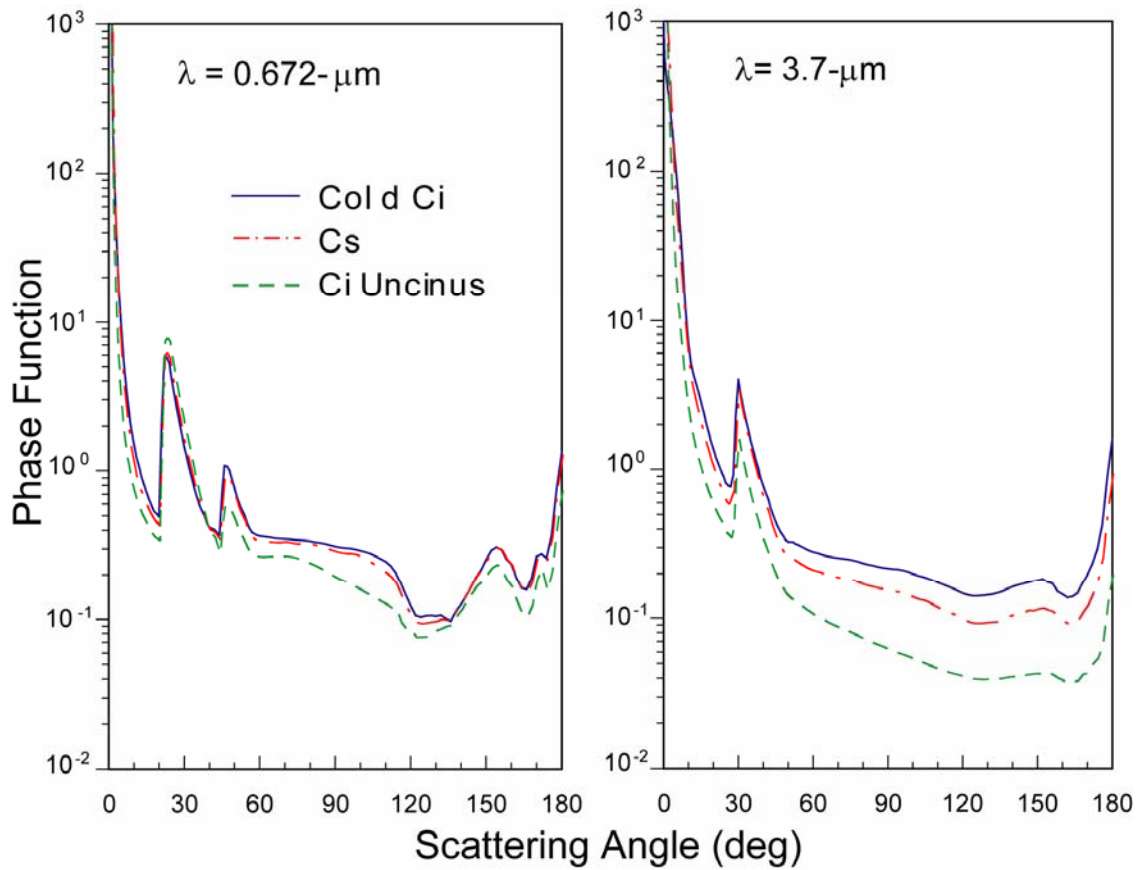


**Fig. 14** Phase functions for (a) 0.672  $\mu\text{m}$  and (b) 3.7  $\mu\text{m}$  wavelengths using Cold Ci, Cirrostratus, and Cirrus Uncinus models (after Ou et al. 2002; 2003).

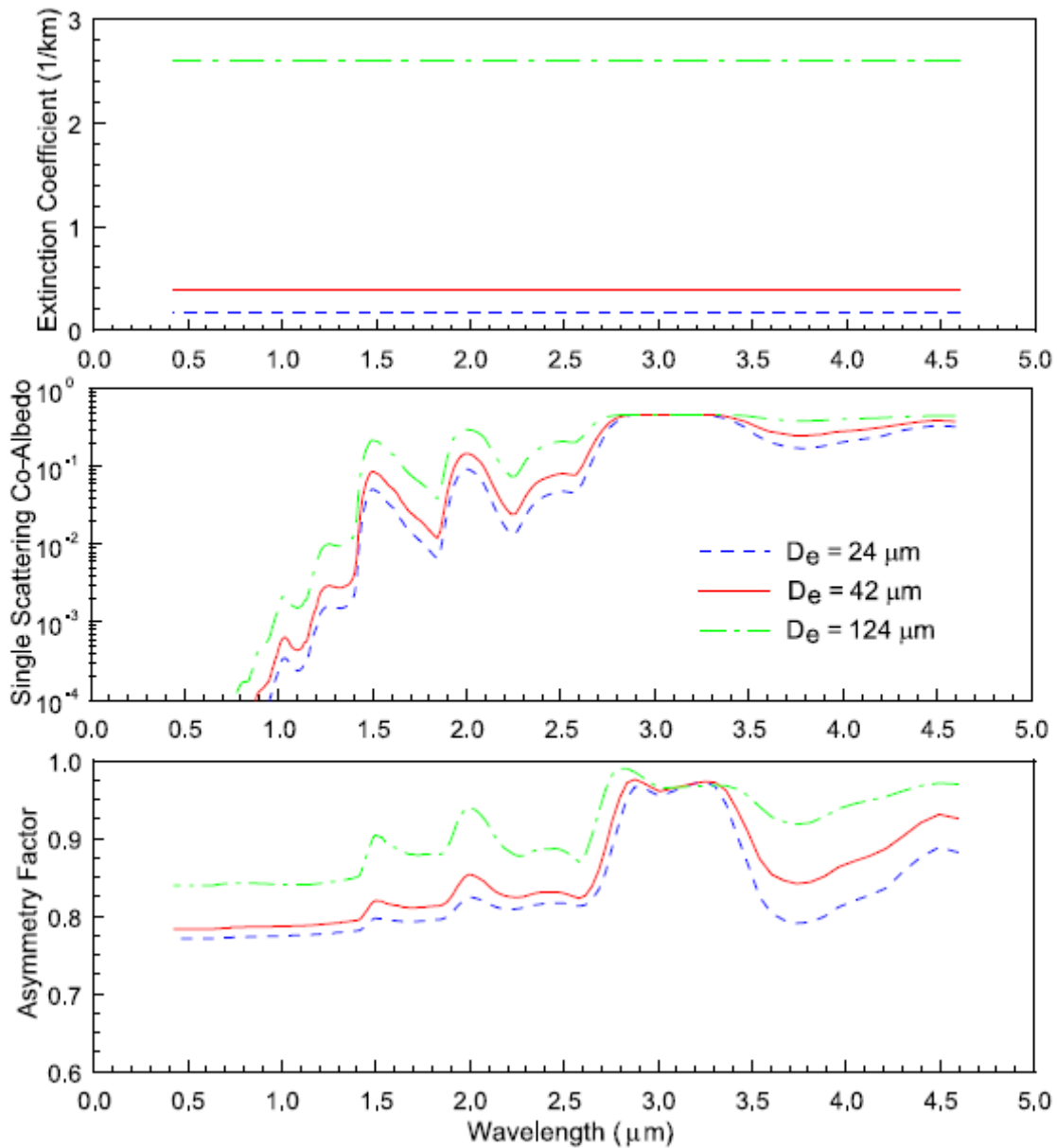


**Fig. 15** Extinction coefficient (top), single-scattering co-albedo ( $1 - \omega$ , middle), and asymmetry factor (bottom), as functions of wavelength from 0.2 to 5  $\mu\text{m}$  for three representative cirrus cloud size distributions. The minima for the extinction coefficient and the maxima for single-scattering co-albedo and asymmetry factor located at 2.85  $\mu\text{m}$  are due to the well-known Christiansen effect (after Ou et al. 2002; 2003).

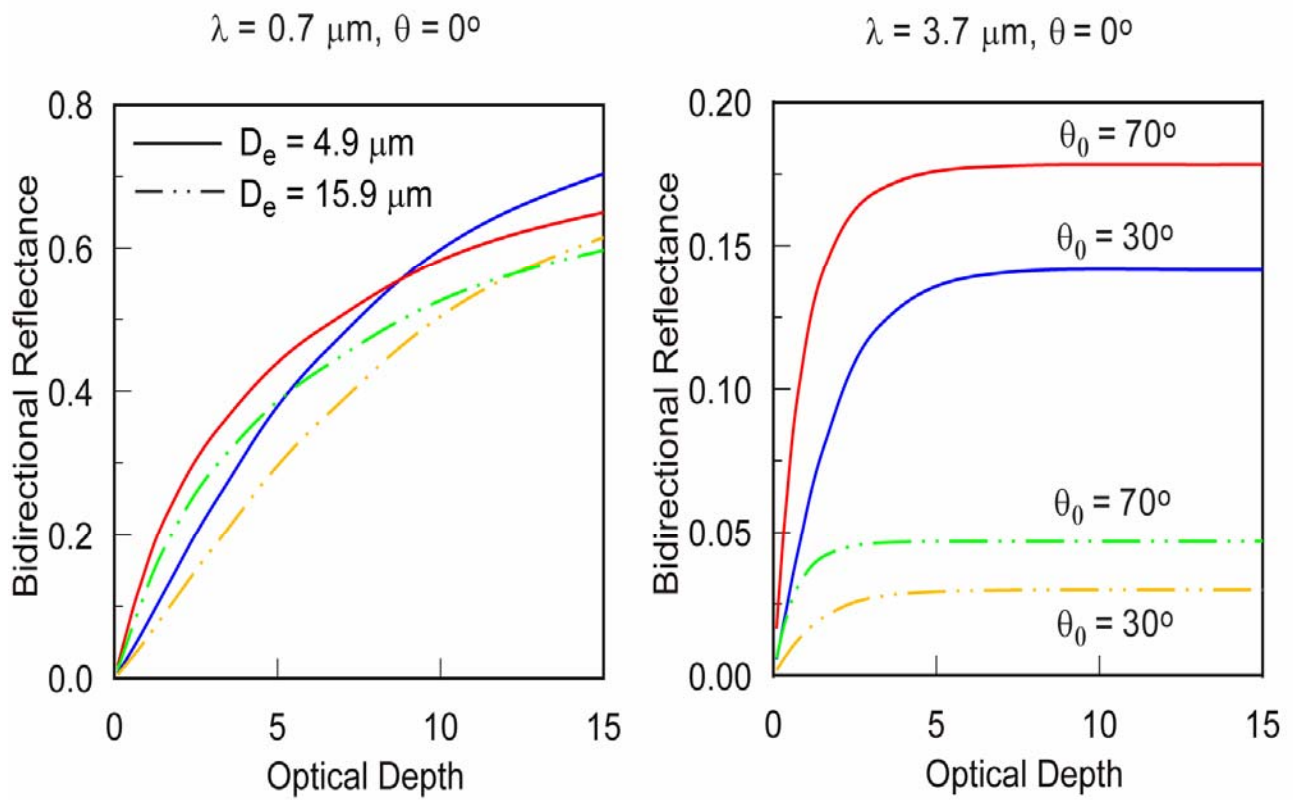


**Fig. 16** Bidirectional reflectances for two contrail size distributions, two solar zenith angles and two wavelengths as functions of optical depth, computed by LBLE model after (Liou et al. 1998).

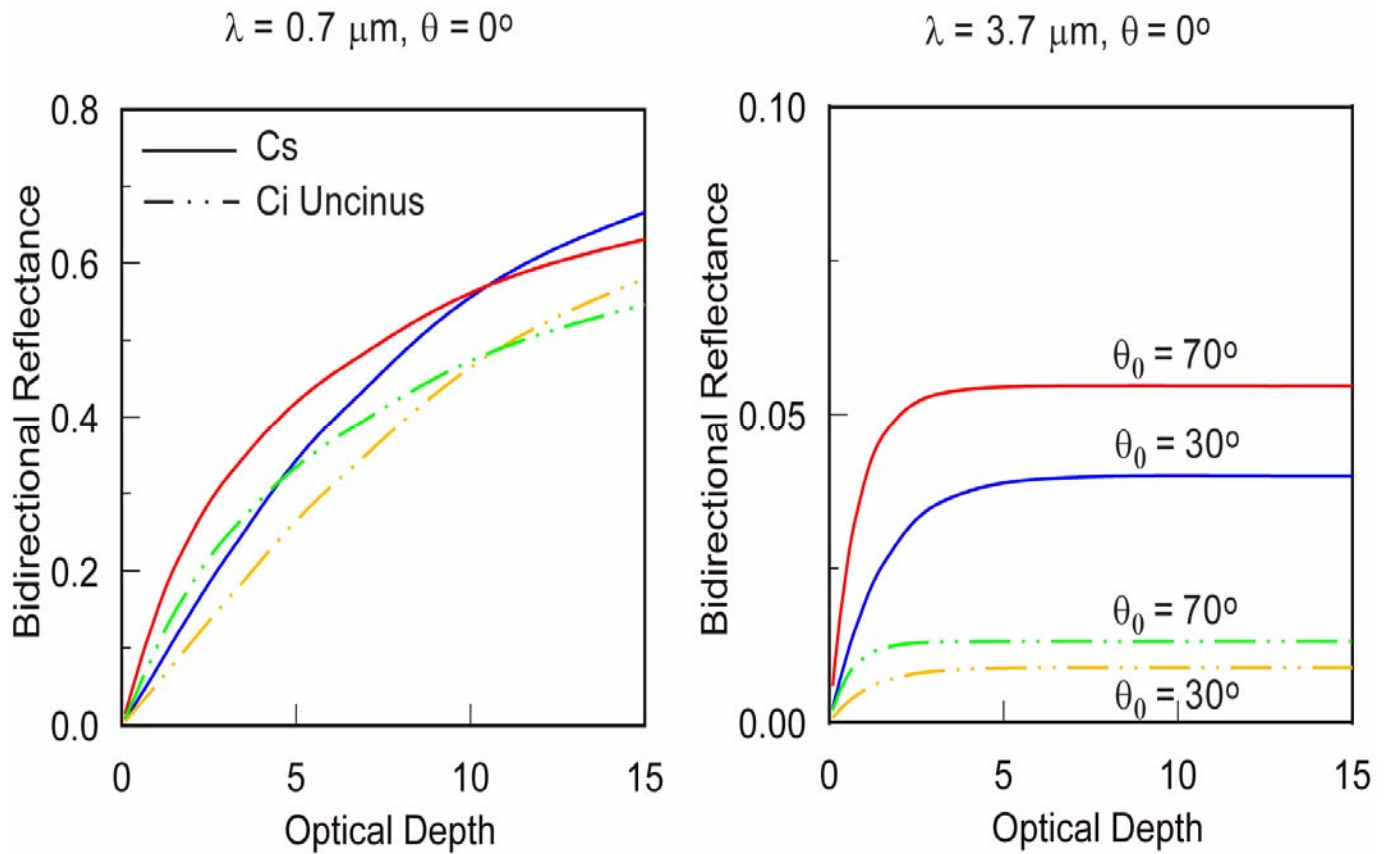


**Fig. 17** Bidirectional reflectances for two cirrus size distributions, two solar zenith angles and two wavelengths as functions of optical depth, computed by LBLE model (after Ou et al. 2002; 2003).

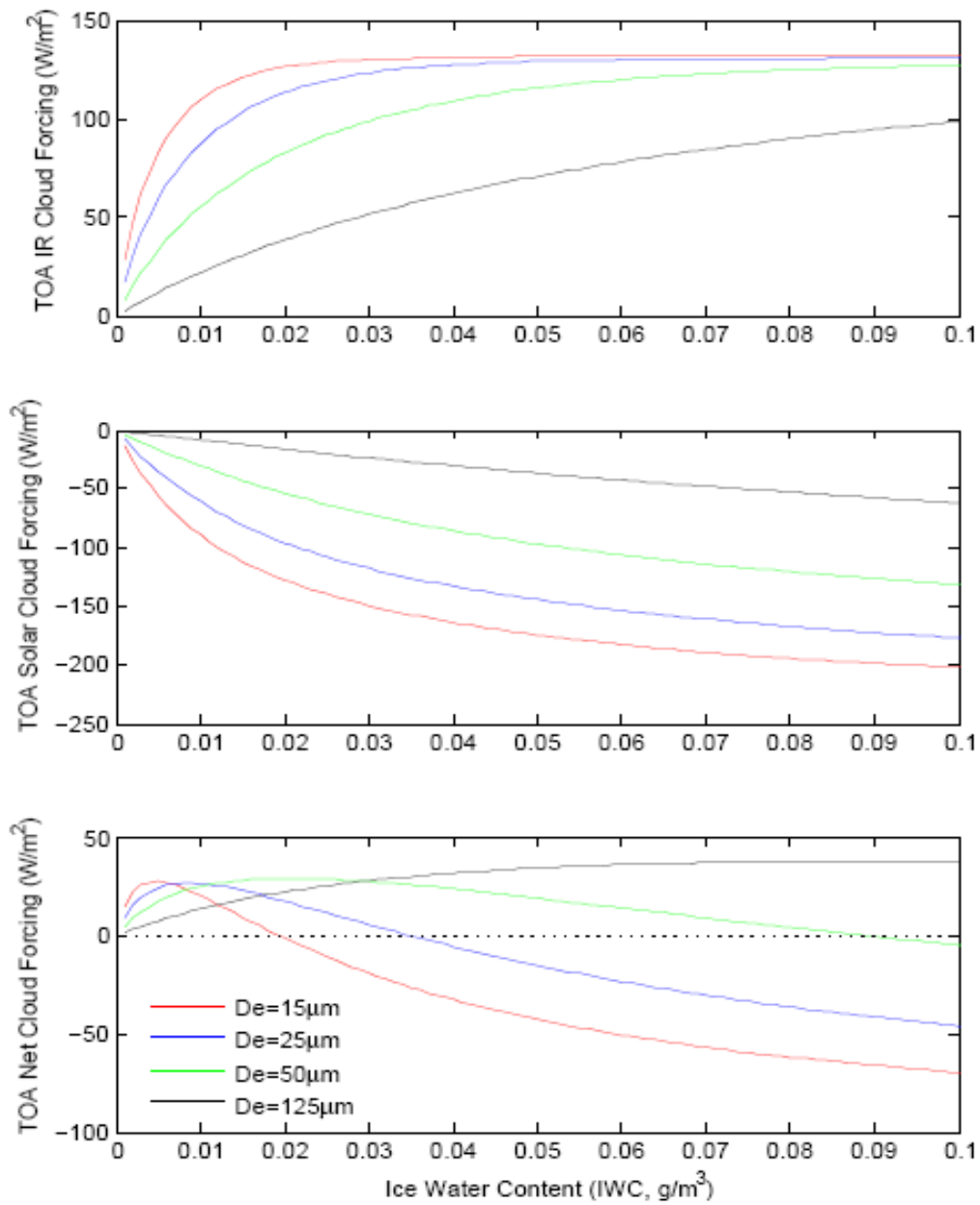


**Fig. 18** Cirrus cloud radiative forcings as function of ice water content for four size distributions computed by Fu-Liou model (after Fu and Liou 1993).

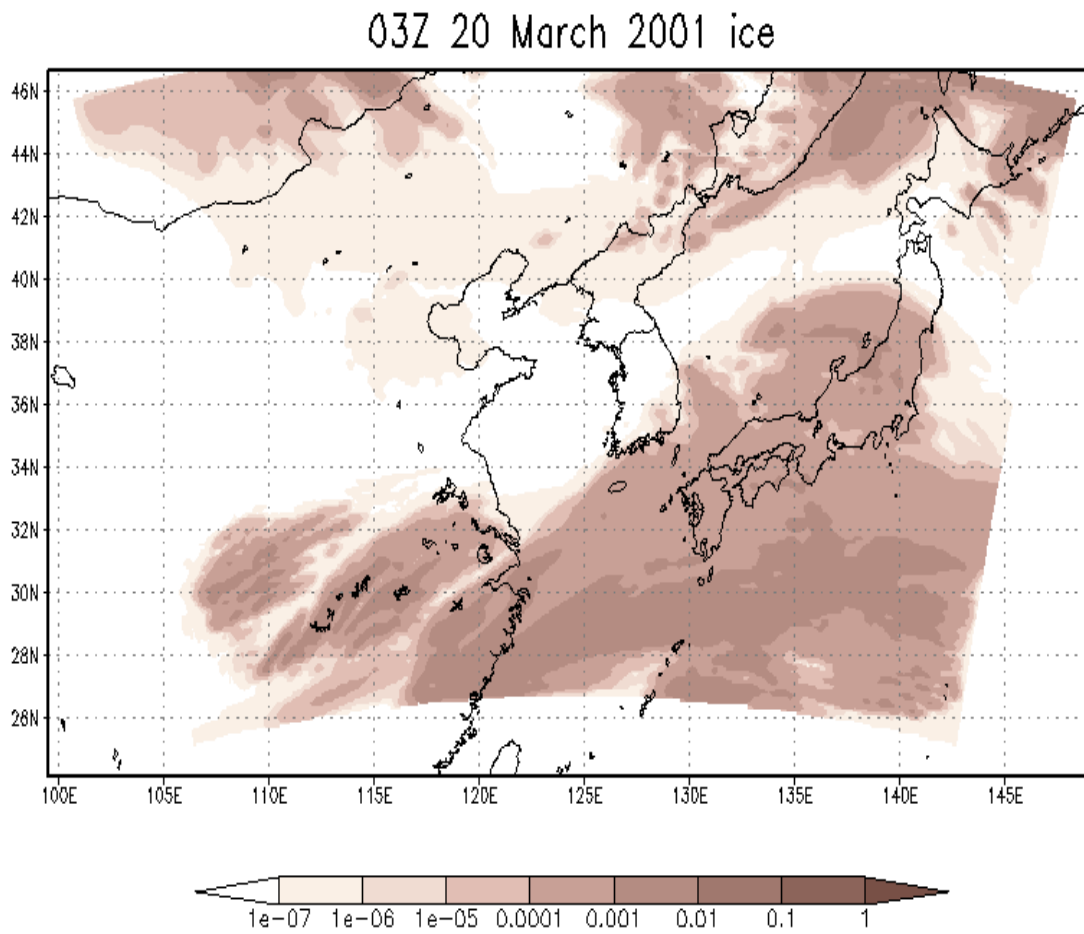


**Fig. 19** A simulation of ice water content field using WRF-ARW over the region corresponding to Fig. 1(d) on March 19-20, 2001.